

AD-A111 068

BATTELLE PACIFIC NORTHWEST LABS RICHLAND WASH

F/G 13/2

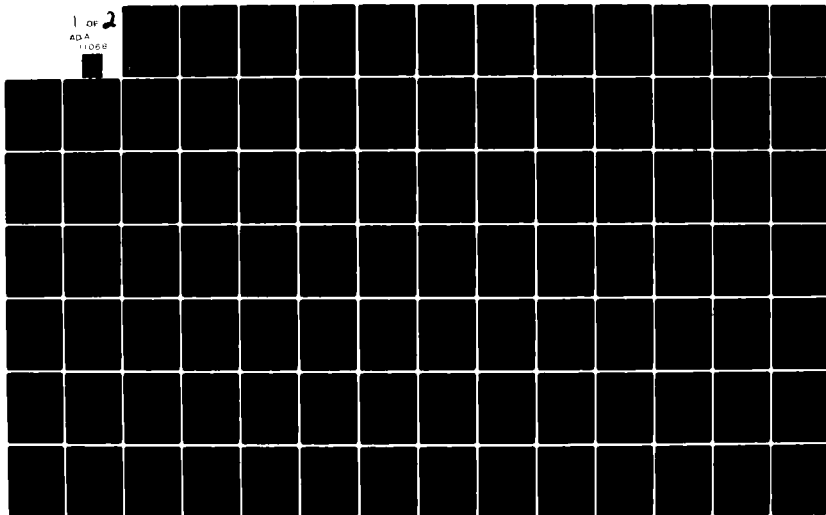
SIMULATION OF THE MIGRATION, FATE, AND EFFECTS OF DIAZINON IN Y--ETC(U)

DEC 81 M A PARKHURST, G WHELAN, Y ONISHI

UNCLASSIFIED

NL

1 OF 2
ADA
11068



AD A111068

LEAD

(12)

Simulation of the Migration, Fate, and Effects of Diazinon in Two Monticello Stream Channels

M. A. Parkhurst
G. Whelan
Y. Onishi
A. R. Olsen

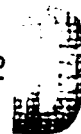
December 1981

Prepared for the
U.S. Army Medical Bioengineering Laboratory
Fort Detrick, Frederick, MD
under Contract 231104483

The views, opinions, and findings contained in this report are those of the authors and should not be construed as an official Department of the Army position, policy, or decision, unless so designated by other documentation.



FEB 18 1982



A



Battelle

Pacific Northwest Laboratories

This document has been approved
for public release and sale; its
distribution is unlimited.

DTIC FILE COPY

LEGAL NOTICE

This report was prepared by Battelle as an account of sponsored research activities. Neither Sponsor nor Battelle nor any person acting on behalf of either:

MAKES ANY WARRANTY OR REPRESENTATION, EXPRESS OR IMPLIED, with respect to the accuracy, completeness, or usefulness of the information contained in this report, or that the use of any information, apparatus, process, or composition disclosed in this report may not infringe privately owned rights; or

Assumes any liabilities with respect to the use of, or for damages resulting from the use of, any information, apparatus, process, or composition disclosed in this report.

SIMULATION OF THE MIGRATION, FATE, AND
EFFECTS OF DIAZINON IN TWO MONTICELLO
STREAM CHANNELS

M. A. Parkhurst
G. Whelan
Y. Onishi
A. R. Olsen

December 1981

Prepared for the
U.S. Army Medical Bioengineering Laboratory
Fort Detrick, Frederick, MD
under Contract 2311104483

Accession For	
NTIS STAR	<input checked="" type="checkbox"/>
DTIC TAB	<input type="checkbox"/>
Unannounced	<input type="checkbox"/>
Justification	
<i>little in file</i>	
By	
Distribution/	
Availability Codes	
Avail and/or	
Dist	Special
<i>H</i>	

Battelle
Pacific Northwest Laboratories
Richland, Washington 99352

A

EXECUTIVE SUMMARY

The U.S. Environmental Protection Agency's (EPA's) Environmental Research Laboratory in Duluth, Minnesota, conducted a field investigation of the aquatic effects of diazinon in experimental stream channels at Monticello, Minnesota during the summer of 1980.

Battelle Pacific Northwest Laboratories (BNW) used the field data provided by EPA to simulate the transport of diazinon in the water and sediments and to assess the toxic risks to fathead minnows using the Chemical Migration and Risk Assessment (CMRA) methodology. This methodology required input of channel and hydrologic characteristics, diazinon characteristics and its release rate into a receiving water body, laboratory concentrations of diazinon exposure causing sublethal effects and mortality, and field observations of actual effects on fathead minnows exposed to diazinon.

Diazinon, an organophosphate insecticide, was injected into the channels at two low-level concentrations (3.0 $\mu\text{g/l}$ and 0.3 $\mu\text{g/l}$ in receiving channels after mixing). Hydrodynamic and sediment transport models were calibrated using the higher concentration channel (3.0 $\mu\text{g/l}$). The models then simulated concentrations in the other (0.3 $\mu\text{g/l}$) channel. The risk assessment used a statistical summary of the modeling results and laboratory toxicity data to determine the probable consequences of continuous exposure of the fish to the two diazinon concentrations.

Results of the modeling application were encouraging. The predicted hydrodynamic simulation concentrations were generally equivalent with measured field concentrations.

Because there was very little data available to indicate the extent of diazinon sorbed by sediment, model calibration and verification for sorbed diazinon transport were very limited. However, diazinon has a very small distribution coefficient, and sediment concentrations in receiving channels were very small. Hence, as simulation results indicated, the effects of sediment-diazinon interactions (such as adsorption of diazinon by sediment, and transport, deposition, and resuspension of sorbed diazinon) on diazinon transport

were very minor. Moreover, this study illustrates ways of estimating necessary input data for the CMRA methodology from limited measured data such as most modelers encounter. The simulation results also provided information regarding the significance of sediment deposition/resuspension, adsorption/desorption, and degradation on the concentration of dissolved diazinon in the channels.

The risk assessment portion of the CMRA methodology was not adequately tested by this application because of the very low diazinon concentrations. The risk evaluation predicted no mortality directly related to diazinon exposure and few (if any) incidents of sublethal effects. EPA's preliminary results indicate no juvenile or adult fish mortality resulting from diazinon exposure. Their only observed effect was an increased number of dead eggs.

Validation of the methodology requires far more field data for comparison than was available in this study. However, results of comparisons that were made indicate that the models can substitute certain assumptions and extrapolations for actual input data and can give creditable results of contaminant concentrations based on hydrodynamic, bed sediment, and chemical characteristics.

The methodology is, in principle, capable of modeling noncontinuous discharge of varying concentrations and has a potential application for comparing the relative concentrations and effects of various chemicals. When combined with its overland transport component, it can be used to model runoff into streams from chemical spills, uncontrolled landfills, or hazardous waste disposal sites and to assess the probable consequences to exposed aquatic life.

ACKNOWLEDGMENTS

The authors wish to extend a special thanks to the EPA staff at Duluth and at the Monticello Ecological Research Station at Monticello, Minnesota for their cooperation, sampling, and analysis on our behalf. We would like to express our gratitude to Dr. Heinz G. Stefan from St. Anthony Falls Hydraulics Laboratory, University of Minnesota for providing hydrodynamic information pertaining to the MERS channels and Mr. Kurt Gunard from the U.S. Geological Survey, St. Paul, Minnesota for providing discharge and water quality data along the Mississippi River. We would also like to thank Miss Fonda L. Thompson for her assistance on the hydrodynamic model and Mr. Daniel B. Carr for his statistical modeling contribution.

CONTENTS

EXECUTIVE SUMMARY	iii
ACKNOWLEDGMENTS	v
1.0 INTRODUCTION	1.1
2.0 METHODOLOGY	2.1
2.1 COMPUTER MODELING	2.2
2.1.1 Sediment-Contaminant Transport Model--(TODAM)	2.2
2.1.2 Hydrodynamic Model--(DWOPER)	2.7
2.2 RISK ASSESSMENT	2.9
3.0 APPLICATION OF THE METHODOLOGY	3.1
3.1 FIELD SAMPLING	3.4
3.1.1 Water Sampling	3.5
3.1.2 Sediment Sampling	3.5
3.1.3 Biological Sampling	3.6
3.1.4 Water Analysis	3.7
3.1.5 Sediment Analysis	3.7
3.1.6 Channel Characteristics.	3.8
3.1.7 Degradation Studies	3.8
3.2 MODEL CALIBRATION	3.9
3.2.1 DWOPER Calibration.	3.9
3.2.2 TODAM Calibration	3.22
3.3 RISK ASSESSMENT.	3.49
4.0 COMPARISON OF SIMULATED VERSUS OBSERVED RESULTS	4.1
4.1 DWOPER--HYDRODYNAMIC MODELING RESULTS	4.1
4.2 CALIBRATION RESULTS OF TODAM	4.5

4.3	MODELING RESULTS OF TODAM.	4.14
4.4	RISK ASSESSMENT.	4.21
5.0	CONCLUSIONS AND RECOMMENDATIONS	5.1
6.0	REFERENCES.	6.1

FIGURES

1.1	Aerial Photograph of the Monticello Experimental Channels	1.3
2.1	Chemical Migration and Risk Assessment (CMRA) Methodology and Required Input Data	2.1
2.2	Summary of Toxicity Curves	2.11
3.1	Layout of Channels 6 and 7	3.3
3.2	Plan View of Channels 6 and 7 with Computational Nodes Included	3.11
3.3	Representation of Pool-Riffle Configuration	3.11
3.4	Average Pool Cross-Sectional Shape	3.13
3.5	Average Riffle Cross-Sectional Shape	3.13
3.6	Concentration vs. Turbidity	3.26
3.7	Sediment Size Distributions	3.38
3.8	Diazinon Concentration (Percentage of Original) when Exposed to Sun	3.47
3.9	Diazinon Concentration (Percentage of Original) when Stored in Shade	3.47
4.1	Observed Versus Computed Stages	4.7
4.2	Observed Versus Computed Depths	4.8
4.3	Longitudinal Variation of Stages	4.9
4.4	Bed Contamination History for Section 604 Test Case 3.1 ppb	4.11
4.5	Diazinon Concentrations in Channel 6	4.12
4.6	Diazinon Concentration Extrapolated Results on Channel 6	4.15
4.7	Bed Contamination History for Section 704 Test Case 0.31 ppb	4.16
4.8	Diazinon Concentrations in Channel 7	4.17
4.9	Extrapolated Diazinon Concentration Results on Channel 7	4.19

TABLES

3.1	Channel Geometry and Hydrodynamic Information	3.14
3.2	Water Surface Slopes, Cross-Sectional Areas, Wetted Perimeters, and Roughness Coefficients of Channel 1 on April 6, 1977	3.19
3.3	Water Surface Slopes, Cross-Sectional Areas, Wetted Perimeters, and Roughness Coefficients of Channel 1 on April 18, 1977	3.20
3.4	Water Surface Slopes, Cross-Sectional Areas, Wetted Perimeters, and Roughness Coefficients of Channel 1 on June 15, 1977	3.21
3.5	Representative Values of Shear Velocity, Flow Velocity, Area and Depth for Riffles and Pools for a Flow of 0.013 m ³ /s	3.23
3.6	Turbidity vs. Concentration	3.25
3.7	Bed Sediment Size Distribution Samples	3.27
3.8	Sediment Specific Weight and Size Computation Information	3.28
3.9	Organic Content of Bed Sediment Samples	3.30
3.10	Sample #1 Distributed by Size Fraction Between Organic and Inorganic Bed Material	3.35
3.11	Sample #2 Distributed by Size Fraction Between Organic and Inorganic Bed Material	3.36
3.12	Combined Sediment Samples Distributed by Size Fraction Between Organic and Inorganic Bed Materials	3.37
3.13	Diazinon Degradation Study Water Samples from Channel 604	3.46
3.14	LC50 Concentrations from Diazinon Exposure (µg/l)	3.51
3.15	Chronic Effects from Diazinon Exposure	3.53
4.1	Measured Diazinon Concentrations in Water Samples in Channel 6	4.2
4.2	Measured Diazinon Concentrations in Water Samples in Channel 7	4.3
4.3	Vertical and Transverse Average Concentration Profiles	4.4
4.4	Average Water Quality Values in Main Pool from May 14 Through July 31	4.5
4.5	DWOPER's Hydrodynamic Results	4.6

4.6	Contaminated Bed Sample from Pool 604	4.13
4.7	Contaminated Bed Sample from Pool 704	4.16
4.8	Computer Simulated Results of the Minutes Before Each Concentration was Achieved in Channel 6	4.21
4.9	Computer Simulated Results of the Minutes Before Each Concentration was Achieved in Channel 7	4.22
4.10	Survival of Caged Fathead Minnows	4.22
4.11	Condition of Fathead Minnow Eggs	4.24
4.12	Distribution of the Predominant Invertebrate Taxa in the Riffles and Pools at a Peak Emergence Period	4.25

1.0 INTRODUCTION

The objectives of this study are to simulate the transport and fate of the organophosphate pesticide, diazinon, in the man-made stream channels at Monticello, Minnesota, and to evaluate the predictive capabilities of the selected models by comparing the results of the modeling analysis with field data. Background information on the modeling methodology and the Monticello field facility are presented before the discussions of sampling, modeling methodology, results, and conclusions. The report focuses primarily on the in-stream simulations. Because the low diazinon concentrations precluded dramatic toxicity results, less attention is centered on the risk assessment.

An approach to predicting the fate and migration of a contaminant in surface waters has been integrated with an evaluation of the toxic risks to aquatic organisms in a single framework called the Chemical Migration and Risk Assessment (CMRA) methodology (Onishi et al. 1979). The methodology predicts the existence and duration of toxic contaminants in streams from point-source and nonpoint-source discharges, and predicts the probability of direct acute and chronic damages to aquatic biota. The methodology, which uses several mathematical models, was initially developed under contract to the Environmental Protection Agency (EPA), Environmental Research Laboratory, Athens, GA, to provide planners and decision makers in government and industry with a sound basis for evaluating the effects of chemical production, use, and disposal.

Many questions remain concerning the methodology's capabilities in predicting concentrations in real stream environments. To determine its usefulness, an application to a field situation was required, allowing us to:

- test the feasibility of applying the CMRA methodology to small streams,
- evaluate the difficulties in collecting necessary data and determine the practicality of present data requirements,
- evaluate the relative significance of various chemical transport and degradation mechanisms and their impacts on exposure to aquatic biota, and

- compare predicted results to measured data to determine the present simulation capabilities of the models.

Few studies to date have looked at the toxicity of a contaminant in a field situation or have had the opportunity to compare field results with laboratory-derived results. Some notable exceptions to this are a copper study on a section of a small river in Ohio (Geckler et al. 1976), a diazinon study that investigated the changes to a benthic community (Morgan 1977), and an acidification study at the Monticello Ecological Research Station (Zischke et al. 1981). The reasons for the lack of field studies are several. Control over the toxicant concentration requires that unidentified external discharge sources must be negligible; thus, the investigator usually must add the necessary contaminant to the stream. This, of course, is seldom an acceptable practice because of the risks posed to downstream organisms or to drinking water. Additionally, in an actual river situation, it is difficult to control the water flow, the aquatic plant growth, and a multitude of other factors. These variables may mask the results and prevent the investigators from drawing accurate conclusions. Finally, the extensive sampling and analytical requirements are prohibitive for most studies.

While considering the possibility of applying the methodology to a field situation, we became aware of an opportunity afforded by EPA-Duluth. The EPA conducted thermal and pH studies in several outdoor channels at its Ecological Research Station at Monticello, Minnesota (Figure 1.1). They believed that their completed studies demonstrated that the channels could provide a way to test the use of laboratory-derived toxicity values to estimate safe concentrations of various chemicals in natural ecosystems. They decided to use these channels to measure and evaluate changes in the population properties of distribution, abundance, growth, and reproduction for selected species during seasonal exposure to a given pesticide.

The Monticello site provided an outdoor "stream" environment, subject to many natural environmental factors with control of some important variables (e.g. hydrodynamic parameters, contaminant concentration, fish species composition). It offered a chance to study the migration and toxic effects in a



FIGURE 1.1. Aerial Photograph of the Monticello Experimental Channels
(Photograph printed courtesy of University of Minnesota,
Stefan et al. 1980)

nearly controlled stream flow condition, with the addition of the contaminant at a constant concentration. Because of these advantages and EPA's cooperation in sampling and analyzing the additional samples needed, Monticello was selected as a site to test the CMRA methodology.

2.0 METHODOLOGY

The CMRA methodology combines overland and in-stream transport models, statistical analysis, and effects data into a single system (Figure 2.1). The models evaluate the migration and fate of a given chemical from the time of its application, particularly to agricultural lands, or from its discharge into a stream. Removal mechanisms handled by the models include surface runoff; soil erosion; volatilization; chemical, microbial, and photochemical transformation or degradation; and uptake by the sediments. The extent of such removal depends on climate, soil conditions, chemical properties, and agricultural management practices (of which surface runoff and soil erosion are recognized as

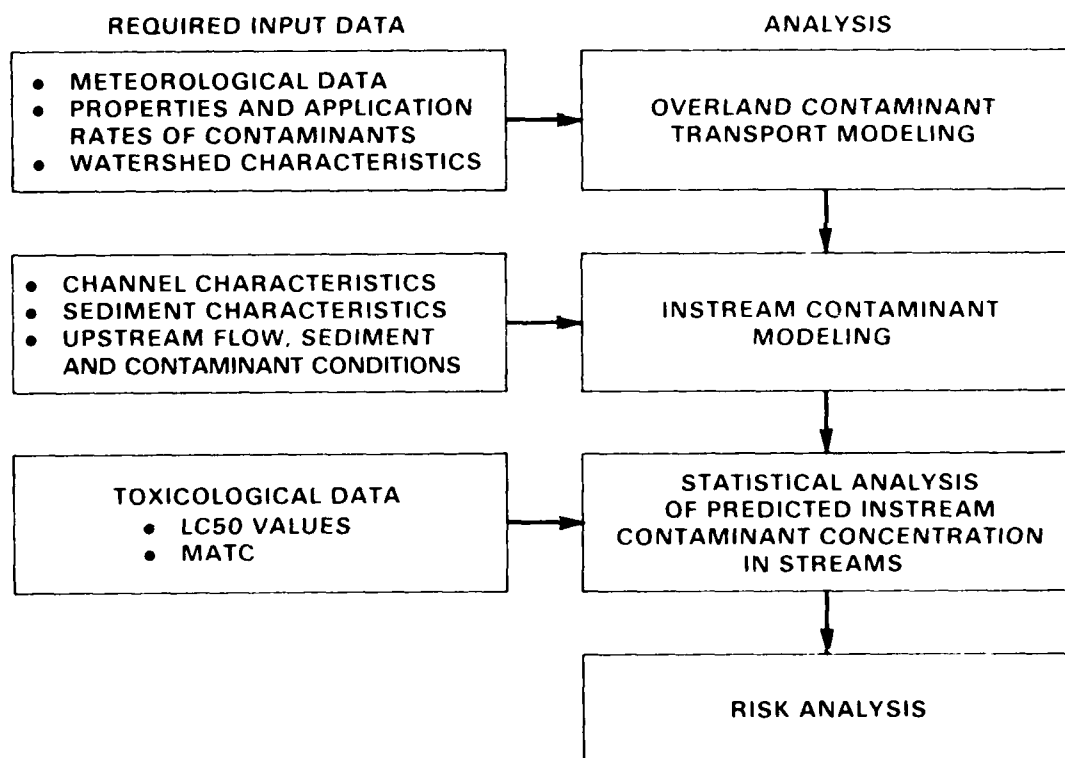


FIGURE 2.1. Chemical Migration and Risk Assessment (CMRA) Methodology and Required Input Data

the dominant mechanisms of removal to a water body). Because the Monticello project entailed a direct discharge into stream channels, modeling of overland transport and fate are not discussed further.

The risk assessment uses a statistical summary of the time-varying concentrations of the chemical being analyzed. It provides a readout of the frequency and duration for which any specified concentration is exceeded during the simulation and can be programmed to indicate when such events occur. This Frequency Analysis of Concentration (FRANCO) code provides a measure of the probability in a risk analysis.

The consequences of the potential risks are evaluated using indicators of lethality and effect/no effect for the organisms at risk. Laboratory toxicological median lethal concentration (LC50) data are used as a measure of mortality. The maximum acceptable toxicant concentration (MATC) is used to define the concentration limit below which no toxic effects have been noted and above which short-term or long-term effects may result. In addition to these laboratory derived data, other observed effects in the lab or the field, as well as relevant chemical properties of the toxicant, are considered to help predict the effects of various toxicant concentrations.

2.1 COMPUTER MODELING

To obtain accurate temporal and spatial distributions of chemical contaminants in streams, a mathematical transport model must include many inter-related complex environmental mechanisms governing the chemical migration and fate phenomena. In addition, the transport model should be combined with a well established, compatible hydrodynamic model. Because of their completeness in formulation and flexibility, the sediment-contaminant transport model(s), SERATRA/TODAM, and the hydrodynamic model, DWOPER, have been combined to simulate the migration and fate of the chemical, diazinon, in the Monticello Ecological Research Station (MERS) channels.

2.1.1 Sediment-Contaminant Transport Model--(TODAM)

Onishi et al. (1976) developed the unsteady two-dimensional (longitudinal and vertical) sediment and contaminant transport model SERATRA

(Sediment-Radionuclide Transport model) as a means of a more realistic prediction of contaminant migration. Onishi, Whelan and Skaggs (1980) simplified SERATRA to the unsteady, one-dimensional sediment and contaminant transport model TODAM (Transient One-Dimensional Degradation and Migration model). The SERATRA/TODAM model is a finite element model that predicts the movement of sediment, chemicals and radionuclides. They use general advection-dispersion equations with decay and sink/source terms and appropriate boundary conditions. The models consist of the following three submodels, coupled to describe sediment-contaminant interaction and migration: 1) a sediment transport submodel, 2) a dissolved-contaminant transport submodel, and 3) a particulate-contaminant (contaminant adsorbed by sediment) transport submodel.

Because the movements and adsorption capacities of sediment vary significantly with size or type, the sediment transport submodel simulates transport, deposition, and resuspension of three size fractions of cohesive and noncohesive sediments. The dissolved-contaminant transport submodel includes mechanisms of adsorption/desorption, as well as decay and degradation resulting from hydrolysis, oxidation, photolysis, volatilization, and biological activity, where applicable. The particulate-contaminant transport submodel simulates transport, deposition, and erosion of contaminants associated with each sediment size fraction.

Adsorption/desorption mechanisms are expressed by a distribution coefficient and a transfer rate that describes how quickly dissolved- and particulate-contaminant concentrations reach their equilibrium condition. These formulations assume that adsorption/desorption mechanisms are completely reversible. However, in reality these mechanisms are not necessarily fully reversible.

SERATRA/TODAM predicts changes of bed conditions for sediment and particulate contaminants, including 1) riverbed elevation changes because of sediment deposition and scour, 2) longitudinal and vertical size distributions of bed sediment, and 3) longitudinal and vertical distribution of particulate contaminant in the riverbed. The model also includes the effects of armoring. Armoring occurs when larger sediment-sized particles in the bed form a protective layer over the smaller particles (Graf 1971).

Input data required by SERATRA/TODAM is fairly extensive and is determined by the modeling scenario. A typical list of input data and simulation output is as follows:

- Common data requirements for all the submodels:
 - channel geometry
 - discharges of tributaries,^(a) overland runoff^(a) and other point and nonpoint^(a) sources
 - longitudinal (TODAM)/vertical (SERATRA) dispersion coefficient
- Additional requirements for hydrodynamic submodel
 - Manning roughness coefficients
 - Initial conditions - depth and velocity distributions
 - Boundary Conditions - depth and/or velocity distributions at the upstream boundary
- Additional requirements for sediment transport submodel
 - sediment size fraction
 - sediment density and fall velocities for sand, silt, and clay
 - critical shear stresses for erosion and deposition of cohesive sediment (silt and clay)
 - erodibility coefficient of cohesive sediment
 - Initial Conditions
 - sediment concentration for each sediment size fraction
 - bottom sediment size fraction distribution
 - Boundary conditions
 - sediment concentration at the upstream end of the study reach
 - contributions of sediments from overland,^(a) tributaries^(a) and other point and nonpoint^(a) sources.

(a) Not considered in this modeling effort.

- Additional requirements for dissolved and particulate contaminant transport submodels
 - Distribution coefficients and transfer rates of contaminant with sediment in each sediment size fraction (i.e., sand, silt, and clay).
 - Degradation and decay rates of contaminants
- Initial conditions
- dissolved contaminant concentration
 - particulate contaminant concentration for each sediment size fraction (i.e., those attached to sand, silt, and clay, etc.)
- Boundary conditions
- dissolved and particulate contaminant concentrations for each sediment size fraction at the upstream end of the study reach
 - contributions of dissolved and particulate contaminant concentrations from tributaries,^(a) overland,^(a) and other point and nonpoint^(a) sources.

With the input data described above, SERATRA/TODAM simulates the following:

1. Hydrodynamic simulation for any given time
 - longitudinal distributions of depth and velocity
2. Sediment simulation for any given time
 - longitudinal distributions of total sediment (sum of suspended and bed load) concentration for each sediment size fraction
 - longitudinal distribution of sediment size fractions in the river bed
 - change in bed elevation (elevation changes due to sediment deposition and/or scour)

(a) Not considered in this modeling effort.

3. Contaminant simulation for any given time

- longitudinal distribution of dissolved contaminant concentration
- longitudinal distribution of contaminant concentration adsorbed by sediment for each sediment size fraction
- longitudinal and vertical distributions of contaminant concentrations in the bottom sediment within the bed for each sediment size fraction.

SERATRA was applied to a large river (the Columbia River--approximately 100-km reach) near the Hanford Site, Washington (Onishi 1977); an intermediate size river (the Clinch River--approximately 37-km reach) near Oak Ridge National Laboratory, Tennessee (Onishi et al. 1979); and very small streams (Four Mile and Wolf Creeks--approximately 68-km reach) in central Iowa (Onishi and Wise 1979). In these cases, SERATRA simulated migration of sediment, radionuclide, and pesticide transport. TODAM has been applied to the Mortandad and South Mortandad Canyons, Los Alamos, New Mexico, (Onishi, Whelan and Skaggs 1980) to simulate the migration and fate of sediment and radionuclides in these canyons, which experience intermittent flows.

The SERATRA/TODAM model(s) has several limitations: 1) it may require extensive input data, which may limit its applicability, 2) it requires extensive computer time, and thus a long-term continuous simulation may be prohibitive, 3) it treats the adsorption/desorption mechanism as completely reversible, and 4) it requires hydrodynamic input from an independent source (e.g., a hydrodynamic model).

In many instances a one-dimensional model (uniform distribution in the vertical and transverse directions) is more applicable than a multi-dimensional model. TODAM is suitable to many rivers and estuaries where vertical and lateral distributions of sediments and contaminants are not a major concern. Because it is a one-dimensional model, it is more compatible with most hydrodynamic codes (which are one-dimensional) than multidimensional models are.

2.1.2 Hydrodynamic Model--(DWOPER)

D. L. Fread (1971, 1973a, 1973b, 1974, 1975, 1976, 1978) of the National Weather Service (NWS) Hydrologic Research Laboratory developed a hydrodynamic routing model based on an implicit finite difference solution of the complete one-dimensional St. Venant equations of unsteady flow. The hydrodynamic model, DWOPER (Dynamic Wave Operational Model), has been implemented on numerous river systems such as the Mississippi, Ohio, Columbia, Missouri, Arkansas, Red Atchafalaya, Cumberland, Tennessee, Willamette, Platte, Kansas, Verdigris, Ouachita, and Yazoo. DWOPER is especially effective in channels in which backwater effects and mild bottom slopes exist. It features the ability to use large time steps for slowly varying floods and to use cross sections spaced at irregular intervals along the river system. The model is generalized for wide applicability to rivers with varying physical features such as irregular geometry, variable roughness parameters, lateral inflows, flow diversions, off-channel storage, and local head losses (e.g., bridge contractions-expansions, lock and dam operations, and wind effects). DWOPER is suited for efficient application to dendritic river systems or to channel networks consisting of bifurcations with weir-type flow into the bifurcated channel. A highly efficient automatic calibration feature determines the optimum roughness coefficients for either a single channel or for a system of interacting channels. It also simulates unsteady flows for purposes of engineering planning, design, or analysis.

DWOPER, however, was not specifically developed for small channels with steep slopes, high flow velocities, and small depths. Under these circumstances the model has difficulty providing meaningful results. Problems appear to be of a convergent type and may be corrected by using a smaller grid size (Ponce 1980). For such cases, a number of other hydrodynamic codes are available. DWOPER is used on the MERS channels because flow velocities are small, slopes are small, a mutual interface exists between TODAM and DWOPER, and results from previous simulations indicate that it is based on a sound methodology.

Input data required by DWOPER is fairly extensive depending on the modeling scenario. Typical data which may be required by DWOPER include:

- General information
 - channel geometry
 - roughness coefficient
 - top width
 - cross-sectional area
 - local head loss coefficients^(a)
 - wind information^(a)
 - weir information^(a)
 - lock and dam information^(a)
 - tributary information^(a)
 - lateral inflow information^(a)
 - discharge
 - stage^(b)
- Initial conditions
 - stage^(c)
 - discharge
- Boundary conditions
 - discharge
 - stage
- Off-channel storage
 - cross-sectional area^(a)
 - stage^(a)
 - top width^(a)

A wide variety of hydrodynamic information can be obtained as output. Most of the data varies spatially and temporally and includes discharge,

(a) Not used in DWOPER for this analysis.

(b) Stage is defined as the elevation or vertical distance of the free surface above a datum (Chow 1959).

(c) Stages were generated via solution of the backwater equation and checked with existing data supplied by MERS' personnel.

velocity, cross-sectional area, flow depth, stage, top width, shear stress, wetted perimeter, etc. Other similar information can relate to storage areas and tributaries.

TODAM and DWOPER are combined in a systematic manner to methodically handle the initial and upstream boundary conditions. For given hydraulic conditions, DWOPER simulates the instream hydrodynamics and supplies the discharge, flow area, flow depth, and shear stress at these locations to TODAM. TODAM completes the in-stream contaminant modeling scenario. As discussed in Chapter 3, this scenario consists of modeling two different channels with different concentrations of diazinon supplied at the upstream boundary. Channel 6, the calibration channel for the model simulation, has an initial inflow concentration of $3.10 \mu\text{g/l}$. Channel 7, the testing/validation channel, has an inflow concentration of $0.31 \mu\text{g/l}$. TODAM supplies the risk-assessment model FRANCO with spatially and temporally varying sediment and contaminant concentrations.

These models are implemented on the Digital VAX/VMS 11/780 computer system and employ standard FORTRAN as the basic language.

2.2 RISK ASSESSMENT

A key component of the CMRA methodology is the transition from the in-stream simulated diazinon concentrations to the assessment of the potential risk. This specific task is completed by the computer code FRANCO (Olsen and Wise 1979). FRANCO supplies a statistical summary of time-varying concentrations and provides the frequency of occurrence and the duration of given diazinon concentrations at specified locations in the channel. Output includes the number of times a given concentration-duration level is exceeded, the length of such incidents, and the concentration levels involved.

The concentration levels and duration times used in the summary are selected to include the actual concentrations simulated in the stream and the median lethal concentration (LC50) and maximum acceptable toxicant concentration (MATC) levels for biota of interest. Where the available data permits, LC50 values are used to define piecewise linear concentration-duration curves. FRANCO provides summaries of the number of times, the length, and the frequency

a given concentration-duration curve is exceeded. In addition to the summary information, each time a diazinon concentration peak exceeds a concentration-duration curve, it may be selected for more detailed analysis by the researcher.

The assessment of risk is generally defined as being equal to the probability of the event multiplied by the consequential effects:

$$\text{Risk} = \text{Probability} \times \text{Consequences}$$

In the CMRA methodology, the FRANCO program provides a statistical probability in terms of the frequency and duration of given concentrations. Consequences of a given exposure to a toxicant are predicted largely from surveying laboratory toxicity data and taking into consideration any unusual chemical properties of the toxicant. The CMRA provides procedures for constructing a concentration-duration curve and describes a method for interpreting toxicological data to define discrete consequence zones of lethality, possible lethality, sublethality, and no effect (see Onishi et al. 1979). These procedures allow the researcher to predict consequences when given a concentration-duration pair representative of toxicant exposure.

The assessment is currently limited to the direct effects of the dissolved form to the chemical. Ingestion as a secondary route is not addressed, nor are indirect effects such as bioconcentration or biomagnification.

LC50 values are used predominately to indicate short-term (acute) lethality to the organisms of interest. The LC50, with its associated duration, is defined as the concentration of a toxicant at which 50% of a given species is killed upon exposure of a stated duration. As a common parameter in aquatic toxicity testing, LC50s estimate the median lethal concentration for the population. When sufficient information exists, a series of time intervals such as 24-, 48-, 96-, and 192-hr LC50 and longer times can be used to form an LC50 concentration-duration curve.

The effect-no effect indicator used by the methodology is the MATC. Long-term sublethality (chronic toxicity) is assumed here to be bounded at the lower

end by the MATC (or the MATC range). Concentrations greater than the MATC may result in a toxic response; values below the MATC presumably will not. Where an MATC has not been generated for the species of concern, it may be possible to use other chronic data or an application factor to estimate an MATC (Eaton 1973).

By selecting specific LC50 concentration-duration levels and the MATC values for the FRANCO analysis, assessment of probable risk can be broken down into concentrations that are projected to be safe and those that may cause acute or chronic toxicity (Figure 2.2).

While this simplified approach is very useful for comparing various chemicals or for determining whether concentrations exceed known thresholds, the results must be evaluated with regard to factors such as water quality, life stages and food sources of the organisms, bioconcentration, and biomagnification to obtain a realistic risk assessment.

RISK ASSESSMENT

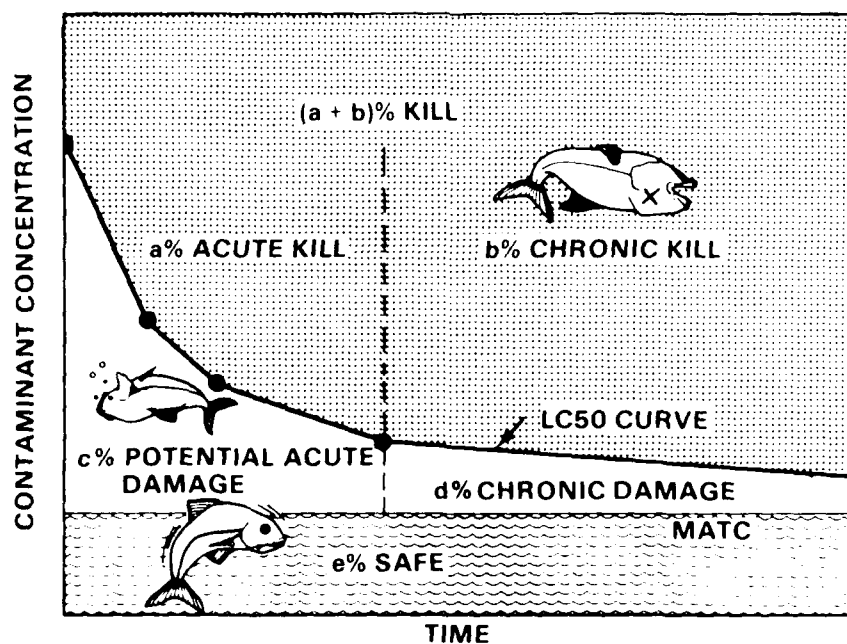
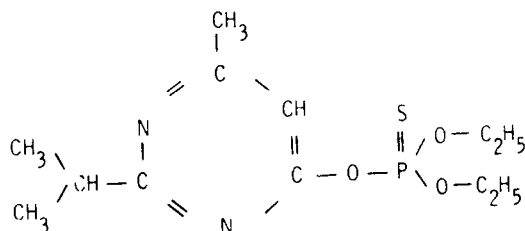


FIGURE 2.2. Summary of Toxicity Curves

3.0 APPLICATION OF THE METHODOLOGY

The U.S. Environmental Protection Agency's Environmental Research Laboratory-Duluth chose the pesticide diazinon for study during the summer of 1980 at the Monticello Environmental Research Station. Diazinon is a widely used insecticide and nematicide that may be found in surface waters from farmland or rangeland runoff. Its biologically effective life in water appears to depend on the pH, abundance of suspended solids, and aerobic/anaerobic condition of the water. These factors determine the variability of diazinon hydrolysis and degradation in water. A half-life of less than two weeks at pH 6.0 has been recorded by Cowart et al. (1971) and of six months at pH 7.4 and four months at pH 9.0 by Gomaa et al. (1969). Degradation is accelerated in aerobic conditions and is inhibited by the presence of suspended solids (Sethunathan and Pathak 1972). Diazinon is an organophosphate:



0,0 - Diethyl 0-(2-isopropyl-4-methyl-6-pyrimidinyl) phosphorothioate

Its water solubility at 20°C is 40 mg/l and it has an octanol/water partition coefficient of about 15 (Dawson et al. 1980).

Diazinon is not a long-lasting pesticide and is not likely to contaminate the sediments long enough to reduce the utility of the Monticello channels. It is toxic to fish at low to moderate levels and to invertebrates at relatively low levels. Its use required a National Pollution Discharge Elimination Systems (NPDES) permit, which EPA obtained for a maximum discharge of 2.7 µg/l of diazinon.

EPA's diazinon study made use of three of the eight 1700-ft channels (Channels 6, 7, and 8) at MERS in Monticello, Minnesota. The channels originally

were constructed for the investigation of effects of thermal pollution to aquatic life utilizing waste heat discharges from the nearby Monticello Nuclear Generating Plant.

The channels consist of alternating 100-ft (30.48 m) sections of deep pools that are about 12 ft (3.66 m) wide and shallow riffles about 4-1/2 ft (1.4 m) wide. There are nine pools and eight riffles in each channel. The approximate geometry of the pool sections is parabolic or trapezoidal. The riffle sections are constricted areas used to increase the flow velocity. They are also trapezoidal and were originally formed by 38 mm (1.5 in.) diameter gravel placed in the channel. As the water stage can be controlled by the bulkhead at the end of each channel, the water depths and surface widths can also be changed. The channels are arranged in pairs, separated by a high berm. Locations in the channel are identified beginning with the number one (1) assigned to the inlet, number two (2) to the first pool, number three (3) to the first riffle, and so forth, up to the outlet, which is designated as number nineteen (19). The first riffle in the study section in Channel 6 is identified as 603; the following pool is 604 (see Figure 3.1). There are, therefore, seventeen channel sections consisting of nine pools and eight riffles. Channels 6 and 7 are illustrated in Figure 3.1. Locations in the channel are designated by the "channel" and the corresponding "section" number. The water filling the channels was pumped from the Mississippi River and introduced into the channels at the first pool, which was used as a settling basin and an upstream barrier. Water flowing through the experimental channels was discharged back to the Mississippi River.

EPA concentrated its study in a 305-ft upstream section of Channels 6, 7, and 8. Each section consists of two 100-ft riffles, the connecting 100-ft pool, and a 5-ft pool between the downstream riffle and the downstream stainless-steel-screen fish barrier. The pools are mud-bottomed and the riffles were constructed with 3/4- to 2-in. diameter gravel. The riffles had been spaded in the fall to reduce silt in these sections. Depending on the time of year, the MERS channels experience various degrees of macrophyte growth. In late March/early April, the channels are relatively free of obstructions, while in June and through the summer the channels usually experience heavy macrophyte growth.

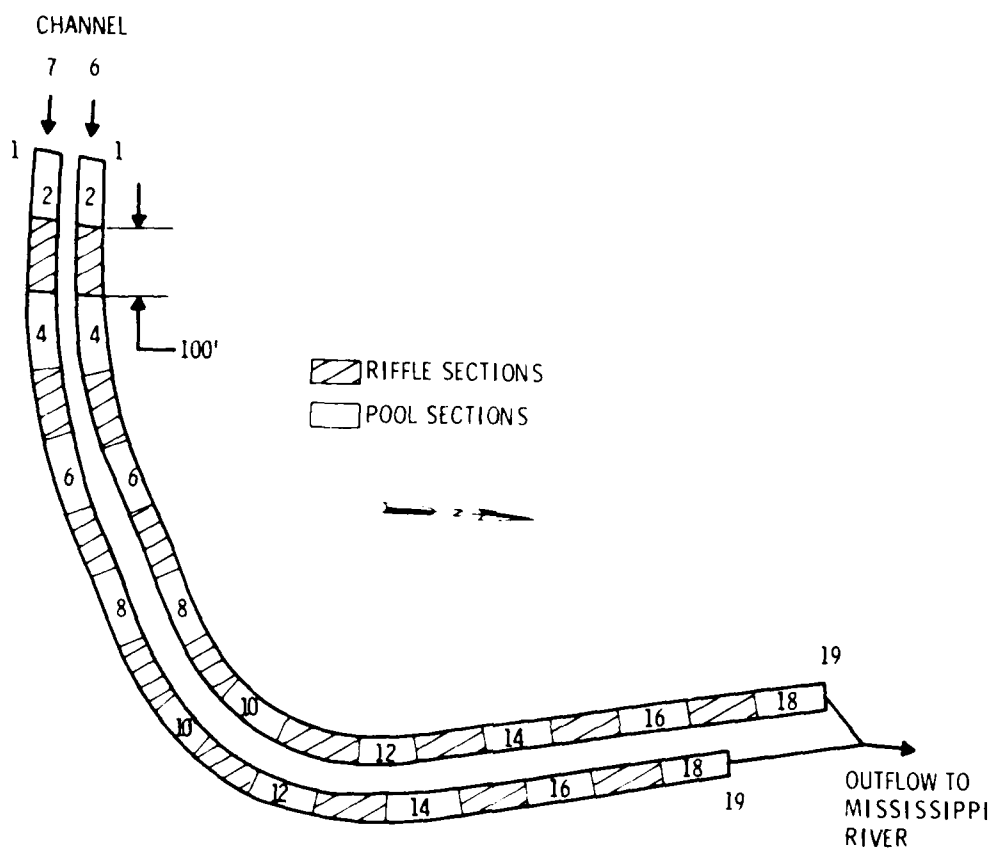


FIGURE 3.1. Layout of Channels 6 and 7 (Gulliver 1977; Stefan 1980)

Shade structures of polypropylene mesh on wooden A frames were erected in EPA's study area to reduce the growth of aquatic plants. The shade modules reduced the available light at the waters surface 70% to 75% under the modules. No shading was provided for the remainder of each channel.^(a)

Technical grade diazinon made by Ciba-Geigy Corporation was mixed in two covered, insulated fiberglass tanks protected by a wooden shed. Temperatures

(a) Hermanutz et al. 1980. "Diazinon's Effects on Populations in MERS Channels," 1980 In-House Work Plan, Monticello Ecological Research Station, January 1980.

were maintained between 4° and 10°C to reduce diazinon degradation. The diazinon solution was metered through industrial grade pumps and delivered to Channels 6 and 7 through PVC tubing. The concentration in Channel 6 was controlled at about 3 µg/l, Channel 7 at 0.3 µg/l. Channel 8 served as the control channel.

EPA chose the fathead minnow Pimephales promelas for the study species. Each channel was stocked with 500 juvenile fathead minnows on May 2, 1980. Two weeks before stocking, water flows were turned off and the channels were treated with rotenone to eliminate fish in the channels without damaging the invertebrate populations. In addition to the above free-roaming fish, three cages with a total of 200 minnows per channel were placed in the first pool within the study area. About 10% of the free-swimming fish were randomly selected to be weighed and measured for EPA's study. Box traps were set up to collect fish weekly for abundance and growth studies.

In addition to the fish study, EPA conducted a macroinvertebrate investigation to study the effects of diazinon on growth, abundance, distribution, and reproduction of the common species in the community.

3.1 FIELD SAMPLING

The computer modeling required several field data points on which to base predictions of dissolved diazinon concentrations in the water and adsorbed onto the suspended and bed sediments. Other required information included hydrologic data on the channel width, depth, roughness (Chow 1959, Henderson 1966), flow rate, and elevation drop. Information required on chemical properties included the diazinon solubility constant in water, the rate of sediment adsorption/desorption and the rate of its evaporation and degradation. This information is provided and discussed in Sections 3.1.2 through 3.3.11.

The toxicological assessment required data concerning the organisms in the channels--what species existed in what abundance, whether they were able to leave the affected areas, what their toxic reaction levels were, how the diazinon affected them, and how much diazinon uptake they were responsible for. The field-sampling techniques and strategies were divided into water, sediment, biological sampling, and channel characteristics.

3.1.1 Water Sampling

Water samples were collected in amber glass gallon jugs for analysis. EPA concentrated on the first two riffles and one pool in each channel where the fathead minnows were confined. Additional samples were routinely taken in the second pool, at a mid-point pool or riffle, and at the downstream end of the channel. A control sample from Channel 8 of the water without diazinon addition was measured during each analysis. Grab samples were generally taken at a mid-point in width and depth in the riffles. Pools were sampled near the center width at the mid-point. Most pool samples were taken at mid-depth.

Diazinon addition began Wednesday, May 14, 1980 at 11 a.m. The upper riffles (603, 703), main pool (604, 704), lower riffles (605, 705), a mid-point pool (612, 712), and the downstream end of the last riffle (617, 717) were sampled at 12 a.m., 1 p.m., 3 p.m., 7 p.m., and 11 p.m. on that first day. Riffle 603 and pool 712, for example, correspond to the 3rd section of Channel 6 and the 12th section of Channel 7. This frequent sampling was done to confirm the solution/dissolution/dispersion of the diazinon in the channels.

Sampling continued once a day for the next two days on at least the first riffle and pool and at the channel discharge. Sampling (at a reduced rate) continued through July, and the first two riffles and the first pool were analyzed about once a week. Vertical and transverse profile samples were collected periodically for pools 604 and 704. Because the diazinon addition rate changed in August, we will limit the discussion of the analysis to May 14 through the end of July.

3.1.2 Sediment Sampling

Bed sediment samples from the gravel-bottom riffles were collected several hours before diazinon addition (May 14) and again on May 15. They were collected one week later and then during the middle of June and the middle of July. Sampling of the riffle sediments from 603 and 605, and 703 and 705 was accomplished by scooping up some of the riffle surface and carefully collecting attached clay from the gravel by stirring and pressing it off the gravel surfaces. The resulting slurry was allowed to settle and the sediment-free portion was decanted. The remaining sediment (muddy water) was transferred to a glass jar.

Pools 604, 704, 612, and 712 were sampled with the same frequency as the riffles. These samples were taken near the center (in length and width) of the pools using wide-mouth glass jars to collect the cores. It was decided that a more precise measure of sample depth was desirable so plastic cores were taken in pool 606 to a depth of 4 in. to collect and separate sequential sediment depths. Previous experimentation determined that diazinon did not adhere to the plastic.

Suspended sediment was not easy to sample or analyze. Because the water had very little turbidity, collecting enough water for diazinon analysis would have required a centrifuge that could pass a large volume of water in a reasonable period of time. This type of centrifuge was not available. Instead, we used the clay fraction in the bed sediment samples to approximate the adsorption of diazinon in the suspended solids. Turbidity measurements were taken on an influent sample daily for several weeks and then as often as samples were collected. An experiment to determine the correlation of turbidity to suspended solids yielded a curve that we used to approximate suspended solids.

3.1.3 Biological Sampling

Fathead minnows free-roaming within the study sites were sampled weekly to determine growth and abundance. Box traps were placed in the main pools (604, 704, 804) of each channel to collect first generation fish for these measurements. Drift nets were used to collect second generation larvae that were drifting downstream. The larvae had passed from the study area through the screen that prevented downstream escape of juveniles and adults. Box traps were also set up periodically in the study sections to collect only second generation juveniles. The number of eggs was sampled by counting the eggs on the plywood spawning substrates set into the channels for this use. The condition of the eggs was noted.

Each month the stomachs of 10 random adult fatheads were examined and the contents identified. Throughout the experiment, all fish collected were examined for morphological aberrations or other symptoms of disease.

Invertebrate samples were collected to determine the distribution, abundance, growth, and reproduction of the channel communities. Benthic samples

were collected from each of the three pools with an Ekman grab sampler. These samples were collected once a month during the season and weekly during the period of peak drift abundance. Emerging adult insects were collected weekly in plexiglass traps.

3.1.4 Water Analysis

Water sample analysis was conducted onsite by EPA-Monticello staff. These samples were analyzed for diazinon, alkalinity, acidity, total hardness, specific conductivity, pH, turbidity, and temperature. The diazinon in the samples was extracted with petroleum ether within a couple of hours of sample collection. The extracted diazinon solutions, which were stable, were analyzed using a Hewlett Packard 5840 gas chromatograph with an electron capture detector. Diazinon recovery in a spiked sample was monitored each day that samples were analyzed. EPA-Duluth ran quality control checks on the water samples and determined that the reported diazinon concentrations showed a recovery of 96% to 99%.

3.1.5 Sediment Analysis

The EPA-Duluth staff analyzed the sediment samples and was faced with several anticipated and unforeseen difficulties. Preliminary testing of extraction procedures, size fractioning, and degradation in storage had not been possible prior to the start of the experiment as it was not originally scheduled by EPA and was done solely in support of this document. Time spent resolving these concerns delayed analysis of certain samples, and trial runs depleted the sample supply. Consequently, there was considerable support documentation and few sediment diazinon data points generated.

After sample collection, some of the samples were stored in a refrigerator; most were freeze dried in liquid nitrogen. Several of the samples were separated into sand, silt and clay fractions to establish the distribution coefficient associated with each fraction. Where possible, macrobiological matter was removed before the samples were analyzed.

Steam distillation was used to extract diazinon from the sediment because it proved more efficient, sensitive, was subject to less interference, and did not present a carryover problem as did soxhlet extraction. The extract was

analyzed using an HP 5736 gas chromatograph with a 6 ft by 2 mm inside diameter column packed with 1.95% OV 17 and 1.5% OV 210 on 100 to 120 mesh chromosorb W. The HP nickel 63 detector temperature was set at 300°C. The injection port temperature was 200°C and the column temperature was set at 185°C.

3.1.6 Channel Characteristics

The channels were constructed to be as nearly identical as possible. Measurement of the width and depth of each section required wading into the pools. To prevent the stirring of sediment, which could affect the partitioning of diazinon in the experimental channels, the control channel (No. 8) was measured, and we assumed that these measurements would closely approximate those of Channels 6 and 7. The width of each section was taken at the water line. Various width measurements were taken on the upstream sections until it was noted that the width within each pool and riffle was nearly uniform. Depth was measured at the center of each riffle and pools were measured at the center, and in some cases, at several other points within the pool. The rest of the points essential for modeling, but not determined by the sampling team, were computed by extrapolating from the known values. The channels became narrower and filled with vegetation toward their downstream end.

Other necessary measurements (e.g., flow rates) were taken with instruments that measured such parameters. The water surface elevation drop from the channel inlet to its outlet was estimated, and channel roughness was estimated from information provided by previous investigators (Hahn 1978; Hahn et al. 1978a; 1978b).

3.1.7 Degradation Studies

It was not possible to analyze each aspect of diazinon degradation (e.g., due to oxidation, hydrolysis, photolysis, and biological activities) and volatilization due to time constraints. While this type of information could have been used by the computer submodels, a degradation breakdown fortunately was not required for the modeling efforts. The situation was complicated by the shading that had been erected over the EPA study area to reduce the algae blooms. To help approximate degradation, EPA collected channel water in two 5-gal jugs and set one in the sun and one in the shade. These were sampled

periodically during the study. A rough estimate of the overall degradation rate in the channels was computed and compared with published values (Dawson et al. 1980). These samples were not sterilized.

3.2 MODEL CALIBRATION

To provide an accurate assessment of the migration and fate of diazinon, a fairly large data base is required for the implementation of the hydrodynamic and contaminant transport models (i.e., DWOPER and TODAM, respectively) used in the study (Section 2.1). Within this data base, hydrodynamic, sediment, and contaminant characteristics are very important. The sediment and contaminant transport model TODAM depends to a large extent on the hydrodynamic results of DWOPER which in turn depends on channel and flow characteristics. An incorrect hydrodynamic simulation may prove costly in accurately assessing the migration of diazinon using TODAM. The fate of a contaminant in a water body depends on sediment characteristics and the characteristics inherent to the specific contaminant. Identifying the nature of the in-stream sediments (such as particle size, fall velocity, specific gravity, etc.) is important because cohesive sediments and organic material have a greater affinity for diazinon than do the noncohesive sediments (Section 3.2.2). In addition, the characteristics inherent to diazinon (such as degradation rate, etc.) play an important role in determining its fate. It, therefore, becomes important to define the hydrodynamic, sediment, and contaminant characteristics as accurately as possible.

3.2.1 DWOPER Calibration

Flow rates in each channel are controlled and metered in the control room of a laboratory building on the MERS grounds. V-notch weirs are installed at the head (inlet) of each channel and are available for installation at the end of each channel. The maximum design flow for a channel is on the order of $1.4 \text{ ft}^3/\text{s}$ ($0.04 \text{ m}^3/\text{s}$).

Numerical Modeling Representation

To numerically model any site, its geometry has to be interpreted for the computer. Channels 6 and 7 were each divided into 44 channel sections. The location of the computation nodes are illustrated in Figure 3.2. A distance

of 33-1/3 ft between the nodes was chosen because of the alternating pools and riffles that compose the channel. The smaller channel section lengths (33-1/3 ft) insure convergence of the modeling effort. The abrupt geometrical change from the pool to the riffle and from the riffle to the pool was represented by a linear approximation. Figure 3.3 illustrates the effect this interpretation has on the channel's geometry. The dotted line represents the approximation and the solid line represents the original channel shape. As Figure 3.3 shows, the channel's longitudinal geometry is changed very little. Because the slopes are mild and the velocities are small, expansion and contraction losses are ignored. Employing this representation should pose no problem since these losses are negligible (Hahn 1978; Hahn et al. 1978a; 1976).

The extreme upstream and downstream pools (sections 2 and 18, respectively) were omitted from the modeling effort. The extreme upstream pool was omitted because this preceded the diazinon addition. Modeling the inflow portion of the channel was unnecessary because no pertinent information would have been obtained. The extreme downstream pool (section 18) was ignored for several reasons: it appeared that section 17 was close to being a critical section;^(a) the slope in section 18 was very steep relative to the upstream sections thereby creating numerical problems with the hydrodynamic code DWOPER; and very little information would have been gained by including section 18 in the modeling effort since section 17 represented the furthest downstream section to be sampled for diazinon.

Data Preparation and Assumptions

To perform hydrodynamic and contaminant transport modeling, information regarding the channel and the flow properties are required. The available data supplied by MERS personnel included:

- an estimated drop in the water-surface elevation of 0.6 ft
- the effective flow area top widths of three pools and five riffles

(a) A critical section exists when the Froude number (i.e., the ratio between inertial and gravitational forces) equals unity.

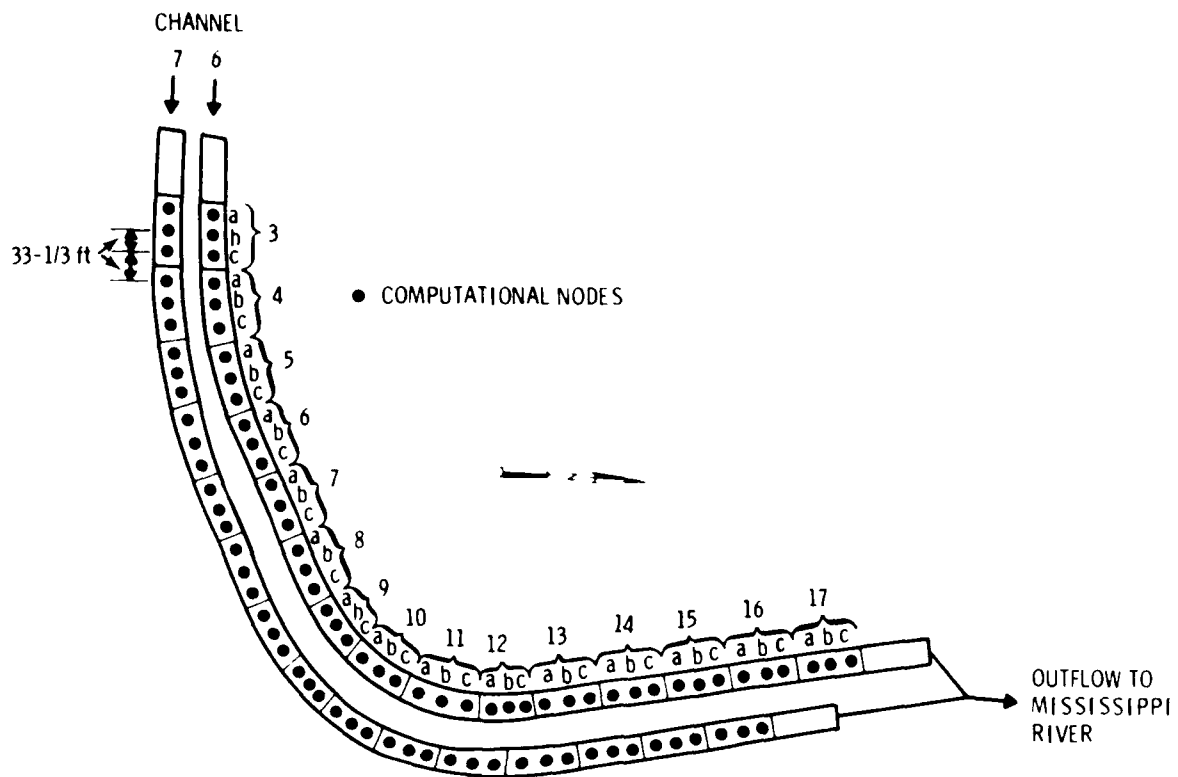


FIGURE 3.2. Plan View of Channels 6 and 7 with Computational Nodes Included (Gulliver 1977; Stefan 1980)

PLAN VIEW

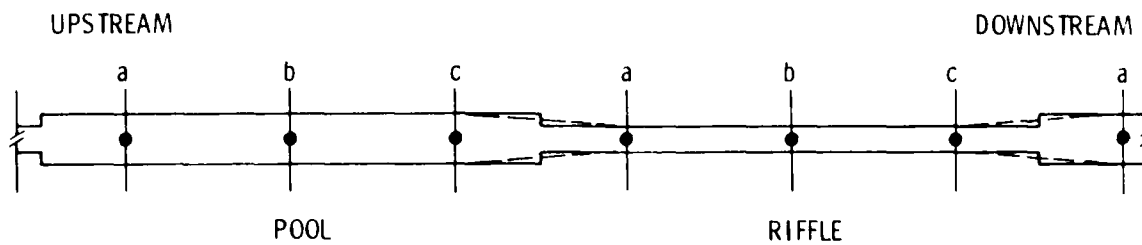


FIGURE 3.3. Representation of Pool-Riffle Configuration

- at least one effective flow depth for each pool and riffle (Within the study area--sections 3, 4, 5, and 6--at least three depths were provided for each section.)
- a discharge equaling $0.445 \text{ ft}^3/\text{s}$ ($0.013 \text{ m}^3/\text{s}$).

Data that were not measured included:

- water-surface slopes for each channel section
- cross-sectional information pertaining to the entire cross section (It should be noted that the banks of the channel were not defined or included in any data provided. The exact location of the known depths and widths is unknown with respect to the banks of the channel. The actual shapes of the channels are therefore unknown.)
- flow velocities
- values for the roughness coefficient
- bed slopes
- storage areas.

To develop reasonable cross-sectional shapes for each node, the available data were used as a guide for estimating these shapes. In addition, several assumptions were made:

- All pools in all channels at MERS can be represented by one generic cross-sectional shape.
- All riffles in all channels at MERS can be represented by one generic cross-sectional shape.
- The largest depth measured at a location closest to each node for each section represents the depth of flow for that node in that channel section.
- Friction slopes provided by other investigators for these channels are on the same order of magnitude as this modeling study. (This assumption provides a mechanism for calculating the roughness of each channel.)
- A monotonic relationship exists between flow discharge and flow area.

From these assumptions the cross-sectional areas, top widths, flow depths, and wetted perimeters for each channel location can be calculated a priori.

Channel Geometry

Generic cross-sectional shapes based on average cross sections as provided by Hahn (1978), Gulliver (1977), and Hahn et al. (1978a; 1978b) were used in this study. Figure 3.4 presents the average pool cross-sectional shape, while Figure 3.5 presents the average riffle cross-sectional shape. These cross sectional shapes were representative of Channel 1 in a 1977 study.

All pertinent cross-sectional data obtained were based on these figures. Given the depth of flow for a channel section and the nodes composing that section, the top flow width and cross-sectional area can be computed. Table 3.1 presents a summary of the hydraulic conditions existing in Channel 8 at the

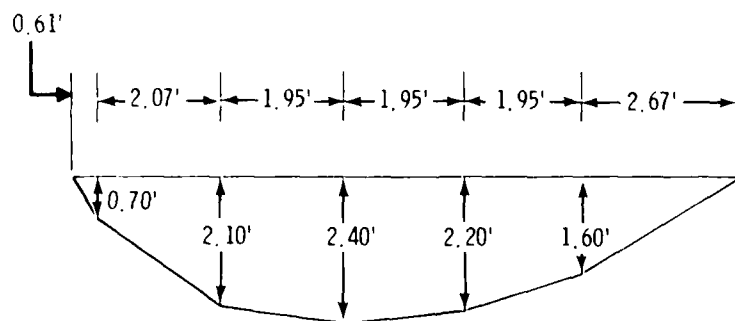


FIGURE 3.4. Average Pool Cross-Sectional Shape

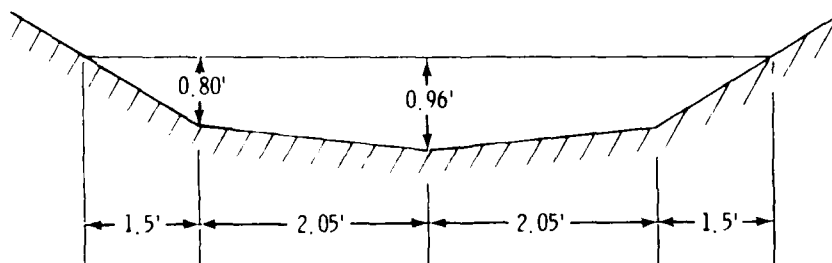


FIGURE 3.5. Average Riffle Cross-Sectional Shape

TABLE 3.1. Channel Geometry and Hydrodynamic Information

(1) Section	(2) Depth (ft)	(3) Top Width (ft)	(4) Area (ft ²)	(5) Computed Mannings Coefficient	(6) Assumed Friction Slope	(7) Averaged Friction Slope	(8) Distance Between Nodes (ft)	(9) Head Loss (ft)	(10) Stage (Assumed) (ft)	(11) Stage (Computed) (ft)
803a	0.492	5.328	1.877	0.0634	0.00043	0.00043	33.333	0.0143	10.000	9.979
803b	0.492	5.328	1.877	0.0634	0.00043	0.00043	33.333	0.0143	9.985	9.962
803c	0.492	5.328	1.877	0.0634	0.00043	0.00024	33.333	0.0080	9.971	9.946
804a	2.198	10.687	15.608	0.4424	0.00005	0.00005	33.333	0.0017	9.963	9.945
804b	2.001	10.186	13.553	0.3629	0.00005	0.00005	33.333	0.0017	9.961	9.944
804c	1.869	9.849	12.229	0.3139	0.00005	0.00024	33.333	0.0080	9.960	9.942
805a	0.574	5.636	2.326	0.0870	0.00043	0.00043	33.333	0.0143	9.952	9.935
805b	0.574	5.636	2.326	0.0870	0.00043	0.00043	33.333	0.0143	9.937	9.920
805c	0.574	5.636	2.326	0.0870	0.00043	0.00024	33.333	0.0080	9.923	9.905
806a	2.100	10.436	14.568	0.4017	0.00005	0.00005	33.333	0.0017	9.915	9.904
806b	2.100	10.436	14.568	0.4017	0.00005	0.00005	33.333	0.0017	9.913	9.903
806c	2.100	10.436	14.568	0.4017	0.00005	0.00024	33.333	0.0080	9.912	9.901

TABLE 3.1. (contd.)

(1) Section	(2) Depth (ft)	(3) Top Width (ft)	(4) Area (ft ²)	(5) Computed Manning's Coefficient	(6) Assumed Friction Slope	(7) Averaged Friction Slope	(8) Distance Between Nodes (ft)	(9) Head Loss (ft)	(10) Stage (Assumed) (ft)	(11) Stage (Computed) (ft)
807a	0.656	5.945	2.800	0.1140	0.00043	0.00043	33.333	0.0143	9.904	9.895
807b	0.656	5.945	2.800	0.1140	0.00043	0.00043	33.333	0.0143	9.889	9.880
807c	0.656	4.945	2.800	0.1140	0.00043	0.00024	33.333	0.0080	9.875	9.867
808a	1.968	10.100	13.211	0.3501	0.00005	0.00005	33.333	0.0017	9.867	9.866
808b	1.968	10.100	13.211	0.3501	0.00005	0.00041	33.333	0.0017	9.865	9.864
808c	1.968	10.100	13.211	0.3501	0.00005	0.000405	33.333	0.0135	9.864	9.863
809a	0.558	5.575	2.234	0.1090	0.00076	0.00076	33.333	0.0253	9.851	9.855
809b	0.558	5.575	2.234	0.1090	0.00076	0.0076	33.333	0.0253	9.826	9.831
809c	0.558	5.575	2.234	0.1090	0.00076	0.00076	33.333	0.0183	9.800	9.809
810a	1.672	9.331	10.338	0.6453	0.00034	0.00034	33.333	0.0113	9.782	9.808
810b	1.739	9.519	10.973	0.7018	0.00034	0.00034	33.333	0.0113	9.771	9.800
810c	1.672	9.331	10.338	0.6453	0.00034	0.00055	33.333	0.0183	9.759	9.789

TABLE 3.1. (contd.)

(1) Section	(2) Depth (ft)	(3) Top Width (ft)	(4) Area (ft ²)	(5) Computed Mannings Coefficient	(6) Assumed Friction Slope	(7) Averaged Friction Slope	(8) Distance Between Nodes (ft)	(9) Head Loss (ft)	(10) Stage (Assumed) (ft)	(11) Stage (Computed) (ft)
811a	0.492	5.328	1.877	0.0843	0.00076	0.00076	33.333	0.0253	9.740	9.750
811b	0.492	5.328	1.877	0.0843	0.00076	0.00076	33.333	0.0253	9.715	9.727
811c	0.492	5.328	1.877	0.0843	0.00076	0.00055	33.333	0.0183	9.689	9.706
812a	1.672	9.331	10.338	0.6453	0.00034	0.00034	33.333	0.0113	9.671	9.705
812b	1.672	9.331	10.338	0.6453	0.00034	0.00034	33.333	0.0113	9.660	9.697
812c	1.672	9.331	10.338	0.6453	0.00034	0.00055	33.333	0.0183	9.648	9.687
813a	0.361	4.834	1.211	0.0436	0.00076	0.00076	33.333	0.0253	9.630	9.642
813b	0.460	5.204	1.704	0.0730	0.00076	0.00076	33.333	0.0253	9.605	9.632
813c	0.329	4.710	1.055	0.0353	0.00076	0.00055	33.333	0.0183	9.579	9.594
814a	1.477	8.718	8.582	0.4972	0.00034	0.00034	33.333	0.0113	9.561	9.593
814b	1.477	8.718	8.582	0.4972	0.00034	0.00034	33.333	0.0113	9.550	9.585
814c	1.477	8.718	8.582	0.4972	0.00034	0.00055	33.333	0.0183	9.538	9.576

TABLE 3.1. (contd.)

(1) Section	(2) Depth (ft)	(3) Top Width (ft)	(4) Area (ft ²)	(5) Computed Mannings Coefficient	(6) Assumed Friction Slope	(7) Averaged Friction Slope	(8) Distance Between Nodes (ft)	(9) Head Loss (ft)	(10) Stage (Assumed) (ft)	(11) Stage (Computed) (ft)
815a	0.262	4.460	0.750	0.0208	0.00076	0.00076	33.333	0.0253	9.520	9.526
815b	0.262	4.460	0.750	0.0208	0.00076	0.00076	33.333	0.0253	9.495	9.504
815c	0.262	4.460	0.750	0.0208	0.00076	0.00055	33.333	0.0183	9.469	9.486
816a	1.477	8.718	8.582	0.4972	0.00034	0.00034	33.333	0.0113	9.451	9.485
816b	1.477	8.718	8.582	0.4972	0.00034	0.00034	33.333	0.0113	9.440	9.477
816c	1.477	8.718	8.582	0.4972	0.00034	0.00055	33.333	0.0183	9.428	9.467
817a	0.153	3.745	0.285	0.0047	0.00076	0.00076	33.333	0.0253	9.410	9.410
817b	0.153	3.745	0.285	0.0047	0.00076	0.00076	33.333	0.0253	9.385	9.385
817c	0.153	3.745	0.285	0.0047	0.00076	0.00076	33.333	0.0253	9.360	9.360

time of the experiment. Column 1 identifies the section and the nodes composing the section. Figure 3.2 identifies the location of each section number. Column 2 identifies the depth at each location along the channel, as reported by the MERS personnel. If only one depth existed for a channel section (e.g., Section 6 of Channel 8), all three nodal locations were assumed the same depth. Based on this depth, the top width and cross-sectional area are presented in columns 3 and 4, respectively, for each channel section. The diazinon modeling was performed on Channels 6 and 7, whereas the channel measurements were made on Channel 8; the averaged cross sections are representative of Channel 1.

Representative Roughness and Stage Computations

To perform the hydrodynamic simulation of the channels at MERS, the slopes, the roughness coefficients, and the initial stage at the downstream boundary had to be estimated. (These parameters were unavailable for the channel sections.) The stage at the downstream boundary can be computed if the water surface slopes or the roughness coefficients are known at each node. Since data pertaining to these variables were not directly available, the information supplied by Hahn (1978) and Hahn et al. (1978a; 1978b) was used as a guide. This information is presented in Tables 3.2, 3.3, and 3.4. The information in these tables represents three different time periods with three different discharges: Table 3.2 represents a channel that was fairly free of macrophyte growth; Table 3.3 represents a channel with light macrophyte growth; and Table 3.4 represents a channel with heavy macrophyte growth.

Based on the information provided in these three tables, either the water surface slope or the roughness coefficient for each node can be assumed. For this modeling effort the water surface slope was assumed as the independent variable. The roughness coefficient was not chosen because:

1. If the friction slope is calculated from an assumed roughness coefficient, the head loss for any given section may be unrealistic. (The total head loss for the channel has to be approximately 0.6 ft.)
2. The roughness coefficient is difficult to assess because the degree of macrophyte growth plays such an important role in its determination. This is especially true of the one-dimensional case because storage areas are also included in the computations.

TABLE 3.2. Water Surface Slopes, Cross-Sectional Areas, Wetted Perimeters, and Roughness Coefficients of Channel 1 on April 6, 1977 (Q = 1.25 ft³/sec) (Hahn 1978)

Station	Slope (ft/ft)	Area (ft ²)	Wetted Perimeter (ft)	Mannings Roughness Coefficient
3	0.000591	3.4	7.0	0.061
4	0			
5	0.000210	4.0	6.7	0.049
6	0			
7	0.000469	4.0	7.1	0.070
8	0.000231			
9	0.000436	3.3	6.7	0.051
10	0			
11	0.000312	3.2	6.3	0.043
12	0			
13	0.000469	3.0	6.2	0.048
14	0.0000526			
15	0.000469	3.2	6.3	0.053
16	-			
17	0.001052	2.3	5.6	0.049

3. The water surface slope at most sections (see Tables 3.2, 3.3, and 3.4) is provided, whereas the roughness coefficient is not.
4. The average water-surface slope in the simulated channel is approximately 0.00041, based on a drop in elevation of 0.6 ft over a distance of 1466.67 ft. This value is similar to the water-surface slopes measured and provided in Tables 3.2, 3.3, and 3.4. The discharge provided in these tables is not the same as the discharge in this study. As only an estimate of parameters is sought, this should pose no problem.

Because the biological sampling for the risk assessment aspect of the modeling effort was confined to the upstream portion of the channels, the channel information (as provided by Tables 3.2, 3.3, and 3.4) was divided into an

TABLE 3.3. Water Surface Slopes, Cross-Sectional Areas, Wetted Perimeter, and Roughness Coefficients of Channel 1 on April 18, 1977 (Q = 1.13 cfs) (Hahn 1978)

<u>Station</u>	<u>Slope (ft/ft)</u>	<u>Area (ft²)</u>	<u>Wetted Perimeter (ft)</u>	<u>Mannings Roughness Coefficient</u>
3	0.000537	3.4	7.0	0.064
4	0			
5	0.000263	4.0	6.7	0.061
6	0.000104			
7	0.000208	4.0	7.1	0.052
8	0.000116			
9	0.000436	3.3	6.7	0.057
10	0.0000531			
11	0.000312	3.2	6.3	0.047
12	0			
13	0.000573	3.0	6.2	0.058
14	0			
15	0.000260	3.2	6.3	0.043
16	0.000104			
17	0.000210	2.3	5.6	0.024

upstream group and a downstream group. The upstream group consisted of sections 3 through 8, while the downstream group consisted of sections 9 through 17. By dividing the channels into regions, each region could reflect the characteristics of the channel more accurately. In addition, the water surface slopes were divided according to pools and riffles because significant differences exist between the two. Based on these assumptions, the friction slope for the upstream pools was calculated by averaging the upstream pool friction slopes provided in Tables 3.2, 3.3, and 3.4. The friction slope for the downstream pools was calculated by averaging the downstream pool friction slopes provided in Tables 3.2, 3.3, and 3.4. The friction slopes for the riffles were calculated in a similar manner. The friction slopes assumed for this modeling effort are:

TABLE 3.4. Water Surface Slopes, Cross-Sectional Areas, Wetted Perimeters, and Roughness Coefficients for Channel 1 on June 15, 1977 (Q = 1.34 ft³/sec) (Hahn 1978)

Station	Slope (ft/ft)	Area (ft ²)	Wetted Perimeter (ft)	Mannings Roughness Coefficient
3	0.000773	6.2	9.1	0.148
4	0.001020	19.1	12.9	0.881
5	0.000505	5.6	8.2	0.109
6	0.000633	19.5	13.0	0.518
7	0.000250	5.9	8.6	0.081
8	0.000185	19.3	13.2	0.376
9	0.000908	5.0	7.2	0.131
10	0	17.6	12.5	0
11	0.000467	5.0	7.4	0.093
12	0.000330	18.3	12.7	0.472
13	0.000142	3.8	6.9	0.107
14	0.000168	17.8	12.9	0.318
15	-	4.3	7.2	
16	-	16.8	12.1	
17	0.001010	2.6	5.6	0.055

S_f (upstream pools) = 0.00005

S_f (downstream pools) = 0.00034

S_f (upstream riffles) = 0.00043

S_f (downstream riffles) = 0.00076

The friction slopes provided above represent a composite between friction slopes from a clean channel and friction slopes from a channel containing heavy growth of macrophytes. When the actual depths of channel were measured, the channel was neither clean nor was it choked with the growth of macrophytes.

Given the cross-sectional information provided in columns two, three, and four of Table 3.1 and the computed friction slopes, the roughness coefficients can be calculated according to Manning's Equation (Henderson 1966). These results are presented in column five of Table 3.1.

The drop in head between nodes was calculated by multiplying the average friction slope by the distance between the respective nodes. The average friction slope, distance between nodes, and the elevation drop between nodes are presented in columns 7, 8, and 9 of Table 3.1, respectively. The stage at the downstream boundary was calculated by summing the head losses (loss of energy) over each section and subtracting them from the arbitrarily assumed upstream stage of 10 ft. The calculated water-surface drop from the head of the channel to the outlet was 0.64 ft. (column 10 Table 3.1).

The stage values presented in column 10 of Table 3.1 represent the steady-state conditions that DWOPER tries to simulate. Only the stage value at the downstream end was used by DWOPER as a boundary condition. The input data supplied to DWOPER comes from columns 2, 3, 4, 5, and 8 of Table 3.1.

Hydrodynamic Simulation

As discussed previously, Table 3.1 presents the hydraulic conditions under which the calibration of DWOPER was performed. The upstream initial and boundary conditions were specified as $1.26 \times 10^{-2} \text{ m}^3/\text{s}$, while the downstream initial and boundary conditions were specified (in stage) as 2.853 m. Based on this information, backwater curves were computed for the channel. Backwater computations were employed because the last node in Section 17 (downstream boundary) represented a critical section (Henderson 1966). (A critical section exists when the Froude number equals unity where the Froude number represents the ratio between inertial and gravitational forces.) The results of the calibration are tabulated in column 11 of Table 3.1.

3.2.2 TODAM Calibration

The calibration procedure of TODAM consisted of defining a number of parameters, performing model runs, inspecting the results, and repeating the procedure until satisfactory results were obtained. Most of these parameters were defined by sediment type (noncohesive, cohesive, and organic) and included: sediment diameter, fall velocity, specific gravity, erodibility coefficient, critical shear stress for resuspension and deposition, rates of adsorption/desorption between dissolved diazinon and sediment, and armoring effects. In

addition, dispersion coefficients, upstream contaminant boundary conditions, and the degradation rate of diazinon were also defined. The methods employed for assigning values to each of these parameters are discussed in the next subsections.

Dispersion Coefficient

Several formulations to estimate a dispersion coefficient have been proposed previously and numerous experiments have been performed for defining the longitudinal dispersion coefficient. Some well-known formulations, along with their estimates, are presented here. Table 3.5 presents the representative values for shear velocity (U_*), flow velocity (V), area (A), and flow depth (h) for riffles and pools.

Elder (1959) presented a formulation based on the von Karman logarithmic velocity flow profile as (Fischer et al. 1979):

$$\epsilon_x = \left(\frac{0.404}{\kappa^3} + \frac{\kappa}{6} \right) h U_* \quad (3.1)$$

in which ϵ_x = longitudinal dispersion coefficient (m^2/s), and κ = von Karman constant (0.41). Based on Equation (3.1), ϵ_x for the riffles and pools were estimated as $0.02 \text{ m}^2/\text{s}$ and $0.09 \text{ m}^2/\text{s}$, respectively.

Gulliver (1979; 1980) presented a formulation based on a power law velocity-flow profile that included the effects of wind. For the no-wind case his results were:

$$\epsilon_x = \epsilon_* V h \quad (3.2)$$

TABLE 3.5. Representative Values of Shear Velocity, Flow Velocity, Area and Depth for Riffles and Pools for a Flow of $0.013 \text{ m}^3/\text{s}$

	Shear Velocity (m/s)	Flow Velocity (m/s)	Area (m ²)	Depth (m)
Riffles	0.021	0.081	0.156	0.14
Pools	0.029	0.013	1.008	0.52

in which ϵ_x is a dimensionless dispersion coefficient. (Based on experiments conducted on Channel 1 at MERS by Gulliver, ϵ_x equalled 1.68 and 1.74 for riffles and pools, respectively.) Hence, ϵ_x for the riffles and pools were computed as $0.02 \text{ m}^2/\text{s}$ and $0.01 \text{ m}^2/\text{s}$, respectively.

Fischer suggested two formulations for computing the longitudinal dispersion coefficient. The first (Fischer 1967) is:

$$\epsilon_x = \frac{0.011 V^2 b^2}{h U_*} \approx \frac{0.011 Q^2}{h^3 U_*} \quad (3.3)$$

in which b = top width (m). The dispersion coefficients for riffles and pools are $0.03 \text{ m}^2/\text{s}$ and $0.0004 \text{ m}^2/\text{s}$, respectively. The second equation is:

$$\epsilon_x = \frac{Vb}{4h} \approx \frac{QA^2}{4h^3} \quad (3.4)$$

in which all parameters are as previously defined. The dispersion coefficients for riffles and pools were computed by Equation (3.3) as $0.18 \text{ m}^2/\text{s}$ and $0.02 \text{ m}^2/\text{s}$.

Dispersion coefficients for both riffles and pools, estimated by the above formulations, vary by one order of magnitude or more. It was assumed that, since a major portion of the values are within the 0.01 to 0.03 range, the dispersion coefficients would be estimated by a median value, and the dispersion coefficients were estimated as $0.02 \text{ m}^2/\text{s}$ and $0.01 \text{ m}^2/\text{s}$ for riffles and pools, respectively. For the transition channel sections between riffles and pools, the average dispersion coefficient value of $0.15 \text{ m}^2/\text{s}$ was assumed.

To assess the impact of the dispersion coefficients on the simulation results, the dispersion coefficient was varied by one order of magnitude. No significant change in the results occurred. This suggests that the advection process dominates and that any of the values for the dispersion coefficient presented could have been employed.

Turbidity Versus Sediment Concentration

EPA-Duluth provided data on turbidity versus sediment concentration. A sample was taken from the bed of one of the test channels at MERS. The size of the sediment included in the analysis was less than or equal to a sieve size of 0.062 mm. The sample was thoroughly mixed and allowed to settle overnight at a temperature of 20°C. The results obtained by EPA are presented in Table 3.6. Turbidity was measured in Nephelometer Turbidity Units (NTU), while concentration was expressed in milligrams per liter. A linear regression analysis was performed on the results and are presented in Figure 3.6. The equation relating turbidity and sediment concentration is:

$$C = 4.806(NTU)^{0.194} \quad (3.5)$$

in which C = sediment concentration (mg/l). The correlation for the relationship is 0.976. The samples analyzed and presented in Table 1 are

TABLE 3.6. Turbidity vs. Concentration

<u>Turbidity, (NTU)</u>	<u>Weight of Sediment per 100 ml, (g)</u>	<u>Concentration, (mg/l)</u>
10.2	0.00759	75.9
	0.00693	69.3
6.3	0.00719	71.9
	0.00671	67.1
3.2	0.00610	61.0
	0.00643	64.3
1.9	0.00557	55.7
	0.00541	54.1
0.38 (background)	0.00383	38.3

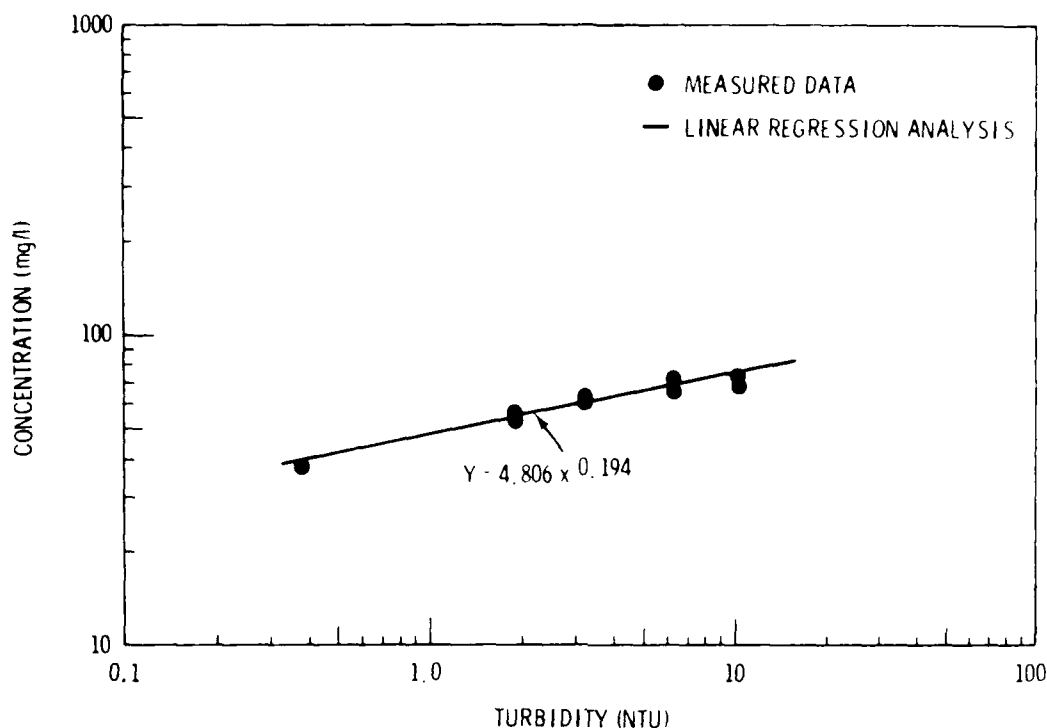


FIGURE 3.6. Concentration vs. Turbidity

representative of the bed and not of the suspended material. Because of a lack of information and data, this relationship is used to relate the measured turbidity at the upstream boundary and suspended sediment concentrations in the channel.

Specific Weight and Sediment Size Computations

The EPA-Duluth provided two samples representative of bed sediment size distribution. Both distribution samples are presented in Table 3.7. The first five sediment sizes were determined from a sieve analysis; the remaining were determined from the pipet method.

The EPA-Duluth also provided information for computing the specific weight for each sediment size equal to and below the 0.062 mm size, as determined from the pipet method. Table 3.8 presents this information for Samples 1 and 2 (Table 3.7). The last column presents the estimated specific weight of each

TABLE 3.7. Bed Sediment Size Distribution Samples

Sediment Size (mm)	Sample #1 Dry Weight (g)	Sample #2 Dry Weight (g)
Sieve Analysis		
2	0.06170	0.22473
1	0.46378	0.54796
0.5	1.19042	1.55702
0.125	7.49991	7.41660
0.062	2.69278	2.48462
Pipet Method Analysis		
0.062	0.19628	0.09513
0.031	0.12102	0.07979
0.016	0.07433	0.04911
0.008	0.05177	0.03374
0.004	0.03021	0.02170
0.002	0.01685	0.01418
0.001	0.00799	0.00776
0.0005	0.00386	0.00515
Background	0.00146	0.00146
Total Dry Weight	22.09000	22.01000

sample. If all of the sediment were alluvial in nature, the specific weight would be approximately 2.65 g/ml. From the results it appears that other material, possibly organic matter, is also contained in the samples.

Computations for the Specific Weight of the Organic Matter

To estimate the amount of the organic content in the bed sediment samples, personnel at the EPA laboratory at Duluth placed two different dry samples (independent of the samples presented in Table 3.8, but from the same bed location), distributed by sediment size, in an oven for 24 hr at 600°C and computed the amount of organic matter consumed. From this information the percent organic content for each sediment size of each sample was calculated. This

TABLE 3.8. Sediment Specific Weight and Size Computation Information (at 20°C)

Sample #1						
Sediment Size (mm)	Sediment-Organic Weight (g)	Total Weight of Mixture (g)	Total Weight of Water (g)	Water Volume (ml)	Sediment Volume (ml)	Estimated Specific Weight (g/ml)
0.062	0.19628	25.03942	24.84314	24.88794	0.11206 ± 0.03	1.38 - 2.39
0.031	0.12102	24.99988	24.87886	24.92372	0.07628 ± 0.03	1.14 - 2.62
0.016	0.07433	24.96102	24.88669	24.93157	0.06843 ± 0.03	0.76 - 1.93
0.008	0.05177	24.94487	24.89310	24.93799	0.06201 ± 0.03	0.56 - 1.62
0.004	0.03021	24.92364	24.89343	24.93832	0.06168 ± 0.03	0.33 - 0.95
0.002	0.01685	24.95332	-	-	-	-
0.001	0.00799	24.94141	-	-	-	-
0.0005	0.00386	24.93659	-	-	-	-

Sample #2						
Sediment Size (mm)	Sediment-Organic Weight (g)	Total Weight of Mixture (g)	Total Weight of Water (g)	Water Volume (ml)	Sediment Volume (ml)	Estimated Specific Weight (g/ml)
0.062	0.09513	24.94464	24.84951	24.89432	0.10568 ± 0.03	0.70 - 1.26
0.031	0.07979	24.96547	24.88568	24.93056	0.06945 ± 0.03	0.80 - 2.02
0.016	0.04911	24.93845	24.88936	24.93422	0.06578 ± 0.03	0.51 - 1.37
0.008	0.03374	24.93204	24.89830	24.94320	0.05680 ± 0.03	0.39 - 1.26
0.004	0.02170	24.92270	24.90100	24.94590	0.05410 ± 0.03	0.26 - 0.90
0.002	0.01418	24.95676	-	-	-	-
0.001	0.00776	24.93675	-	-	-	-
0.0005	0.00515	24.95214	-	-	-	-

information is presented in Table 3.9. (NOTE: The samples presented in Tables 3.8 and 3.9 are not the same.)

Information from Tables 3.8 and 3.9 was used in calculating an estimated specific weight of the organic matter, assuming that the alluvial material (sand, silt, and clay) has a density of 2.65 g/ml. The sediment information from Table 3.8. was combined with the percent organic information from Table 3.9 to compute the specific weight of the organic matter. The computations for calculating the density of the organic matter within the bed are presented below:

Sample 1

Sediment size = 0.062 mm

% organic content (Table 3.9) = 11.37

Total weight of sample (Table 3.8) = 0.19628 g

Total volume of sample (Table 3.8) = 0.11206 ± 0.03 ml

$$W_T = W_S + W_O = 0.19628 \text{ g} \quad (3.6)$$

$$V_T = V_S + V_O = 0.11206 \pm 0.03 \text{ ml} \quad (3.7)$$

$$W_O = \%W_T = (0.1137)(0.19628) = 0.022317 \text{ g} \quad (3.8)$$

$$W_S = W_T - W_O = 0.19628 - 0.022317 = 0.173963 \text{ g} \quad (3.9)$$

$$V_S = W_S / 2.65 = 0.173963 / 2.65 = 0.0656464 \text{ ml} \quad (3.10)$$

$$V_O = V_T - V_S \quad (3.11)$$

$$V_O \text{ (minimum)} = 0.11206 - 0.03 - 0.0656464 = 0.0164136 \text{ ml} \quad (3.12)$$

$$V_O \text{ (maximum)} = 0.11206 + 0.03 - 0.0656464 = 0.0764136 \text{ ml} \quad (3.13)$$

$$\gamma_O = W_O / V_O \quad (3.14)$$

TABLE 3.9. Organic Content of Bed Sediment Samples

Sediment Size (mm)	Sample 1				Sample 2				Combined Percent Organic
	Total Weight (g)	Loss (g)	Percent Organic Content	Seive Size (mm)	Total Weight (g)	Loss (g)	Percent Organic Content	Weighted Average Percent Organic Content	
2	shells, etc.				2	-	-	-	7.33
1	twigs, rocks, etc.				1	-	-	-	
0.5	1.18876	0.01842	1.5	0.5	1.55556	0.03211	2.1	1.84	
0.25	7.49845	0.14916	2.0	0.25	7.41514	0.14011	1.9	1.94	
0.125	2.69132	0.12151	4.5	0.125	2.48316	0.10667	4.3	4.41	
0.062	0.19482	0.02201	11.3	0.062	0.09367	0.01080	11.5	11.37	
0.031	0.11956	0.01602	13.4	0.031	0.07833	0.01022	13.0	13.26	
0.016	0.07287	0.01054	14.5	0.016	0.04765	0.00657	13.8	14.20	
0.008	0.05031	0.00791	15.7	0.008	0.03228	0.00533	16.5	16.03	
0.004	0.02875	0.00496	17.3	0.004	0.02024	0.00307	15.2	16.39	
0.002	0.01539	0.00230	14.9	0.002	0.01272	0.00178	14.0	14.51	
0.001	0.00653	0.00047	7.2	0.001	0.00630	0.00045	7.1	7.17	
0.0005	0.00240	0.00025	10.4	0.0005	0.00369	0.00039	10.6	10.51	

$$\gamma_o \text{ (maximum)} = 0.022317/0.0164136 = 1.36 \text{ g/ml} \quad (3.15)$$

$$\gamma_o \text{ (minimum)} = 0.022317/0.0764136 = 0.29 \text{ g/ml} \quad (3.16)$$

in which W_T = total weight of samples (g), W_S = weight of alluvial sediment(g), W_O = weight of organic matter(g), α = percent organic matter contained in sample, V_T = total dry volume (ml), V_S = dry volume of alluvial sediment (ml), V_O = dry volume of organic matter (ml), and γ_o = specific weight of organic matter (g/ml). Similar calculations were performed for all other sediment sizes for both samples in Table 3.8. The only other sample that provided results in which the specific weight was greater than unity was sediment size 0.031 mm from Sample 1. Its results were:

$$\gamma_o \text{ (maximum)} = 2.41 \text{ g/ml} \quad (3.17)$$

$$\gamma_o \text{ (minimum)} = 0.24 \text{ g/ml} \quad (3.18)$$

Because only the first two sediment sizes from Sample 1 produced organic specific weights greater than unity, these were used to compute the specific weight employed in the modeling effort. The others were not used because if the specific weight was allowed to be less than unity, all material in the bed would float to the surface. This cannot occur because the samples being analyzed are from the bed.

From this information an upper limit can be estimated by averaging the maximum specific weight of the two sediment sizes:

$$\gamma_{o \text{ upper limit}} = (2.41 + 1.36) / 2 = 1.885 \text{ g/ml} \quad (3.19)$$

Because the minimum specific weight values for both sediment sizes were well below unity, they were not employed in estimating a lower limit. Instead, the procedure below was employed.

In studying the fall velocity of geometric shapes and sand grains, the shapes of the particles have been expressed by a shape factor, SF, given by:

$$SF = \frac{c}{\sqrt{ab}} \quad (3.20)$$

in which a, b, and c are, respectively, the lengths of the longest, intermediate, and shortest mutually perpendicular axes of the particle (Vanoni 1975). It was assumed that the shape factor of the organic matter was 0.5 with the shortest and intermediate axes being equal (see Vanoni 1975.) With these assumptions it can be shown that

$$a = 4c \quad (3.21)$$

It was also assumed that the size of the sieve opening is just larger than the length of the minor axis of the particle or

$$2a = 2c = \text{size of sieve} \quad (3.22)$$

From the last two equations an equivalent diameter d_o based on volume, can be calculated:

$$\frac{4}{3} \pi \left(\frac{d_o}{2}\right)^3 = \frac{4}{3} \pi ac^2 = \frac{16}{3} \pi c^3 \quad (3.23)$$

or

$$\frac{d_o}{2c} \leq 1.59 \approx 1.6 \quad (3.24)$$

For the pipet method of analysis it is possible to get sediment sizes larger than 0.062 mm. Based on this, it was assumed that Equation (3.24) formed an upper limit for the size of the organic matter relative to the alluvial material. Therefore,

$$d_o < 1.6 d_s \quad (3.25)$$

in which d_o = diameter of an organic particle (mm) and d_s = diameter of an alluvial particle ($\approx 2c$ in mm). As diameters are based on fall velocities and densities in the pipet method, the following relationship can be made based on Stokes' law (assuming a temperature of 20°C):

$$\frac{w_s}{w_o} = \left(\frac{d_s}{d_o}\right)^2 \left(\frac{\gamma_s - 0.9982}{\gamma_o - 0.9982}\right) \approx 1 \quad (3.26)$$

in which w_s = fall velocity of inorganic particle (m/s), w_o = fall velocity of organic particle, γ_s = specific weight of sediment (2.65 g/ml). By combining Equations (3.25) and (3.26) γ_o becomes

$$\gamma_o > 1.64 \quad (3.27)$$

γ_o is now defined within an upper limit (1.885 g/ml) and a lower limit (1.64 g/ml). By assuming the average will reflect the actual specific weight, γ_o becomes

$$\gamma_o = 1.7525 \approx 1.76 \quad (3.28)$$

The specific weight of the organic matter used for the modeling effort is assumed as 1.76 g/ml. Because γ_o was re-estimated, recalculating the ratio between the organic and inorganic sediment sizes by way of Equation (3.26), gives

$$\frac{w_s}{w_o} = \left(\frac{d_s}{d_o}\right)^2 \left(\frac{2.65 - 0.9982}{1.76 - 0.9982}\right) \approx 1 \quad (3.29)$$

or

$$d_o \approx 1.4725 d_s \quad (3.30)$$

Since the specific weight of the organic matter is physically less than the specific weight of inorganic sediment, the sediment diameter has to be smaller for the organic and inorganic sediment to have equivalent fall velocities [see Equations (3.26) and (3.29)]. Equation (3.30) meets the criterion of Equation (3.25) and is used in calculating the diameters of the organic material. The diameters of each sediment type are calculated in the next section.

Sediment Size Calculations

Cohesive sediment, noncohesive sediment, and organic matter represent the three sediment types used in the modeling effort. Noncohesive sediments are represented by sand (≥ 0.062 mm) and cohesive sediments are represented by silt and clay (< 0.062 mm). Table 3.9 presents the combined organic content total which is 7.33%. This is the percentage of the organic content composing the combined samples presented in Table 3.7 or 3.8. In addition, the percentages of the cohesive and noncohesive inorganic bed sediment, based on the combination of Samples 1 and 2 in Table 3.7 or 3.8 are 39.67% and 53.00%, respectively. The bed material was divided into these three categories because 1) a significant amount of bed material is organic, 2) 50% of the sediment entering at the upstream boundary condition is organic (see p. 3.49), 3) the majority of the inorganic sediment is either sand or clay (very little silt), and 4) organic matter has a high affinity for chemical contaminants; therefore, small amounts of organic material should not be neglected. Because these three sediment types are being modeled, equivalent diameters for each type are required. Tables 3.10 and 3.11 present the size distribution of the organic and inorganic bed material of Samples 1 and 2, respectively (these samples were previously presented in Tables 3.7 and 3.8). In addition, Table 3.12 presents the combined sediment size distribution by sediment size of Samples 1 and 2 for the organic and inorganic bed materials. An equivalent sediment diameter was calculated for each sediment type (non-cohesive, cohesive, and organic), and weighted according to the amount of sediment in each size fraction. Based

TABLE 3.10. Sample #1 Distributed by Size Fraction Between Organic and Inorganic Bed Material

Sediment Size (mm)	Sediment Weight (g)	Organic Weight (g)	Percent Weight of Sediment	Percent Finer of Sediment
2	0.061700	-	0.30	99.70
1	0.463780	-	2.28	97.42
0.50	1.168520	0.021900	5.74	91.68
0.125	7.169160	0.330750	35.23	56.45
0.092	-	0.022317	-	-
0.062	2.560574	0.306169	12.58	43.87
0.046	-	0.016043	-	-
0.032	0.104973	-	0.52	43.35
0.023	-	0.010555	-	-
0.016	0.063775	-	0.31	43.04
0.012	-	0.008299	-	-
0.008	0.043471	-	0.21	42.83
0.006	-	0.004951	-	-
0.004	0.025259	-	0.12	42.71
0.003	-	0.002445	-	-
0.002	0.014405	-	0.07	42.64
0.0014	-	0.000573	-	-
0.001	0.007417	-	0.04	42.60
0.0007	-	0.000406	-	-
0.0005	0.003454	-	0.02	42.58
~0.00036	-	1.017273	-	-
~0.0002	8.661822	-	42.58	0

on this, the equivalent diameters for the non-cohesive, cohesive, and organic sediments were 0.2164 mm, 0.00065 mm, and 0.03920 mm, respectively.

The sediment distributions as presented in Tables 3.10 and 3.11, were plotted in Figure 3.7. The solid curve represents Sample 1 and the broken curve represents Sample 2. Based on these curves, the mean diameter of the sediment (D_{50}) was assumed as 0.075 mm.

TABLE 3.11. Sample #2 Distributed by Size Fraction Between Organic and Inorganic Bed Material

Sediment Size (mm)	Sediment Weight (g)	Organic Weight (g)	Percent Weight of Sediment	Percent Finer of Sediment
2	0.224730	-	1.10	98.90
1	0.547960	-	2.67	96.23
0.5	1.528371	0.028649	7.45	88.78
0.125	7.272718	0.143882	35.44	53.34
0.092	-	0.010816	-	-
0.062	2.286433	0.282501	11.14	42.20
0.046	-	0.01058	-	-
0.032	0.069210	-	0.34	41.86
0.023	-	0.006974	-	-
0.016	0.042136	-	0.21	41.65
0.012	-	0.005409	-	-
0.008	0.028331	-	0.14	41.51
0.006	-	0.003557	-	-
0.004	0.018143	-	0.09	41.42
0.003	-	0.002058	-	-
0.002	0.012122	-	0.06	41.36
0.0014	-	0.000556	-	-
0.001	0.007204	-	0.04	41.32
0.0007	-	0.000541	-	-
0.0005	0.004609	-	0.02	41.30
~0.00036	-	0.995561	-	-
~0.00020	8.476949	-	41.30	0

Fall Velocities

The fall velocities of the three sediment types were calculated according to their representative diameter sizes. Because the pipet method was employed for the cohesive sediments, Stokes' Law (Vanoni 1975) was employed for calculating the fall velocities of cohesive sediment and the organic matter. For the non-cohesive sediments, Ruby's formula (Vanoni 1975) was employed for cal-

TABLE 3.12. Combined Sediment Samples Distributed by Size Fraction
Between Organic and Inorganic Bed Materials

<u>Size (mm)</u>	<u>Combined Sediment Weight (g)</u>	<u>Combined Organic Weight (g)</u>
2	0.28643	-
1	1.01174	-
0.5	2.69689	0.05055
0.125	14.44188	0.47463
0.092	-	0.03313
0.062	4.84701	0.58867
0.046	-	0.02662
0.032	0.17418	-
0.023	-	0.01753
0.016	0.10591	-
0.012	-	0.01371
0.008	0.07180	-
0.006	-	0.00851
0.004	0.04340	-
0.003	-	0.00450
0.002	0.02653	-
0.0014	-	0.00113
0.0010	0.01462	-
0.0007	-	0.00095
0.0005	0.00806	-
~0.00036	-	2.01283
~0.0002	17.13877	-

culating the fall velocity. The fall velocities of non-cohesive, cohesive, and organic sediments were estimated to be 2.510×10^{-2} m/s, 3.765×10^{-7} m/s, and 6.300×10^{-4} m/s, respectively.

Critical Shear Stress, Erodibility Coefficient, and Bed Armoring

From observations of the site there appeared to be little or no sediment erosion or deposition in the channels. The top layer of the bed in the riffle

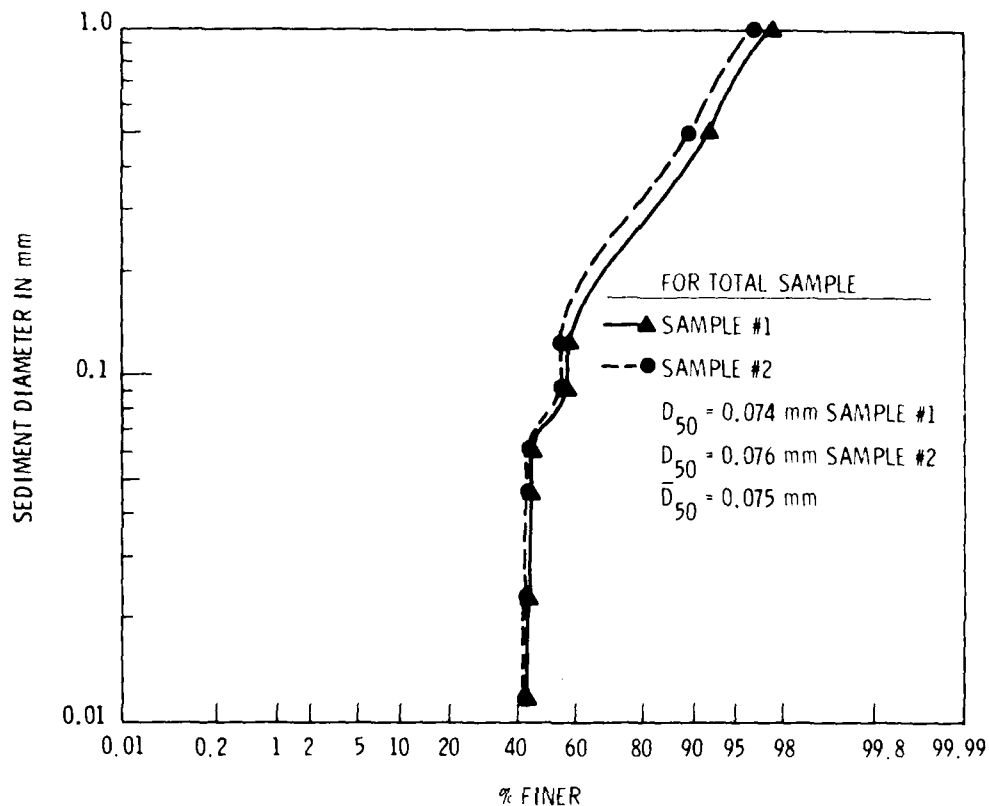


FIGURE 3.7. Sediment Size Distributions

sections, though, appeared to be 95% armored with gravel and the remaining 5% was distributed between the three sediment types (noncohesive, cohesive, and organic). Only the cohesive and organic sediments require estimates of the critical shear stress and the erodibility coefficient because the noncohesive sediments were estimated in TODAM by using either Colby's or Toffaleti's sediment discharge formula (Vanoni 1975).

Two types of critical shear stress for cohesive sediments and organic matter are employed in the modeling effort: one for sediment erosion and one for deposition. The critical shear stress for erosion defines the point above which the bed sediment is resuspended. For the organic matter, Shield's diagram (Vanoni 1975) was employed in calculating the critical shear stress for motion in the riffles and pools. Based on Table 3.5, a specific weight of

1.76 g/ml, and a representative diameter size of 0.0392 mm, the critical shear stress for motion of the organic matter in the pools and riffles was selected as $3.3 \times 10^{-3} \text{ kg/m}^2$ and $4.5 \times 10^{-3} \text{ kg/m}^2$, respectively. For the channel sections between the pools and riffles, the average shear stress of $3.9 \times 10^{-3} \text{ kg/m}^2$ was used. The diameter size for the cohesive sediments was too small to use Shield's diagram. This indicates that a large shear stress would be required because the particles tend to move as a group rather than as individual particles. If the curve on Shield's diagram is extrapolated, the computed critical shear stress becomes very large. Based on Shield's diagram, the critical shear stress for the cohesive sediments in the pools and riffles was assumed to be 5.5 kg/m^2 .

As there was no appreciable deposition observed in the channels, the critical shear stress was assumed to be $1.0 \times 10^{-5} \text{ kg/m}^2$ for all sediment types for all pools and riffles.

The ability of a sediment size to be resuspended is a function of its exposed area in the top layer. Only 5% of the exposed area in the top layer of the riffles is composed of the three sediment types (non-cohesive, cohesive, and organic). To reflect this, the erosion rates in the riffles were reduced by a factor, 0.05. Note that 100% of the erosion rate still applies in the pools.

The erodibility coefficient is a parameter defining the amount of cohesive or organic sediments eroded from the bed. Because there is little erosion or deposition, it was arbitrarily assumed to be 0.0432% or $4.32 \times 10^{-4} \text{ kg/m}^2\text{-day}$. By assigning the erodibility coefficient in this manner, the sediments are assured of being carried through the system without deposition.

Distribution Coefficient Calculations

The distribution coefficient is a measure of the affinity between diazinon and sediment. It is a ratio of the particulate diazinon concentration and the dissolved diazinon concentration. In this particular modeling effort three sediment types are considered: cohesive, noncohesive, and organic. Each has its own distribution coefficient.

The personnel at EPA-Duluth supplied information so the distribution coefficients for the three sediment types in the MERS channels could be computed:

1. on September 19, 1980, 50 ml of a sediment-organic-water mixture from the bed of Channel 6 was placed in a beaker with Lake Superior water until a 250 ml mixture was attained.
2. The mixture was thoroughly combined and allowed to settle for 33 minutes, at which time, the top 200 ml of mixture was removed and placed in a second beaker. (It was assumed that Beaker No. 1 contained noncohesive-organic material.) Lake Superior water was then added to Beaker No. 2 until a mixture of 250 ml was attained.
3. 25 ml of the mixture was then removed from Beaker No. 2. From this mixture the dry weight of sediment-organics was obtained. By extrapolating for the entire 250 ml mixture, the total weight of sediment and organic matter was estimated as 1.6466 g.
4. The remaining 90% of the mixture from Beaker No. 2 was used to calculate the total amount of diazinon present. This included the diazinon in solution and adsorbed onto the cohesive sediment and organic matter. The total amount of diazinon estimated for Beaker No. 2 adjusted for the 250 ml mixture was 3.0297×10^{-11} kg.
5. The total amount of diazinon in Beaker No. 1 was measured as 2.8823×10^{-10} kg. This beaker also contained a dry weight of 12.7534 g of noncohesive sediment and organic matter.
6. Based on the computations earlier that 7.33% of the bed contained organic material, the distribution between sediments and organic matter can be computed in each beaker.

For Beaker No. 1:

Weight of noncohesive sediment (W_s)

$$(1 - 0.0733)(1.27534 \times 10^{-2} \text{ kg}) = 1.182 \times 10^{-2} \text{ kg} \quad (3.31)$$

Weight of organic matter (W_{O1})

$$(0.0733)(1.27534 \times 10^{-2} \text{ kg}) = 9.348 \times 10^{-4} \text{ kg} \quad (3.32)$$

For Beaker No. 2:

Weight of cohesive sediment (W_c)

$$(1 - 0.0733)(1.6466 \times 10^{-3} \text{ kg}) = 1.526 \times 10^{-3} \text{ kg} \quad (3.33)$$

Weight of organic matter (W_{O2})

$$(0.0733)(1.6466 \times 10^{-3} \text{ kg}) = 1.206 \times 10^{-4} \text{ kg} \quad (3.34)$$

7. Based on the specific weight of the organic and inorganic material computed earlier, the volume of water in each beaker can be computed.

For Beaker No. 1:

Volume of Water (V_1)

$$50 \times 10^{-6} \text{ m}^3 - \frac{1.182 \times 10^{-2} \text{ kg}}{2650 \text{ kg/m}^3} - \frac{9.348 \times 10^{-4} \text{ kg}}{1760 \text{ kg/m}^3} = 45.073 \times 10^{-6} \text{ m}^3 \quad (3.35)$$

For Beaker No. 2:

Volume of water (V_2)

$$250 \times 10^{-6} \text{ m}^3 - \frac{1.526 \times 10^{-3} \text{ kg}}{2650 \text{ kg/m}^3} - \frac{1.206 \times 10^{-4} \text{ kg}}{1760 \text{ kg/m}^3} = 249.355 \times 10^{-6} \text{ m}^3 \quad (3.36)$$

8. By definition, six additional equations can be developed:

$$(a) K_{d1} = \left(\frac{D_s}{W_s} \right) / \left(\frac{D_{d1}}{V_1} \right) \quad (3.37)$$

$$(b) K_{d2} = \left(\frac{D_c}{W_c}\right) / \left(\frac{D_{d2}}{V_2}\right) \quad (3.38)$$

$$(c) K_{d3'} = \left(\frac{D_{o1}}{W_{o1}}\right) / \left(\frac{D_{d1}}{V_1}\right) \quad (3.39)$$

$$(d) K_{d3''} = \left(\frac{D_{o2}}{W_{o2}}\right) / \left(\frac{D_{d2}}{V_2}\right) \quad (3.40)$$

$$D_{T1} = D_{d1} + D_s + D_{o1} \quad (3.41)$$

$$D_{T2} = D_{d2} + D_c + D_{o2} \quad (3.42)$$

in which K_{d1} = distribution coefficient for noncohesive sediment (m^3/kg), K_{d2} distribution coefficients for cohesive sediment (m^3/kg), $K_{d3'}$ = distribution coefficient for organic matter in Beaker No. 1 (m^3/kg), $K_{d3''}$ = distribution coefficient for organic matter in Beaker No. 2 (m^3/kg), D_s = weight of diazinon associated with noncohesive sediment (kg), D_c = weight of diazinon associated with cohesive sediment (kg), D_{o1} = weight of diazinon associated with organic matter in Beaker No. 1 (kg), D_{o2} = weight of diazinon associated with organic matter in Beaker No. 2 (kg), D_{d1} = dissolved weight of diazinon in Beaker No. 1 (kg), D_{d2} = dissolved weight of diazinon in Beaker No. 2 (kg), D_{T1} = total weight of diazinon in Beaker No. 1 (kg), and D_{T2} = total weight of diazinon in Beaker No. 2 (kg).

At this point in the analysis, there are 14 equations and 18 unknowns. Based on the information presented, four additional assumptions were made.

9. It is assumed that the equilibrium coefficients for organic matter in Beakers No. 1 and 2 are equal:

$$K_{d3'} = K_{d3''} \quad (3.43)$$

(Rename $K_{d3'}$ and $K_{d3''}$ as K_{d3} .)

10. It is assumed that 3/4 of the dissolved diazinon was transferred from Beaker No. 1 to Beaker No. 2. This is a crude estimate and may be incorrect:

$$D_{d2} = 3 D_{d1} \quad (3.44)$$

11. According to Onishi et al. (1979) and Dawson et al. (1980), the distribution coefficient of diazinon for silty-sand with 1% to 3% organic matter is $0.05 \text{ m}^3/\text{kg}$. With the information presented by Onishi et al. (1979) and Dawson et al. (1980), it is assumed that the distribution coefficient is based on a sample consisting of 1% organic matter and 99% inorganic matter. This distribution coefficient is a composite of noncohesive sediment and organic matter. It is further assumed that the composite distribution coefficient is distributed between the distribution coefficients for noncohesive sediment and organic matter according to the amount present; thereby giving:

$$0.05 = 0.99 K_{d1} + 0.01 K_{d3} \quad (3.45)$$

(If 2% or 3% were used, K_d values would have been negative.)

12. It is assumed that the ratio of the distribution coefficients of cohesive and noncohesive sediments is equal to the ratio of the surface areas of the two sediment sizes assuming an equal volume of each (based on the spherical shape). In addition, a representative sand size as 0.15 mm and a representative clay size as 0.001 mm is assumed. Based on this information:

$$K_{d2} = 150 K_{d1} \quad (3.46)$$

This is strictly an estimation and may be incorrect. The finer sediments have a greater affinity for diazinon than do the larger sizes. This is largely because of the increased surface area of the finer material.

There are now 18 equations and 18 unknowns. In summary, the equations are:

$$D_{T1} = 2.8823 \times 10^{-10} \text{ kg} \quad (3.45)$$

$$D_{T2} = 3.0297 \times 10^{-11} \text{ kg} \quad (3.46)$$

$$W_s = 1.182 \times 10^{-11} \text{ kg} \quad (3.31)$$

$$W_{o1} = 9.348 \times 10^{-4} \text{ kg} \quad (3.32)$$

$$W_c = 1.526 \times 10^{-3} \text{ kg} \quad (3.33)$$

$$W_{o2} = 1.206 \times 10^{-4} \text{ kg} \quad (3.34)$$

$$V_1 = 45.073 \times 10^{-6} \text{ m}^3 \quad (3.35)$$

$$V_2 = 249.355 \times 10^{-6} \text{ m}^3 \quad (3.36)$$

$$K_{d1} = \left(\frac{D_s}{W_s} \right) / \left(\frac{D_{d1}}{V_1} \right) \quad (3.37)$$

$$K_{d2} = \left(\frac{D_c}{W_c} \right) / \left(\frac{D_{d2}}{V_2} \right) \quad (3.38)$$

$$K_{d3'} = \left(\frac{D_{o2}}{W_{o1}} \right) / \left(\frac{D_{d1}}{V_1} \right) \quad (3.39)$$

$$K_{d3}'' = (D_{o2}/W_{o2}) / (D_{d2}/V_2) \quad (3.40)$$

$$D_{T1} = D_{d1} + D_s + D_{o1} \quad (3.41)$$

$$D_{T2} = D_{d2} + D_c + D_{o2} \quad (3.42)$$

$$K_{d3} = K_{d3}' = K_{d3}'' \quad (3.43)$$

$$D_{d2} = 3 D_{d1} \quad (3.44)$$

$$0.05 = 0.99 K_{d1} + 0.01 K_{d3} \quad (3.45)$$

$$K_{d2} = 150 K_{d1} \quad (3.46)$$

Solving these equations for K_{d1} , K_{d2} , K_{d3} gives:

$$K_{d1} = 0.00027 \approx 0.0003 \text{ m}^3/\text{kg} \quad (3.47)$$

$$K_{d2} = 0.0407 \approx 0.04 \text{ m}^3/\text{kg} \quad (3.48)$$

$$K_{d3} = 4.97 \approx 5.0 \text{ m}^3/\text{kg} \quad (3.49)$$

Hence, distribution coefficients for noncohesive, cohesive, and organic matter were selected to be $0.0003 \text{ m}^3/\text{kg}$, $0.04 \text{ m}^3/\text{kg}$, and $5.0 \text{ m}^3/\text{kg}$, respectively.

Degradation Constant for Diazinon

Several contaminated water samples were taken from Section 4 of Channel 6 at MERS for the purpose of estimating the degradation rate of diazinon. A summary of the samples and their diazinon concentrations are presented in

Table 3.13. Each sample was divided into two specimens. One sample was exposed to sunlight; the second was not. The specimens exposed to sunlight showed a rate of degradation of approximately 4% per day which translates to a half-life of approximately 17 days. Mathematically, this may be expressed as

$$\hat{C} = 124.23 \text{ Exp}(-0.040 t) \quad (3.40)$$

in which \hat{C} is the least squares estimate of the percentage of the original concentration after t days. The linear equation is $\hat{C} = 99.5 - 1.65 t$. Results are provided in Figure 3.8, which presents the temporal variation of the diazinon concentration as a percentage of the original concentration. If the equation is forced through $t = 0$, $C = 100$, it becomes $\hat{C} = 100e^{-0.034t}$.

The shaded samples exhibited a slower degradation rate as would be expected without photolysis as a significant contributor to degradation. The least squares equation for this data is

$$\hat{C} = 110.48e^{-0.018 t}$$

which has been plotted as the percentage of the original concentration after t days (Figure 3.9). The linear equation is

$$\hat{C} = 103.7 - 1.17 t$$

TABLE 3.13. Diazinon Degradation Study Water Samples from Channel 604

	Date	Sun	Shade
Run 1	5-14	3.0 µg/l	3.0 (initial concentration)
	5-30	2.00	2.90 µg/l
	6-10	1.50	2.10
	6-25	1.01	1.76
	7-8	0.25	1.00
Run 2	7-8	2.10	2.30 (initial concentration)
	7-22	1.70	1.90
	7-30	1.40	1.90

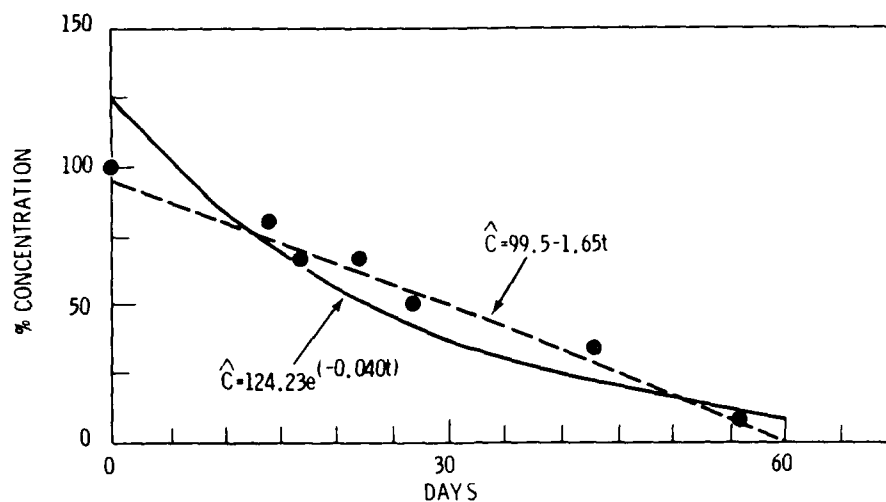


FIGURE 3.8. Diazinon Concentration (Percentage of Original) when Exposed to Sun

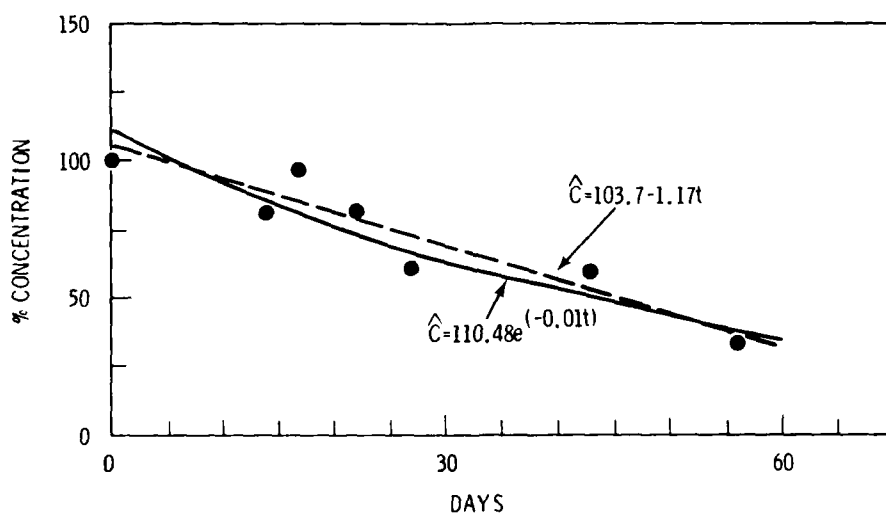


FIGURE 3.9. Diazinon Concentration (Percentage of Original) when Stored in Shade

and the equation when forced through $t = 0$, $C = 100$ is

$$\hat{C} = 100e^{-0.015 t}.$$

The overall degradation rate was about 2% per day which calculates to a half-life of 39 days.

A number of seasonal changes such as increased water temperature, development of bacteria capable of breaking down diazinon, or changes in dissolved oxygen or pH may tend to change the rate of degradation. More frequent testing of the water may allow detection of such trends.

The overall first-order degradation rate from the sun exposed results was assumed as $4.6 \times 10^{-7} \text{ s}^{-1}$. This is similar to the estimate presented by Onishi et al. (1979), Dexter (1979), and Dawson et al. (1980) of $3.65 \times 10^{-7} \text{ s}^{-1}$. The shaded degradation rate was not used because the shaded portion of the channels extended for only about 300 ft of each channel. Because of the lack of data, the overall degradation constant was employed in the model as opposed to individual degradation rates from such processes as hydrolysis, photolysis, oxidation, biochemical processes, and volatilization. In addition, the half-life of the diazinon well exceeds the travel time in the channel from the inlet to the outlet, thereby reducing its influence on the simulation results.

Upstream Contaminant Boundary Conditions

Discharges of diazinon to Channels 6 and 7 occurred at the inlet (entrance) of each channel. No significant lateral inflow of water or sediment occurred in either channel.

Diazinon released to the channels was first mixed and stored in a large stock tank with an initial concentration of 30.9 mg/l ($30.9 \times 10^{-3} \text{ kg/m}^3$). This stock tank supplied both channels (6 and 7) with diazinon. Channel 6 received an inflow rate of 76 ml/min ($1.2667 \times 10^{-6} \text{ m}^3/\text{s}$) of the contaminated solution from the stock tank, (a diazinon flux of $3.914 \times 10^{-8} \text{ kg/s}$). Channel 7 received an inflow rate of 7.6 ml/min ($1.2667 \times 10^{-7} \text{ m}^3/\text{s}$) of the solution from the stock tank, (a diazinon flux of $3.914 \times 10^{-9} \text{ kg/s}$). The mixture of diazinon and water were added at the inlet of each channel through metered piping from

the stock tank. The pipes discharged the contaminated solution into the channel just above the water surface. Flow rates in each channel were maintained at 200 gal/min ($1.26 \times 10^{-2} \text{ m}^3/\text{s}$). V-notched weirs were used to control the flow rates. Based on the constant flow rate in each channel (200 gal/min) and the diazinon flux supplied to the channels, the diazinon concentrations representing the upstream boundary conditions in Channels 6 and 7 were computed as $3.10 \times 10^{-6} \text{ kg/m}^3$ (3.1 $\mu\text{g/l}$), and $3.10 \times 10^{-7} \text{ kg/m}^3$ (0.31 $\mu\text{g/l}$), respectively. This assumes instantaneous mixing between the diazinon and the receiving flow.

Water flowing through all channels was supplied by the Mississippi River. This water was unfiltered and its suspended sediment contained approximately 50% organic matter, 45% cohesive sediment, and 5% non-cohesive sediment. This information is based on five years of data (1974-1979) supplied by the St. Paul, Minnesota District office of the U.S. Geological Survey (USGS) for the gaging station at Royalton, Minnesota, approximately 50 miles upstream of MERS. The information provided contains a wide range of water quality data including organic content, particle size distribution for suspended sediment, turbidity, and pesticide concentrations. In addition to water quality information supplied by the USGS, MERS personnel supplied turbidity information for the inlet of Channel 8 during the testing period. Weekly turbidity values at the inlet were supplied, including a maximum, minimum, and mean value. The mean turbidity during the testing period was 3.2 NTU. Based on this value and Equation (3.5), the sediment concentration was estimated to be approximately 60 mg/l ($60 \times 10^{-3} \text{ kg/m}^3$). Distributing the 60 mg/l, according to the Mississippi sediment distribution of 50% organic matter, 45% cohesive sediment, and 5% noncohesive sediment from the USGS, gives:

- 30 mg/l as organic matter
- 27 mg/l as cohesive sediment
- 3 mg/l as noncohesive sediment.

These were the sediment concentrations used as the upstream boundary conditions for Channels 6 and 7.

3.3 RISK ASSESSMENT

Previous use of the CMRA risk assessment has been based on the acute toxicity indicator LC50 and a chronic indicator, MATC, for the different species

of interest. For noncontinuous chemical discharges, a time-LC50 curve is constructed, and the risk evaluation depends heavily on the frequency and duration of which points on the LC50 line or the MATC range are exceeded. Interpretation is based on these values to indicate a measure of the potentially hazardous conditions existing through the modeling duration. Actual interpretation requires much more information, but the graphs provide a framework.

This specific situation is different from most theoretical studies because of the control of several variables. For instance, the flow (addition) of diazinon is almost constant. The only time a diazinon concentration at a given location fluctuates significantly is at start-up when it goes from 0 to the steady concentration. This eliminates the value of a statistical summary of events exceeding an LC50 curve unless startup values exceed LC50 values, which is not the case for fathead minnows, the only fish planned for study.

The toxicity information we chose to use borrows extensively from the data MERS has gathered. Fish and invertebrate LC50 data are provided in Table 3.14. Two separate bioassays of fathead minnows exposed to diazinon resulted in LC50s of 6900 $\mu\text{g/l}$ and 7800 $\mu\text{g/l}$ at 96 hr. Chronic toxicological information is summarized in Table 3.15. Morbidity analysis and potential problems in spawning, and the reduced viability of eggs has been shown in much lower concentrations for fathead minnows. Spinal scoliosis has been diagnosed by Allison and Hermanutz (1977) at a concentration of 3.2 $\mu\text{g/l}$ for 18 weeks.

Four locations were selected within both Channels 6 and 7 for FRANCO analysis. These are sections designated in Channel 6 as 604, 605, 612, and 617 and in Channel 7 as 704, 705, 712, and 717. The site for the first three sections in both these series was at the midpoint of each section. Riffles 617 and 717 were analyzed at the downstream ends of the riffles. The points correspond to field-sampling sites.

The FRANCO summary was programmed to indicate diazinon concentrations for the first 5 days using 3-minute timesteps which were used by TODAM.

TABLE 3.14. LC50 Concentrations from Diazinon Exposure ($\mu\text{g/l}$)

<u>Fish</u>	<u>24 hr</u>	<u>48 hr</u>	<u>96 hr</u>	<u>Other LC50 Data</u>	<u>References</u>
<u>Lepomis macrochirus</u> (bluegill sunfish)	52	30	22 90		Cope 1965 Johnson and Finley 1980
<u>Pimephales promelas</u> (fathead minnow)			7800 6900		Allison and Hermanutz 1977 Jarvinen and Tanner 1981
<u>Salmo gairdneri</u> (rainbow trout)	380	170	90 170		Cope 1965 Johnson and Finley 1980
<u>Salmo clarki</u> (cutthroat trout)			1700		Johnson and Finley 1980
<u>Salvelinus fontinalis</u> (brook trout)			770		Johnson and Finley 1980
<u>Salvelinus namaycush</u> (lake trout)			600		Johnson and Finley 1980
<u>Invertebrates</u>					
<u>Acroneuria lycorias</u>			1.7	30 day LC50-1.25	Bell 1971
<u>Acroneuria ruralis</u>	294				Morgan 1977
<u>Asellus communis</u>			21		Morgan 1976
<u>Baetis intermedius</u>	55				Morgan 1977
<u>Cheumatopsyche oxa</u>				3 hr LC50-190	Morgan 1977
<u>Chironomus tentans</u>	1		0.03		Morgan 1977
<u>Crangonyx sp.</u>			14		MERS 1980 (unpublished)
<u>Daphnia magna</u>				50 hr LC50-4.3 21 days TL50-0.26	Sanders and cope 1966 Biesinger 1971

TABLE 3.14. (contd.)

Invertebrates (contd.)	24 hr	48 hr	96 hr	Other LC50 Data	References
<u>Daphnia pulex</u>		0.9			Sanders and Cope 1966
<u>Ephemereilla subvaria</u>				30 day LC50-1.05	Bell 1971
<u>Gammarus lacustris</u>	800	500 229	200		Sanders 1969 Morgan 1977
<u>Gammarus pseudolimnaeus</u>		3	0.2	30 day LC50-0.27	Morgan 1977 Johnson and Finley 1980 Bell 1972
<u>Helisoma trivolis</u>				168 hr LC50-528	Morgan 1977
<u>Hyalrella azteca</u>		22			Morgan 1977
<u>Hydropsyche sparna</u>				3 hr LC50-220	Morgan 1977
<u>Hydropsyche bettoni</u>				30 day LC50-3.54	Bell 1971
<u>Leptocella albeda</u>				3 hr LC50-220	Morgan 1977
<u>Ophiogomphus rupinsulensis</u>				30 day LC50-2.2	Bell 1971
<u>Orconectes propinquus</u>		537			Morgan 1977
<u>Paraleptophlebia pallipes</u>		134			Morgan 1977
<u>Physa gyrina</u>			48		Morgan 1977
<u>Pteronarcys californica</u>	155	60	25		Sanders and Cope 1968
<u>Pteronarcys dorsata</u>				30 day LC50-4.6	Bell 1971
<u>Simocephalus serrulatus</u>		1.8			Sanders and Cope 1968

TABLE 3.15. Chronic Effects from Diazinon Exposure

<u>Fish</u>	<u>Description</u>	<u>Reference</u>
<u>Jordanella floridae</u> (flag fish)	Reduced egg hatchability - 18 weeks at 90 µg/l	Allison 1977
<u>Pimephales promelas</u> (fathead minnow)	Reduced hatching and increase in incidence of scoliosis at 3.2 µg/l	Allison and Hermanutz 1977
<u>Salvelinus namaycush</u> (brook trout)	Reduced progeny growth at 0.55 µg/l for 37 weeks	Allison and Hermanutz 1977
<u>Cyprinodon variegatus</u> (sheepshead minnow)	Reduced fecundity at 0.47 g/l for 108 days	Goodman et al. 1979
<u>Invertebrates</u>		
<u>Daphnia</u>	Interfered with reproduction - 21 days at 0.3 µg/l	Biesinger 1971
<u>Chironomus tentans</u>	Effectuated egg development - 109 days at 0.003 µg/l	Morgan 1977

4.0 COMPARISON OF SIMULATED VERSUS OBSERVED RESULTS

The simulation^(a) time for the transport and fate of the chemical diazinon in the channels at MERS was for a time span of five days. A longer simulation was unnecessary for several reasons:

1. There was not enough information regarding the bed contamination for the extended time period past five days.
2. The simulated contaminant concentrations in channel sections 3, 4, and 5 after five days of simulation were very close to steady-state conditions. A ten-day trial simulation was performed and no significant differences resulted in the simulation.
3. Due to steady-state hydrodynamic conditions, all hydrodynamic parameters were constant.
4. The temporal variation of the diazinon concentration in those downstream channel sections where the steady-state equilibrium condition had not been attained was very small, thereby allowing for extrapolation of the simulated results.

The observed diazinon concentrations for Channel 6 are listed in Table 4.1 and Channel 7 concentrations in Table 4.2. The background level of diazinon in the Mississippi River water was generally below the detection limit; only occasionally was a trace of diazinon found. All concentrations in Tables 4.1 through 4.3 represent values above background. Vertical and transverse profiles on one pool in channels 6 and 7 were analyzed on several occasions during the study. Results of these analyses are given in Table 4.3. A summary of routinely analyzed water quality parameters is given in Table 4.4.

4.1 DWOPER--HYDRODYNAMIC MODELING RESULTS

The hydrodynamic model DWOPER was used to simulate flow conditions in Channel 8 under steady-state conditions with a constant flow discharge of

(a) The terms "simulated" and "computed" refer to model results, while the terms "observed" and "measured" refer to data observed or measured at the MERS' site.

TABLE 4.1. Measured Diazinon Concentrations in Water Samples in Channel 6

Date	Time	Channel 6 ($\mu\text{g/l}$)				
		603	604	605	611	617
5-14	1200(a)	2.2	2.1	1.4	0	0
	1300	2.3	2.2	2.1	0	0
	1600	2.2	2.3	2.3	1.5	1.5
	1900	2.4	2.3	2.3	2.2	1.7
	2300	2.4	2.5	2.5	1.8	1.9
5-15	1100	2.9	2.8	2.8	2.9	2.6
	mid-depth	2.9	2.7	2.8	2.9	2.6
5-16		3.1	3.1	3.1	-	2.8
5-17		3.3	2.9	-	-	2.8
5-21		2.9	3.0	3.2	2.9	2.9
5-22		-	3.6	-	-	-
5-23		3.9	3.5	3.9	-	3.5
6-11		-	2.9	-	-	-
6-13		3.2	3.1	3.2	-	-
6-16		3.2	-	-	-	-
6-27		3.6	3.6	3.6	-	-
6-30		3.4	-	-	-	3.2
7-11		2.7	2.9	2.7	-	-
7-14		2.5	-	-	-	2.2
7-25		2.8	2.8	2.7	-	-
7-28		1.9	-	-	-	1.7

(a) Sampling took about 20 minutes

TABLE 4.2. Measured Diazinon Concentrations in Water Samples in Channel 7

Date	Time	Channel 7 (ug/l)				
		703	704	705	711	717
5-14	1200(a)	0.25	0.17	trace(b)	0	trace(b)
	1300	0.24	0.16	0.16	0	0
	1600	0.28	0.26	0.26	0.05	0
	1900	0.3	0.3	0.28	0.25	0.13
	2300	0.31	0.31	0.24	0.23	0.24
5-15	1100	0.3	0.32	0.32	0.22	0.25
	mid-depth	0.3	0.3	0.32	0.22	0.25
5-16		0.36	0.37	-	-	0.31
5-17		0.40	0.76	0.37	-	0.31
5-21		0.38	0.39	0.39	0.36	0.33
5-22		-	0.54	-	-	-
5-23		0.42	0.58	0.57	-	0.38
6-11		-	0.3	-	-	-
6-13		0.44	3.5	0.33	-	-
6-16		0.35	-	-	-	-
6-27		0.33	0.38	0.35	-	-
6-30		0.31	-	-	-	0.23
7-11		0.27	0.39	0.23	-	-
7-14		0.31	-	-	-	0.37
7-25		0.24	0.24	0.24	-	-
7-28		0.14	-	-	-	0.19

(a) Sampling took about 20 minutes

(b) Trace <0.1 ppb

TABLE 4.3. Vertical and Transverse Average Concentration Profiles

	<u>Number of Samples</u>	<u>Average Concentration</u>	<u>Standard Deviation</u>
Pool 604 - Vertical Profile			
surface	12	3.1	0.77
30 cm ^(a)	12	2.8	0.89
10-15 cm ^(a)	12	2.7	0.76
2-5 cm ^(a)	12	2.9	0.52
Pool 604 - Transverse Profile			
north edge ^(b)	4	3.2	0.33
mid-pool ^(b)	4	3.2	0.36
south edge ^(b)	4	3.2	0.36
Pool 704 - Vertical Profile			
surface	12	0.34	0.11
30 cm ^(a)	12	0.33	0.14
10-15 cm ^(a)	12	0.32	0.13
2-5 cm ^(a)	11	0.35	0.15
Pool 704 - Transverse Profile			
north edge ^(b)	3	0.37	0.16
mid-pool ^(b)	3	0.33	0.05
south edge ^(b)	3	0.31	0.09

(a) Distance above bottom

(b) Samples taken about 10 cm below surface

$1.26 \times 10^{-2} \text{ m}^3/\text{s}$. The channel consisted of fifteen channel sections with alternating pools and riffles of equal lengths of 30.48 m. Three nodes were used to describe each channel section; the distance between nodes was 10.16 m. Therefore, forty-five nodes described the entire channel. (See Figures 3.1 and 3.2). Table 3.1 presents the hydraulic conditions used in the modeling simulation. The results of the calibration are also included in Table 3.1 under Column 11.

TABLE 4.4. Average Water Quality Values in Main Pool from
May 14 through July 31

	<u>Channel 6</u>	<u>Channel 7</u>	<u>Channel 8</u>
Alkalinity (mg/l)	161	159	159
Acidity (mg/l)	4.1	4.2	5.2
Total Hardness (mg/l)	192	192	170
Sp. Conductivity	387	381	384
pH ^(a) (Units)	8.1 to 9.1	8.0 to 9.1	7.0 to 9.1
Turbidity (NTU Units) ^(b)	---	---	3.6

(a) Range

(b) Measurement from upper riffle in Channel 8

The results presented in Table 4.5 are graphically depicted in Figures 4.1, 4.2, and 4.3. Figures 4.1 and 4.2 present the observed versus the computed stages and depths, respectively, for all 45 nodes. The diagonal line (45° angle) represents a perfect simulation between the observed and computed values. Figure 4.3 presents the longitudinal variation of stages from the extreme upstream node to the outlet. The curve represents the observed stages, while the points represent the simulated stages. The total elevation drop predicted by the modeling scenario from the inlet to the outlet equalled 0.619 ft and the observed (roughly estimated) drop in stage elevation was 0.6 ft. The standard deviation for the stages equalled 0.021 ft.

4.2 CALIBRATION RESULTS OF TODAM

The contaminant transport model TODAM was used to simulate the migration and fate of the chemical pesticide diazinon. TODAM simulated the particulate and dissolved phases of the contaminant as well as bed contamination. Channel 6 was designated as the calibration channel. The diazinon concentration at the upstream boundary was $3.1 \times 10^{-6} \text{ kg/m}^3$ (3.1 $\mu\text{g/l}$).

The calibration procedure consisted of adjusting the bed contaminant transfer rate (K_{bj}) and the in-stream contaminant transfer rate (K_j) until simulated concentrations instream and in the bed matched observed concentrations instream and in the bed, respectively. K_{bj} defines the rate at which

TABLE 4.5. DWOPER's Hydrodynamic Results (in feet)

Section	Measured Depth	Assumed ^(a) Stage	Computed Stage	Computed Depth	Error
803a	0.492	10.000	9.979	0.471	0.021
803b	0.492	9.985	9.962	0.469	0.023
803c	0.492	9.971	9.946	0.467	0.025
804a	2.198	9.963	9.945	2.180	0.018
804b	2.001	9.961	9.944	1.984	0.017
804c	1.869	9.960	9.942	1.851	0.018
805a	0.574	9.952	9.935	0.557	0.017
805b	0.574	9.937	9.920	0.557	0.017
805c	0.574	9.923	9.905	0.556	0.018
806a	2.100	9.915	9.904	2.089	0.011
806b	2.100	9.913	9.903	2.090	0.010
806c	2.100	9.912	9.901	2.089	0.011
807a	0.656	9.904	9.895	0.647	0.009
807b	0.656	9.889	9.880	0.647	0.009
807c	0.656	9.875	0.867	0.648	0.008
808a	1.968	9.867	9.866	1.967	0.001
808b	1.968	9.865	9.864	1.967	0.001
808c	1.968	9.864	9.863	1.967	0.001
809a	0.558	9.851	9.855	0.562	-0.004
809b	0.558	9.826	9.831	0.563	-0.005
809c	0.558	9.800	9.809	0.567	-0.009
810a	1.672	9.782	9.808	1.698	-0.026
810b	1.739	9.771	9.800	1.768	-0.029
810c	1.672	9.759	9.789	1.702	-0.030
811a	0.492	9.740	9.750	0.502	-0.010
811b	0.492	9.715	9.727	0.504	-0.012
811c	0.492	9.689	9.706	0.509	-0.017
812a	1.672	9.671	9.705	1.706	-0.034
812b	1.672	9.660	9.697	1.709	-0.037
812c	1.672	9.648	9.687	1.711	-0.039
813a	0.361	9.630	9.642	0.373	-0.012
813b	0.460	9.605	9.632	0.487	-0.027
813c	0.329	9.579	9.594	0.344	-0.015
814a	1.477	9.561	9.593	1.509	-0.032
814b	1.477	9.550	9.585	1.512	-0.035
814c	1.477	9.538	9.576	1.515	-0.038
815a	0.262	9.520	9.526	0.268	-0.006
815b	0.262	9.495	9.504	0.271	-0.009
815c	0.262	9.469	9.486	0.279	-0.017
816a	1.477	9.451	9.485	1.511	-0.034
816b	1.477	9.440	9.477	1.514	-0.037
816c	1.477	9.428	9.467	1.516	-0.039
817a	0.153	9.410	9.410	0.153	0.0
817b	0.153	9.385	9.385	0.153	0.0
817c	0.153	9.360	9.360	0.153	0.0

(a) Upstream stage assumed as 10 ft

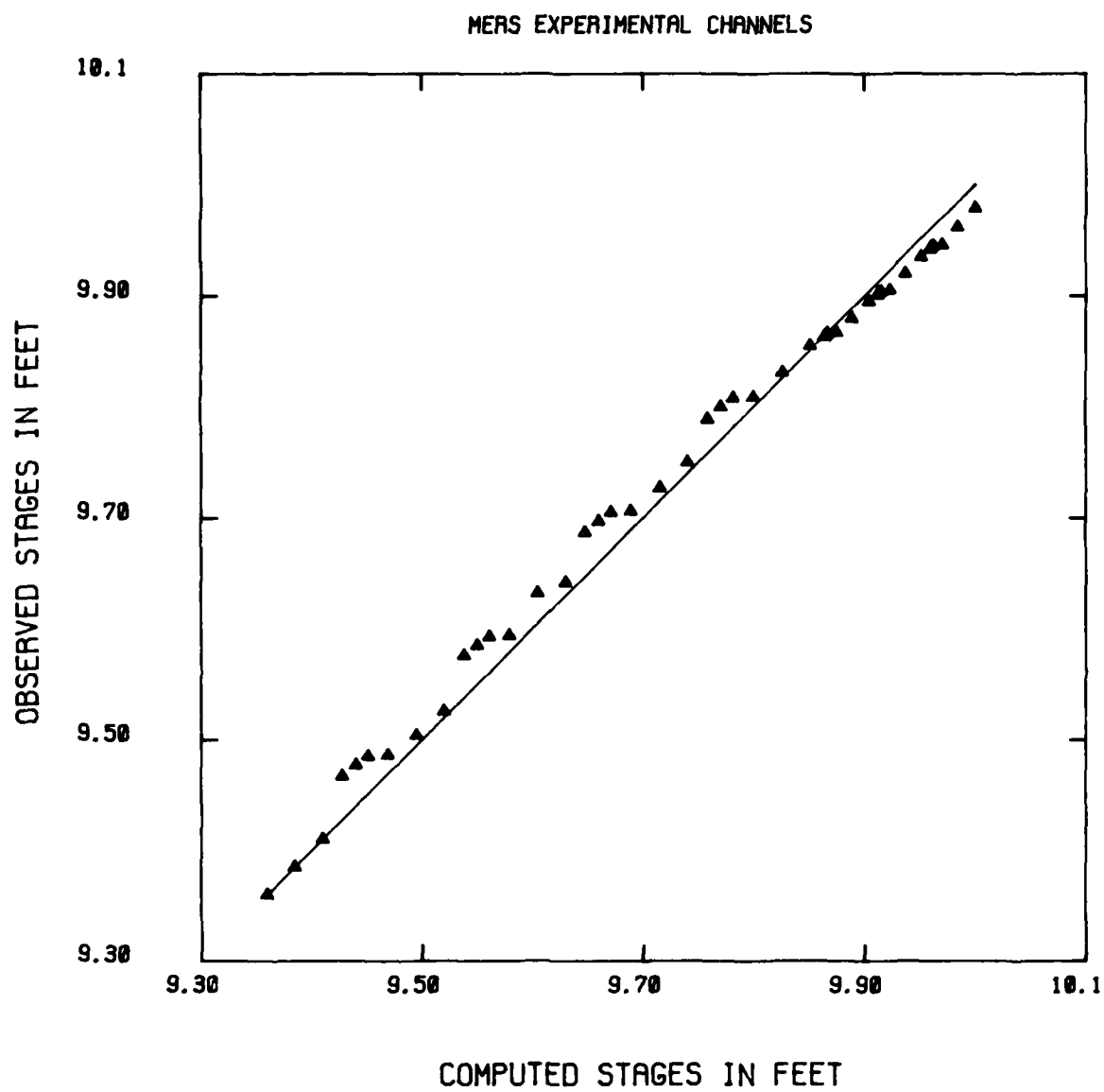


FIGURE 4.1. Observed Versus Computed Stages

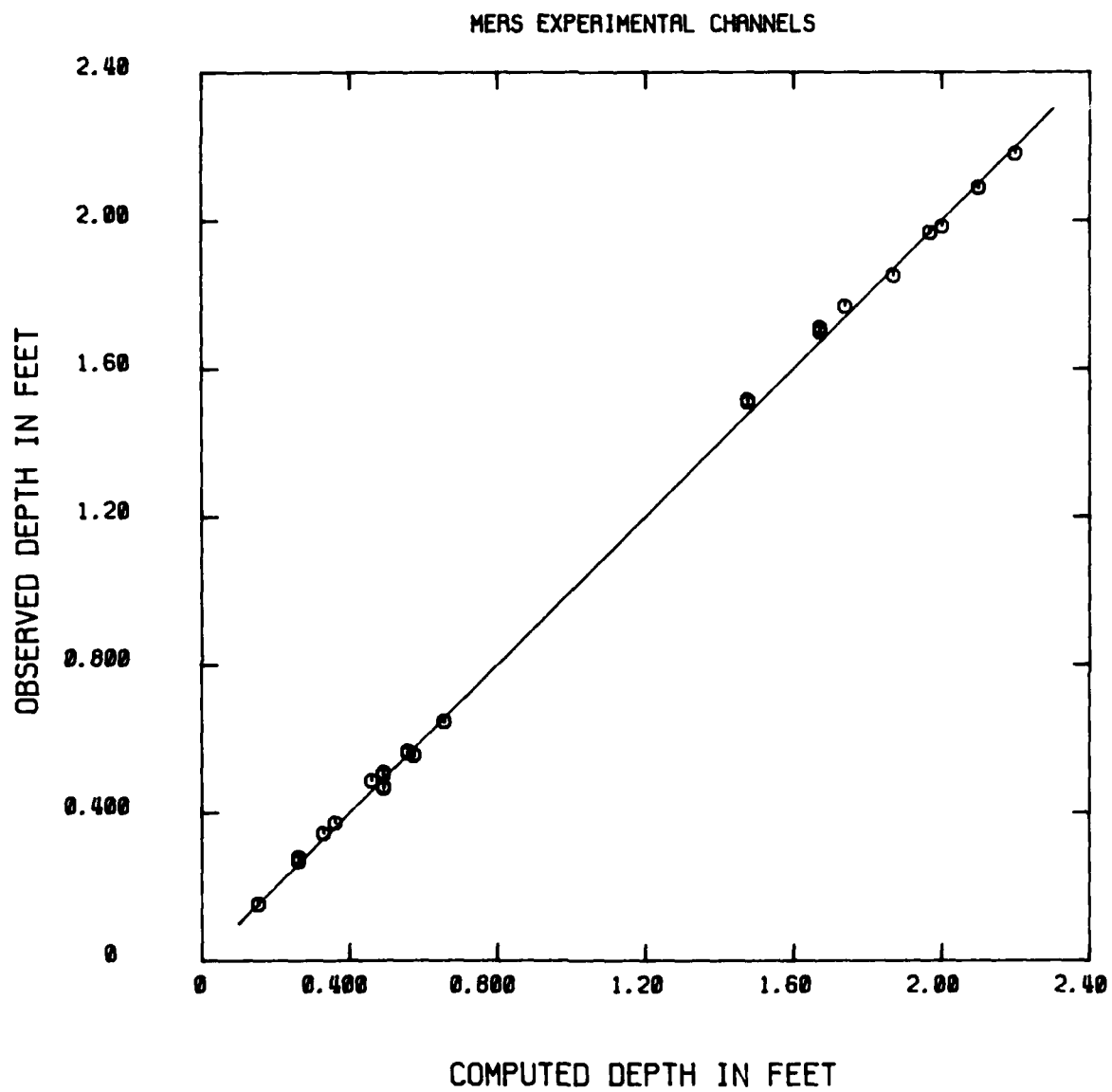


FIGURE 4.2. Observed Versus Computed Depths

MERS EXPERIMENTAL CHANNELS

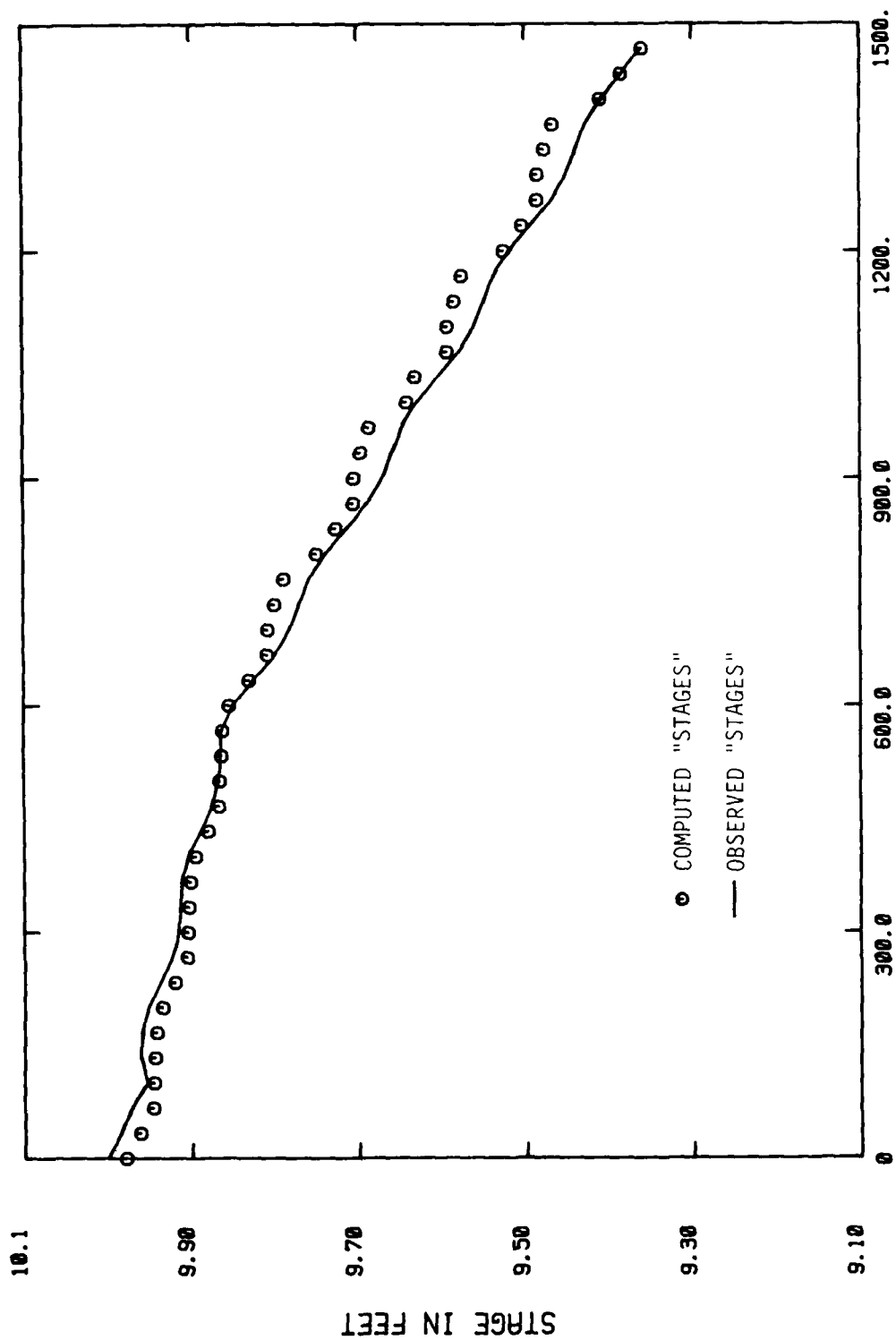


FIGURE 4.3. Longitudinal Variation of Stages

the contaminant concentrations between the dissolved phase instream and the particulate phase in the top layer of the bed proceed to an equilibrium state. K_j defines the rate at which the contaminant concentrations between the dissolved and particulate phases in-stream proceed to an equilibrium state.

Each sediment type has a bed contaminant transfer rate (K_{bj}) and an instream contaminant transfer rate (K_j) associated with it. The bed contaminant transfer rate was considered equal for each sediment type. Likewise, the in-stream contaminant transfer rate for each sediment type was considered equal. The assumption of a constant K_j and K_{bj} value between sediment types is probably incorrect, but due to a lack of data, this assumption appears necessary.

Strictly speaking, values of K_{bj} and K_j should be selected from field or laboratory testing and should not be subjected to model calibration. However, a lack of information on K_{bj} and K_j required these values to be selected as part of the model calibration. K_j and K_{bj} were adjusted until an acceptable simulation resulted. K_j and K_{bj} were calibrated as $9.0 \times 10^{-6} \text{ s}^{-1}$ and $3.136 \times 10^{-5} \text{ s}^{-1}$, respectively. It should be noted that the value of K_{bj} should be smaller than the value of K_j (adsorption/desorption with bed sediment is slower than with suspended sediment). K_j could have been increased with little adjustment to K_{bj} . Since K_j adjusts the in-stream diazinon distribution between particulate and dissolved phases, the total in-stream diazinon amount would have been effected very little.

The results of the calibration are presented in Figures 4.4 and 4.5. Figure 4.4 presents the concentration of diazinon by weight, varying temporally, in the bed in channel section four. The plotted points represent the measured amount of diazinon adsorbed to bed sediment, while the curve represents the simulated results. Table 4.6 presents the measured diazinon in bed samples from pool 604 during the five days of computer simulation. The measured and simulated concentrations of diazinon coincide for the first 24 hr, after which the measured diazinon concentration decreases to approximately zero at the 72-hr mark, while the simulated concentrations apparently increase at a

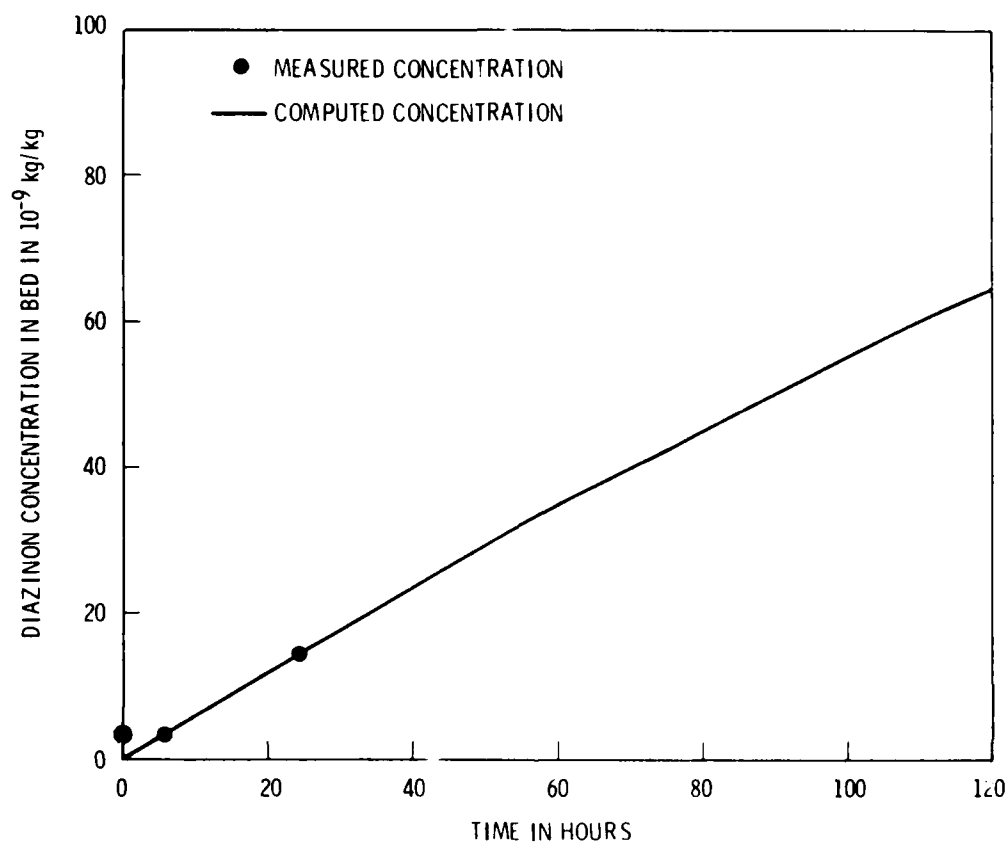


FIGURE 4.4. Bed Contamination History for Section 604 Test Case 3.1 ppb

linear rate. This apparent linear rate is expected in the initial hours of the simulation because the bed was practically devoid of diazinon. With time, the rate of increase of the diazinon concentration in the bed is expected to decrease as the distribution coefficient between the dissolved phase of diazinon in-stream and the particulate phase in the top layer of the bed for each sediment type is approached.

As the deposition and resuspension of contaminated sediment is assumed to be insignificant, the major mechanism generating the contamination in the top layer of the bed appears to be direct adsorption between the dissolved diazinon in-stream and bed sediment. Based on this, the contaminant concentration in

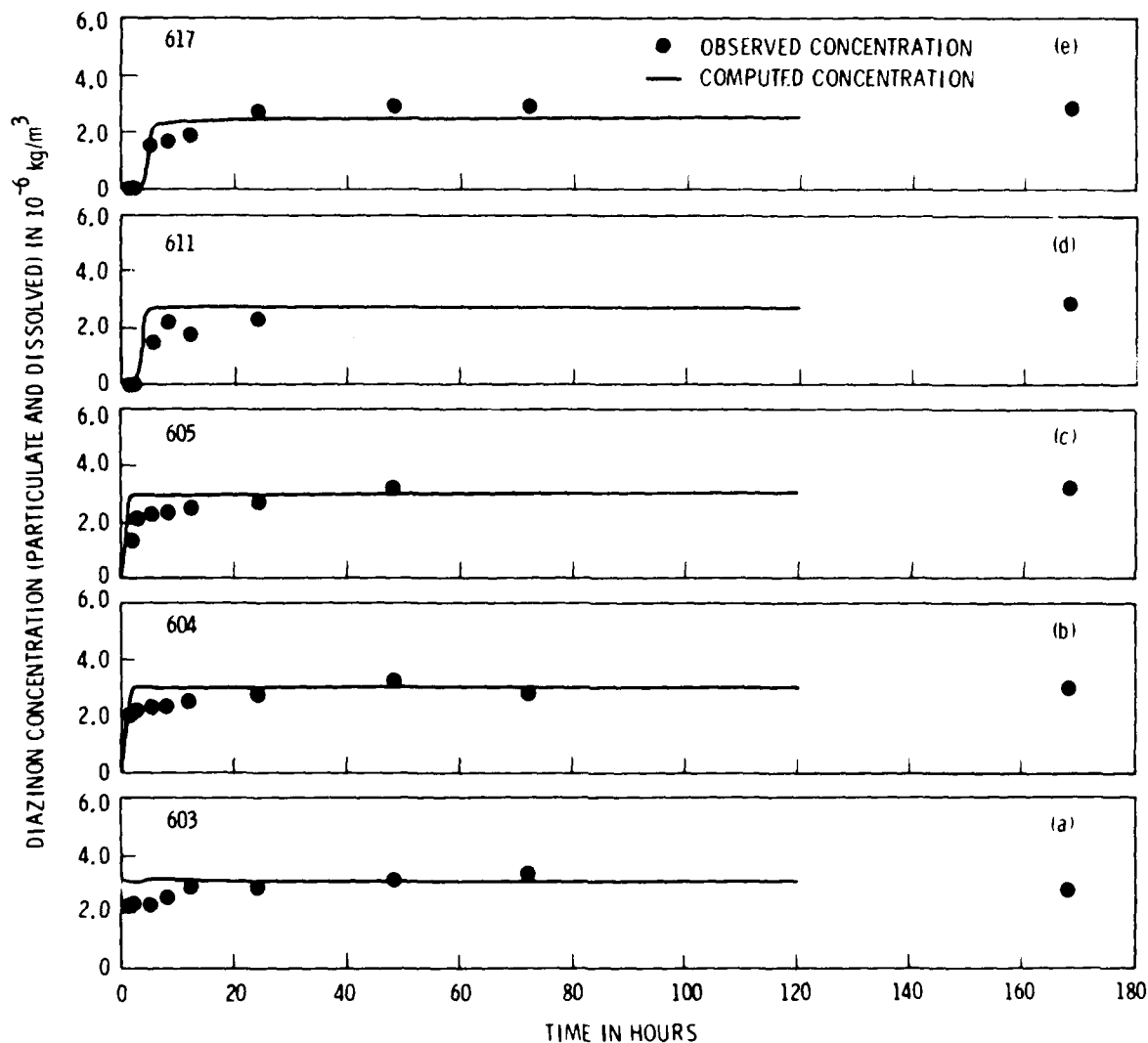


FIGURE 4.5. Diazinon Concentrations in Channel 6

the bed should be increasing with time, not decreasing, because the equilibrium point between the dissolved diazinon phase in-stream and the particulate phase in the bed has not been reached or exceeded. The last two subsamples as presented in Table 4.5, therefore, appear to contradict the physics-based phenomena occurring in-stream. Because of this discrepancy only the first two subsamples presented in Table 4.6 were used in calibrating K_{bj} and K_j in the model. This discrepancy may have been the result of degradation before the

TABLE 4.6. Contaminated Bed Sample from Pool 604

<u>Subsample Number</u>	<u>Date Sampled</u>	<u>Date Analyzed</u>	<u>Storage Procedure</u>	<u>Concentration (10^{-9} kg/kg)</u>
1	05/14/80	08/05/80	refrigerated	3.3
2	05/15/80	09/19/80	refrigerated	14.2
3	05/16/80	09/24/80	refrigerated	10.3
4	05/17/80	09/30/80	refrigerated	<1.1

samples were analyzed. Analysis of sediment sampled from pool 606 on July 9, 1980 and analyzed on July 11, 1980, has a concentration of 34×10^{-9} kg/kg which agrees with the expected trend of increasing diazinon concentration in the bed until equilibrium is reached.

Because K_j indicates how quickly diazinon reaches its equilibrium conditions (determined by K_d) between dissolved and particulate phases, it does not affect the total amount of diazinon in-stream. It can affect the amount adsorbed onto the bed sediment, since the amount of diazinon in the bed depends on the dissolved amount in-stream. Because there was little deposition or resuspension of sediments, only the adsorption/desorption process occurs between the dissolved phase of diazinon in-stream and the diazinon amount in the bed. Because diazinon has small distribution coefficients and sediment concentrations in these two channels were small, the amount of sorbed diazinon (suspended and in the bed) was small compared to the amount in-stream.

Figure 4.5 presents the concentration of diazinon varying temporally at sections 3, 4, 5, 11, and 17. The plotted points represent the measured in-stream concentration, while the curve represents the simulated results. Each section (3, 4, 5, 11, and 17) in Figure 4.5 exhibits two distinct regions: the unsteady region and the steady-state region. Based on measured concentrations, the unsteady region generally encompasses the first 24 hours in which the concentration increases until it reaches a value of approximately 2.8×10^{-9} kg/kg (2.8 ppb). The lag time between the observed and simulated concentrations in this region is 1 to 10 hours. A 1- to 10-hr lag time indicates that possibly the concentration levels are being monitored at non-representative locations, the model is simulating the initial contaminant migration inaccurately, or that

the water and diazinon channel are not well mixed. This is especially evident in section 3. After 8 hr, the measured diazinon concentration at the extreme upstream boundary ($2.4 \mu\text{g/l}$) is still 23% below the upstream boundary condition of $3.1 \mu\text{g/l}$. This problem is alleviated as the diazinon moves downstream, indicating more mixing of diazinon within the flow.

The steady-state region coincides with any time greater than 24 hours. The long-term simulation results of the diazinon concentration in Channel 6 at sections 3, 4, 5, 11, and 17 are presented in Figure 4.6. The solid curves represent the simulated diazinon concentrations by TODAM (The first 5 days). The broken curves represent the extrapolated diazinon concentrations based on TODAM's five-day results. The plotted points represent the observed diazinon concentrations. The extrapolations of the simulated concentrations in channel sections 3, 4, and 5 consisted simply of extending the computed curves, since near steady-state conditions were reached by the time the extrapolation was performed. The extrapolations of the simulate results in sections 11 and 17 were performed by continuing the rate of change in concentration at the same rate of the last few simulated time steps. This procedure appears valid since the temporal variation of the diazinon concentration in these sections was very small (e.g., $\sim 10^{-14} \text{ kg/kg-s}$). The general trends between the simulated and observed concentrations are the same. In fact, for the steady-state case the error is approximately 3% to 6%. The deviation in observed and measured concentrations is approximately $\pm 0.20 \times 10^{-9} \text{ kg/kg}$. The smallest discrepancies between the computed and observed depths were located in the upstream half of the channel where the risk assessment was performed.

4.3 MODELING RESULTS OF TODAM

The contaminant transport model TODAM was calibrated on Channel 6 of the MERS channels. The test run was performed on Channel 7, with a diazinon concentration at the upstream boundary of $3.1 \times 10^{-7} \text{ kg/m}^3$ ($0.31 \mu\text{g/l}$). Table 4.7 presents the measured contaminated bed samples from pool 704. The results of the test run are presented in Figures 4.7 and 4.8. Figure 4.7 presents the concentration of diazinon by weight, varying temporally, in the bed in channel section four. The dotted line represent the range of the

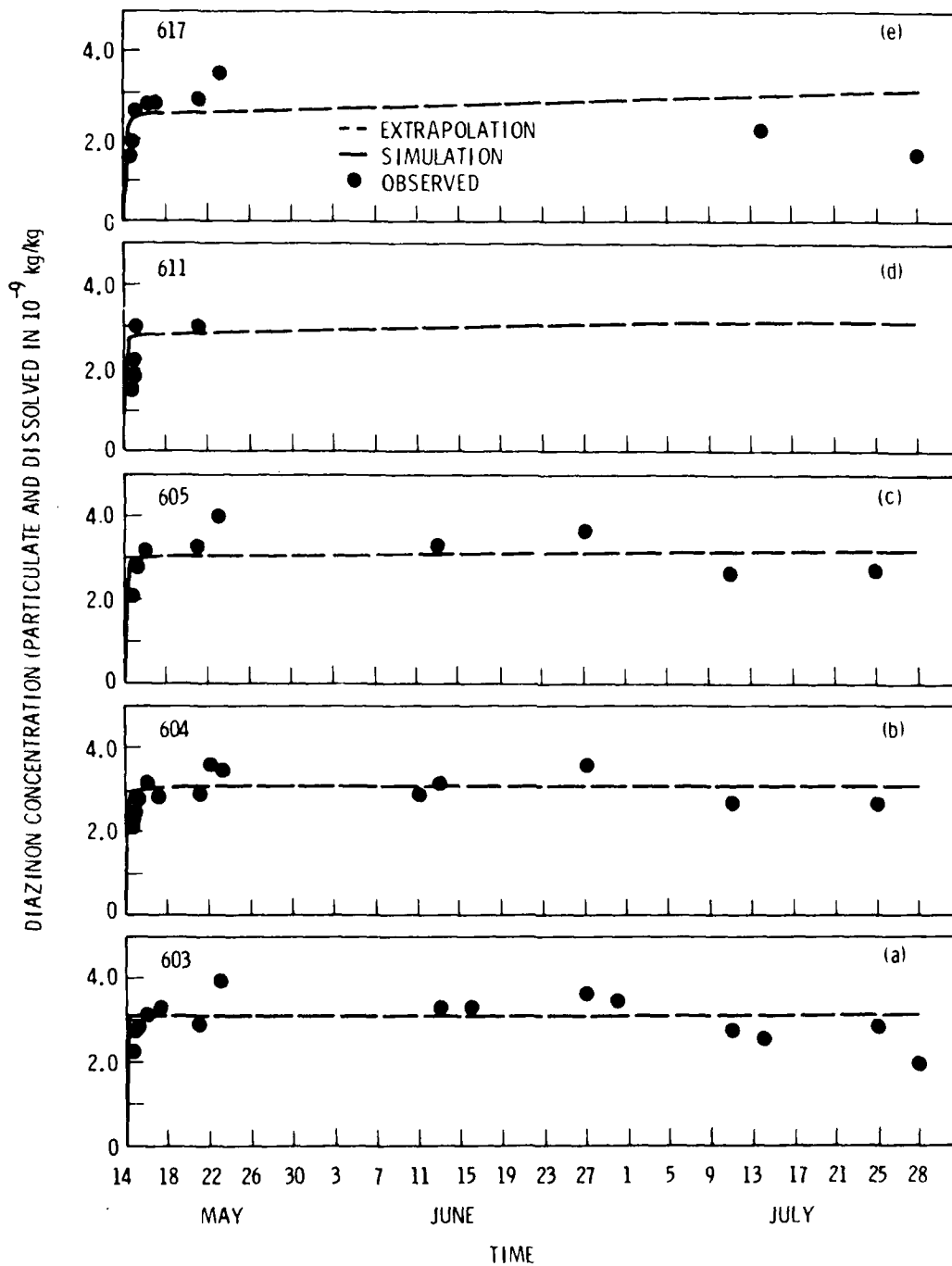


FIGURE 4.6. Diazinon Concentration Extrapolated Results on Channel 6

TABLE 4.7. Contaminated Bed Sample From Pool 704

Number	Date Sampled	Date Analyzed	Storage Procedure	Concentration (10^{-9} kg/kg)
1	05/14/80	08/07/80	refrigerated	<5.4
2	05/16/80	09/23/80	refrigerated	<1.6

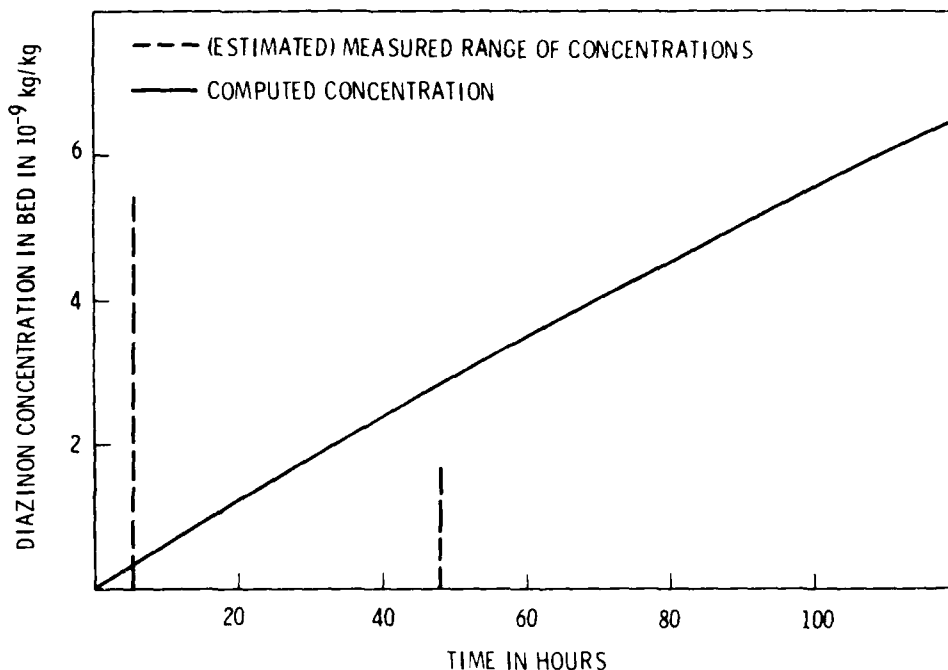


FIGURE 4.7. Bed Contamination History for Section 704 Test Case 0.31 ppb

diazinon concentration in the bed as provided by MERS personnel, while the curve represents the computer simulation of the bed contamination. For the time period presented in Figure 4.7 the simulated contamination of the bed by diazinon appears to steadily increase, whereas the range of the diazinon concentrations in the bed appears to decrease with time. As discussed earlier in Section 4.1 (with respect to Figure 4.4), the simulated increase of diazinon in the bed with time was expected. The rate of contamination is expected to decrease as the distribution coefficient between the dissolved phase of diazinon in-stream and the particulate phase in the top layer of the

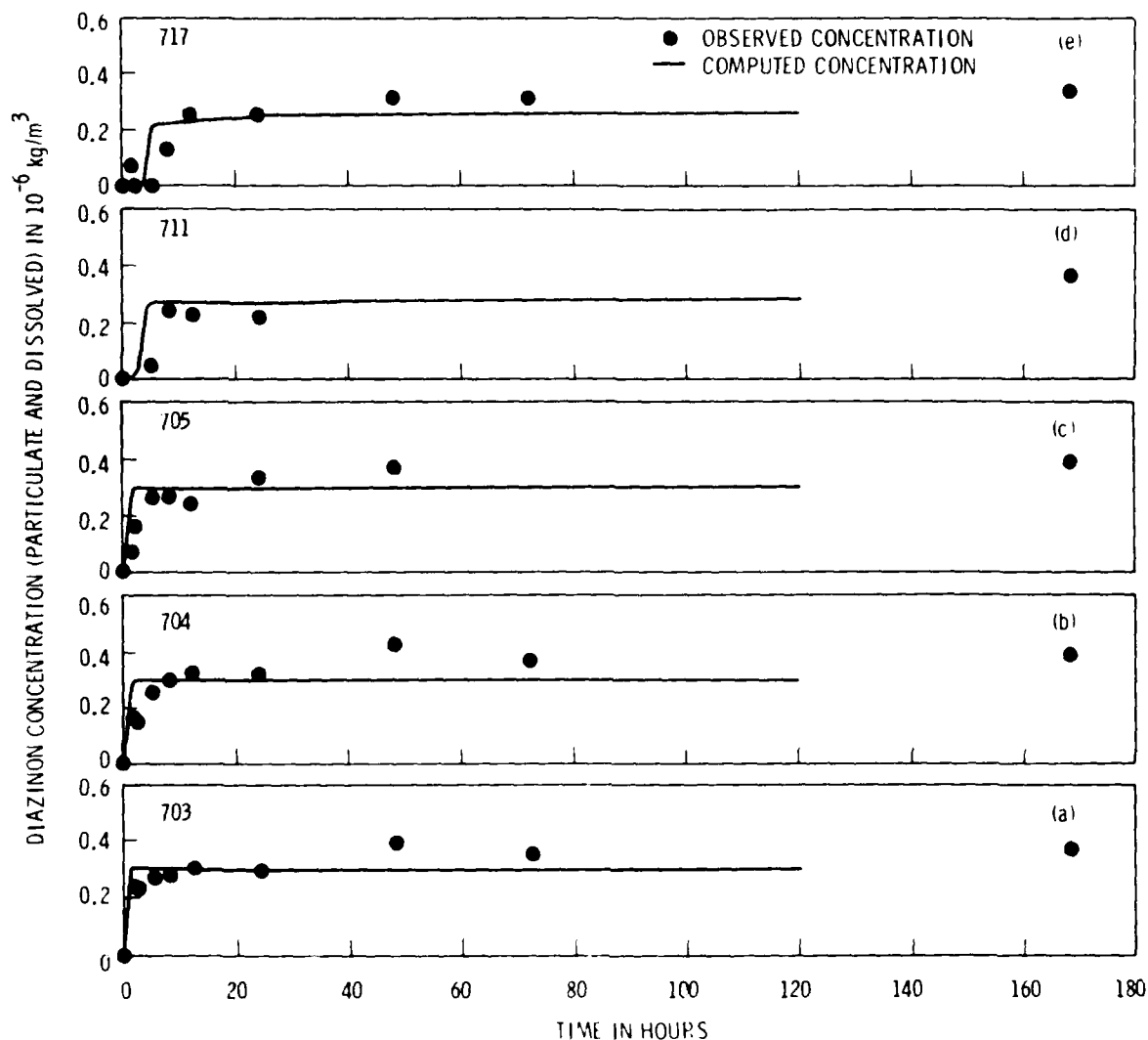


FIGURE 4.8. Diazinon Concentrations in Channel 7

bed for each sediment type is approached. The concentration range (as roughly measured) appears to continually decrease as time increases. As the major mechanism generating the contamination in the top layer of the bed appears to be direct adsorption between the dissolved diazinon in-stream and bed sediment (as explained earlier), the contaminant concentration in the bed should be increasing, not decreasing. One reason for this discrepancy was discussed in Section 4.1 (with respect to Figure 4.4). In addition, two other reasons are mentioned below:

1. The measured concentrations presented in Figure 4.7 represent a range of the concentration. The range should not necessarily imply a decrease in bed contamination.
2. Because the simulated results presented in Figure 4.7 are indirectly based on the measured results presented in Figure 4.4, the simulated results may be inaccurate.

Figure 4.8 presents the concentration of diazinon varying temporally at sections 3, 4, 5, 11, and 17. The plotted points represent the measured in-stream diazinon concentration, while the curve represents the simulated results. As in the calibration case, there appear to be two distinct regions for each section (3, 4, 5, 11, and 17) in Figure 4.8: an unsteady region and a steady-state region. Based on measured concentrations, the unsteady region appears to encompass the first 8 to 12 hr, in which the concentration increases until it reaches a value of approximately 3.0×10^{-10} kg/kg (0.30 μ g/l). The lag time between the observed and simulated concentrations in this region is approximately 4 hours. As discussed previously in Section 4.1 (with respect to Figure 4.5), a 4-hr lag time indicates that either the concentration levels are being monitored at non-representative locations, the model is simulating the initial contaminant migration inaccurately, or that the water and diazinon in the channel are not well mixed. This point is illustrated in Section 3. After 5 hr the measured concentration at the extreme upstream boundary (0.275 μ g/l) is still 11% below the upstream boundary condition of 0.31 μ g/l. The lag time appears less prevalent in the test Channel 7 than in the calibration Channel 6.

The steady-state region coincides with any time greater than 12 hours. The long-term in-stream contamination simulation at five section locations (3, 4, 5, 11 and 17) in Channel 7 is presented in Figure 4.9. The solid curves represent the simulated diazinon concentrations by TODAM (the first five days). The broken curves represent the extrapolated diazinon concentrations based on TODAM's five-day results. The plotted points represent the observed diazinon concentrations. The extrapolation of the simulated concentrations in sections 3, 4, and 5 consisted simply of extending the computed curves, since near steady-state conditions were reached by the time the extrapolation was

AD-A111 068

BATTELLE PACIFIC NORTHWEST LABS RICHLAND WASH
SIMULATION OF THE MIGRATION, FATE, AND EFFECTS OF DIAZINON IN T--ETC(U)
DEC 81 M A PARKHURST, G WHELAN, Y ONISHI

F/6 13/2

UNCLASSIFIED

NL

2 OF 2

AD-A
11068



END
DATE
FILMED
13-82
DTIC

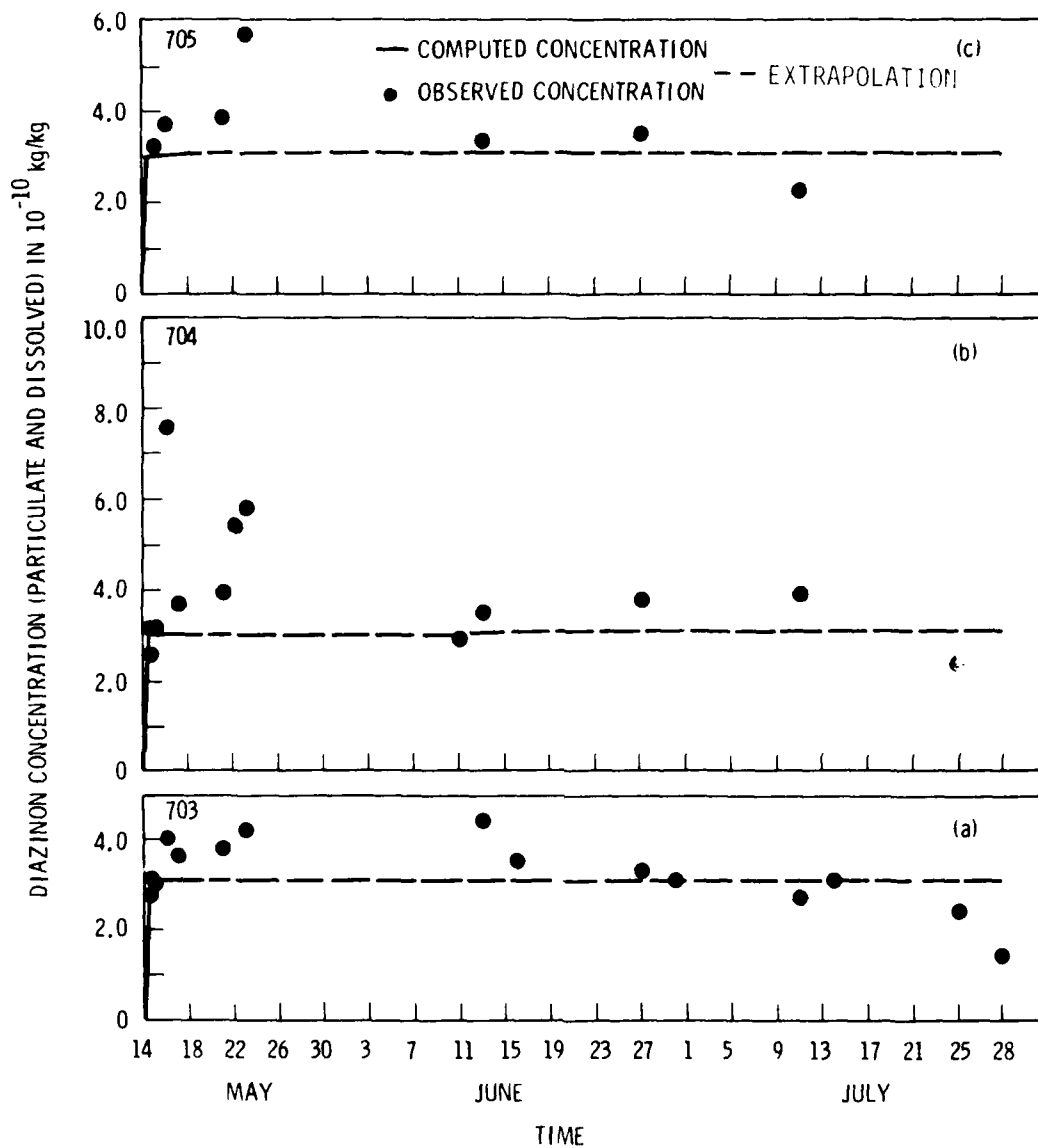


FIGURE 4.9. Extrapolated Diazinon Concentration Results on Channel 7

performed. The extrapolation of the simulated results in sections 11 and 17 was performed by continuing the rate of change in concentration at the same rate of the last few simulated time steps. This rate was of the order of 10^{-15} kg/kg-s. In this region the measured concentrations appear consistently higher than the simulated concentrations. The concentration levels

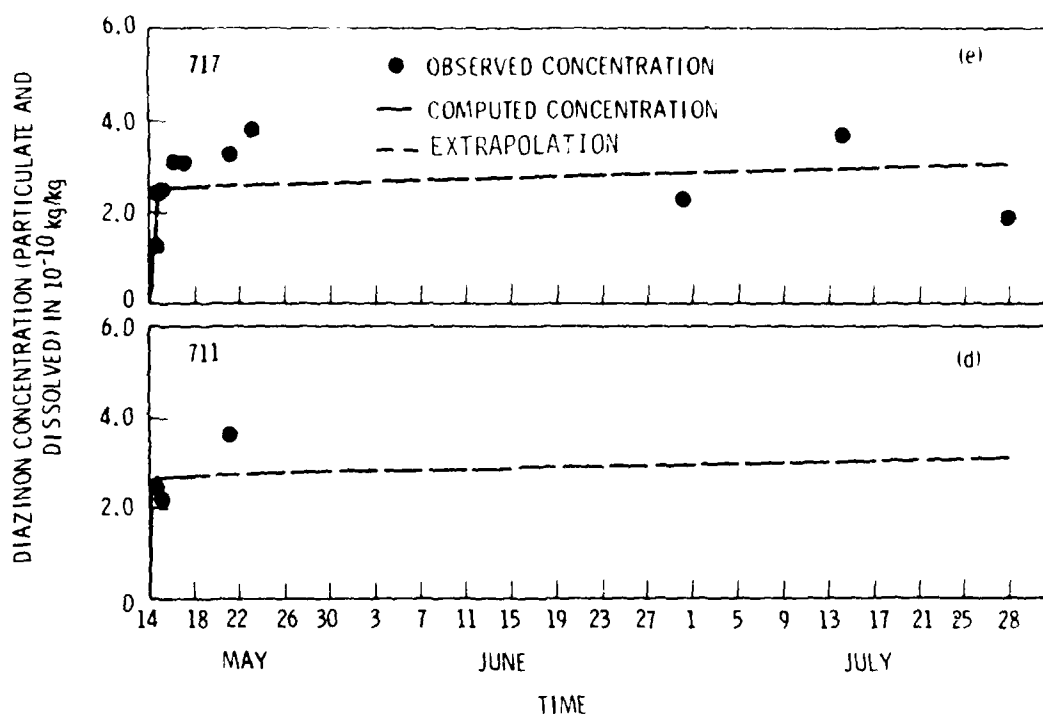


FIGURE 4.9. (contd.)

measured in Channel 7 are one order of magnitude less than the concentration levels in Channel 6. Because of the smaller concentrations, insignificant variabilities experienced in Channel 6 were significant in Channel 7. For the steady-state case, the variability is on the order of 15% to 30% with a deviation of 0.05 to 0.10×10^{-9} kg/kg. In addition, channel section four appears to have a measured outlier associated with it at the 48-hr mark. The measured concentration here is 7.6×10^{-10} kg/kg ($0.76 \mu\text{g/l}$), which is approximately 200% higher than the other measured concentrations. This concentration should be considered an outlier, as its effects do not appear in any upstream or downstream location at anytime. One would expect an increase in the downstream concentrations after the 48-hr mark. This concentration measurement could possibly be caused by sample contamination or a recording error.

4.4 RISK ASSESSMENT

The CMRA risk assessment usually relies on LC50 and MATC curves to help interpret the probable effects of simulated toxicant concentrations to the fish species of interest. However, because the concentrations were below LC50 values for the fathead minnow and an MATC has not been established, the usual approach was not applied to this situation.

The FRANCO analysis was used to provide a summary of the concentration over the five days at four sites in Channels 6 and 7. From this summary it was possible to determine how long it took for each site to reach its highest and continuous concentrations. In the first pool of the study area in both channels, the intended concentrations of 3.0 and 0.3 $\mu\text{g/l}$ were reached in an hour (Tables 4.8 and 4.9). The model simulation predicted that riffles 617 and 717 reached concentrations no higher than 2.4 and 0.24 $\mu\text{g/l}$, respectively, in the first five days.

The acute and chronic laboratory data generated for fathead minnows (Tables 3.16 and 3.17) indicate that lethality has been noted with a 96-day exposure to 6900 $\mu\text{g/l}$ of diazinon. The MATC may be close to 3.2 $\mu\text{g/l}$ though some spinal deformity (scoliosis) has been observed at this concentration (Allison and Hermanutz 1977).

Considering the relatively high concentration noted for acute lethality, we predict that there should have been no mortality resulting strictly from

TABLE 4.8. Computer Simulated Results of the Minutes Before Each Concentration was Achieved in Channel 6

Concentration ($\mu\text{g/l}$)	Section			
	604	605	612	617
0.001	12	21	129	186
0.010	12	24	141	204
0.10	15	27	165	234
1.0	24	48	213	301
2.0	36	66	249	342
2.5	45	84	282	---
3.0	60	--	---	---

TABLE 4.9. Computer Simulated Results of the Minutes Before Each Concentration was Achieved in Channel 7

Concentration ($\mu\text{g/l}$)	Section			
	704	705	712	717
0.001	12	24	141	204
0.010	12	27	165	234
0.10	24	48	213	301
0.20	36	66	249	342
0.25	45	84	282	---
0.30	60	--	---	---

diazinon exposure at 0.3 or 3.0 $\mu\text{g/l}$ to the population. Because of the nearly constant low concentrations, this can be concluded without the formal risk assessment procedure. The only channel data with which to compare the mortality studies is the study of caged minnows in each stream, which were originally intended for ovary and gonad study. In this study, two cages were placed in each channel. Cages A and B each had 80 adult fish that were placed in the channels on June 4, 1980. This is in addition to the free-roaming juveniles originally stocked in the channel study sections. By July 29, mortality approached 40% (Table 4.10). Most of this mortality probably occurred shortly after caging as adult fish appear to be more susceptible to injury and death from caging than juveniles are. However, the fish were not counted until the end of July so there is no verification of this. These data present no evidence of increased mortality of the fish when exposed to diazinon. We applied two different statistical procedures to the data, a simple chi-square test and

TABLE 4.10. Survival of Caged Fathead Minnows

Date	Number of Fish per Cage					
	Control		3.0 $\mu\text{g/l}$		0.3 $\mu\text{g/l}$	
	A	B	A	B	A	B
06/05	80	80	80	80	80	80
07/29	47	47	45	41	45	51
08/14	40	44	42	41	42	51

the Kruskal-Wallis nonparametric test for differences among several samples. The results were essentially the same: no differences in fish mortality among the three channels can be inferred. This tends to confirm that diazinon concentrations of 3.0 $\mu\text{g/l}$ are not high enough to cause mortality in adult minnows. This concentration would not be expected to directly kill other fish species having a higher LC50 than the minnow.

Sublethality predictions cannot be quantified with results of the concentration simulations and the known chronic data. Laboratory investigations have not conclusively determined whether long-term exposure of fathead minnows to concentrations less than 3.2 $\mu\text{g/l}$ are responsible for detrimental effects. We can predict from this information that some incidence of scoliosis may be present, and possible reduced resistance to sublethal effects to progeny may occur. According to these data and other information known about this chemical including its persistence, we would not project dramatic detrimental effects.

The results of EPA's biological experimentation are still preliminary. EPA investigators analyzing the data have come to several tentative findings regarding the fathead minnow population. The first is that the 3 $\mu\text{g/l}$ channel had a significant increase in dead eggs compared to Channels 7 and 8 though there was no significant difference between the control channel and the treatment channels in the average number of eyed eggs per observation (Table 4.11). A second finding is that the 3.0 $\mu\text{g/l}$ channel yielded mostly medium-sized second-generation fish. The median size peaked sharply at 50 mm and showed little variation. This contrasted with Channels 7 and 8, which produced less size uniformity. A third finding is that there were fewer juvenile minnows found downstream in Channel 6 when compared to Control Channel 8. These juveniles represent the progeny of the originally stocked fish. As larvae, they were able to pass through the screen barriers at the end of the study sections and swim freely in the downstream sections of the channels where their populations were sampled. A probable explanation for the extremely low juvenile population in Channel 7 is that there was a large population of carnivorous brook stickleback fish residing in the lower reaches of Channel 7.

TABLE 4.11. Condition of Fathead Minnow Eggs

	<u>Channel 6</u>	<u>Channel 7</u>	<u>Channel 8</u>
Percent "Eyed" Eggs	45.3	40.1	43.6
Percent Dead Eggs	4.9	0.05	0.17

The reduced number of juveniles in Channel 6 (downstream) cannot be attributed only to diazinon because within the two riffle-one pool study sections there was no significant difference in the number of second generation juveniles among the channels.

An additional result from EPA's analysis is that no incidence of scoliosis in the fathead minnows was detected by the field crew in their routine sampling.

Invertebrates tend to be more sensitive to diazinon than fish (Table 3.16), and those with LC50s less than the concentrations in the channels may suffer lethal or sublethal effects. Results of the emergence of predominant taxa during the period May 22 to June 12 are recorded in Table 4.12 but conclusions have not been drawn.

Although we would like to extend the risk assessment to cover invertebrates, three major reasons prevent us from making comparisons of field versus laboratory conclusions on the invertebrates: 1) the primary invertebrates found in the channel are not the same species as those previously studied for diazinon exposure; 2) EPA has compiled only preliminary data on the invertebrates and has not completed its analysis; 3) not enough information has been generated on exposure mechanisms.

All of the above field data were supplied by EPA-Monticello and appear in their Preliminary Data Summary. More extensive information on their procedures, analysis, results and conclusions will be presented in their final report after the analysis on the 1980 diazinon study is complete.

Their data on the fathead minnow suggest that the continuous 3.0 $\mu\text{g/l}$ concentration has some effect on increasing the numbers of dead eggs and modifying the size of the offspring. Because there was no significant difference in the number of apparently viable (eyed) eggs, it is difficult to

TABLE 4.12. Distribution of the Predominant Invertebrate Taxa in the Riffles and Pools at a Peak Emergence Period

	Total Numbers Emergence		
	Riffle	Pool	Period
Control Channel			
<u>Chironomus attenuates</u>	4	122	May 29 - June 5
<u>Cricotopus</u> sp.	72	15	No discrete peak
<u>Dicrotendipes fumidus</u>	279	252	May 29 - June 5
<u>Micropsectra</u> sp.	100	63	May 22 - May 29
<u>Orthocladiinae</u>	92	27	May 29
<u>Tanytarus</u> spp.	129	92	May 29 - June 5
<u>Cheumatopsyche</u>	56	3	
Low Concentration Channel			
<u>Chironomus attenuates</u>	15	112	May 29 - June 5
<u>Cricotopus</u> sp.	55	7	May 29
<u>Dicrotendipes fumidus</u>	58	15	June 5
<u>Micropsectra</u> sp.	269	2	May 22 - May 29
<u>Orthocladiinae</u>	257	2	May 22 - June 12
<u>Tanytarus</u> spp.	140	49	May 29 - June 5
High Concentration Channel			
<u>Chironomus attenuates</u>	52	102	May 29 - June 12
<u>Corynoneura</u> sp.	1	-	No discrete peak
<u>Dicrotendipes fumidus</u>	200	308	May 29 - June 12
<u>Micropsectra</u> sp.	132	3	May 22 - May 29
<u>Tanytarus</u> spp.	48	17	June 5

(a) Predominate taxa are insects comprising >5.0% abundance within an order or family.

NOTE: Chironomid abundance expressed by number of males present.

determine this as an effect on population abundance. Likewise, the uniform size of the second generation is a curious result, but hardly dramatic enough to determine it a particularly dangerous effect without further study.

5.0 CONCLUSIONS AND RECOMMENDATIONS

The hydrodynamic modeling simulation results by DWOPER were comparable to the measured conditions in-stream. Discrepancies between observed and measured flow depths were very small and were within the range of measurement accuracy. These results, therefore, tend to confirm the credibility of the assumptions used in the model (i.e., generic cross sections and water surface slopes). Because of the macrophyte growth and possible storage areas created by this growth, the hydrodynamic flow condition may not have been simulated with the accuracy suggested by the results. Because of this macrophyte growth, the total cross section may contain storage areas where the flow velocity is negligible. In such a case, the effective flow area would be smaller and the effective flow velocity would be higher than what the simulation results suggest. Based on the overall results and on the results from other investigators (Hahn 1978; Hahn et al. 1978a; 1978b), the discrepancy appears to have an insignificant effect on the final results.

The calibration procedure of TODAM was based on the diazinon contamination levels in-stream and within the bottom sediment. The calibration of the bed contamination was based on very little data. Additionally, the sediment data showed considerable variation in diazinon concentration which may have been due to changes in the sampling depth as well as to degradation occurring during sample storage. Results of other portions of sediment analysis such as size fraction distribution and organic content provided much of the necessary data and support for assumptions made to fill certain data gaps. Although many necessary input data for modeling were not directly measured, we could estimate them indirectly from various available information. However, since simulation results depend highly on integrity of the input data, model calibration and verification were limited.

The calibration of the in-stream contamination was based on samples at five locations: Sections 3, 4, 5, 11, and 17 in Channel 6. The general trends between the simulated and observed concentrations are the same. There is some variability, though, between the simulated and observed concentrations. This may be due to several factors two of which are storage areas not accurately

simulated and possible complications caused by macrophyte growth. The channel areas around the macrophyte growth could act as storage areas for diazinon thereby allowing diazinon, to be released later in the simulation.

The test/validation run for the in-stream contamination was based on samples at five locations: Sections 3, 4, 5, 11, and 17 in Channel 7. The simulated concentrations from TODAM were compared to the observed concentration levels of diazinon in the bed and in-stream in Channel 7. Because of an inadequate supply of bed contamination levels for Channel 7 and because of the 4 to 5 month lag time before bed samples were analyzed, a cogent analysis identifying the degree of accuracy between simulated and observed bed concentrations was not possible. The general trends between the simulated and observed concentrations are the same except for the time period between May 16 and May 24. The discrepancy during this time period may be due to several things including storage areas not accurately simulated and possible complications caused by macrophyte growth and possible build-up of diazinon in the biota. The simulated concentrations for the remaining time period matched the observed concentrations fairly well. Since the concentrations in Channel 7 are one order of magnitude lower than the concentrations in Channel 6, a wider range of variability about the mean was expected.

Steady-state (but nonuniform) flow conditions with a constant flux of diazinon entering as a point source at the inlet of the channels represented the controlled (dependent) parameters in this study. The mechanisms governing the migration and fate of diazinon were not individually isolated. These mechanisms included:

- deposition and resuspension of three sediment types (i.e., cohesive, noncohesive, and organic matter)
- adsorption/desorption process between the dissolved phase of diazinon and the particulate phase in-stream and in the bed
- degradation
- dispersion.

It should be noted that other parameters (such as salinity, temperature, pH, etc.) in this study also affect the fate of chemicals, but were not considered.

For this study, the only measureable mechanism for bed contamination appeared to be the direct adsorption/desorption mechanisms between the dissolved diazinon and sediments in the top layer of the bed. The sediment (and corresponding diazinon adsorbed onto the sediment) deposition and resuspension mechanism were relatively insignificant. The degradation phenomenon was also insignificant because the half-life of the contaminant was much longer (~18 days) than the time for the diazinon to travel the entire length of the channel (~12 hr). Since the latter two mechanisms were insignificant in reducing the diazinon levels in-stream, more diazinon was available to affect the in-stream aquatic life.

In-stream diazinon concentrations of 3.0 and 0.3 $\mu\text{g/l}$ were too low to provide much of a test of the risk assessment portion of the methodology. The validity of the risk assessment has three major aspects. First, it requires accurate in-stream modeling of the toxicant from the migration and fate codes. This was the parameter we were able to partially evaluate. Second, the risk assessment relies heavily on the validity of using laboratory-derived data to predict field mortality or morbidity. Evaluating this issue for diazinon for certain organisms was one of EPA's objectives for the diazinon channel experiment. EPA's conclusions on this aspect are not yet available. The third aspect of the assessment is the validity of the investigator's interpretation of the above results. Discrepancies may result from chemical sensitivity, resistivity, or a tendency of the organisms to migrate from the contaminated area. Relative comparisons of various toxicants should produce accurate results if the modeling has been properly applied, if differences between laboratory and field results are factored in the analysis, and if unusual synergistic or antagonistic mechanisms do not drastically change the effective exposure concentration.

From the results of the Monticello study, these conclusions regarding the risk assessment can be made:

- This study was not adequate to test the risk assessment portion of the methodology.
- A more strenuous test with higher and variable concentrations would be useful to evaluate the predictive risk assessment results versus

actual field results. This kind of test could reveal weaknesses in the methodology where models could be modified to better simulate the results.

- The risk assessment predicted no mortality of fathead minnows from long-term exposure to diazinon. Preliminary field results show no significance in mortality between either diazinon-treated channels or the control channel.
- Little or no chronic toxicity to fathead minnows was projected to occur over the season. The possibility of scoliosis in the adults and reduced hatchability of the eggs could be expected in Channel 6. Field results revealed no positive evidence of scoliosis and ambiguous results on egg hatchability.
- Toxicological information such as LC50s and MATCs may have real value in approximating effects in a field situation. The 3.0 µg/l concentration, which approaches the apparent MATC for fathead minnows, did appear to "protect" the minnows from lethality or obvious population parameter changes though some increase in nonviable eggs did occur.

Recommendations for Future Field Modeling Studies

Estimation of the potential risk posed by the release of chemical substances into the environment requires that methodologies be established that fit the nature and magnitude of the release and the desired resolution of environmental effects. The CMRA methodology predicts the occurrence and longevity of a given chemical in the environment and evaluates the probability of acute and chronic damages to biota by using mathematical models. The effectiveness of this methodology depends on: 1) the correlation between laboratory experimental work and actual field occurrences, and 2) how accurately the sediment-contaminant transport codes simulate the in-stream migration of the chemicals.

As with most codes, when a new sediment-contaminant code is developed, some sort of verification technique is usually initiated by the developer. However, the techniques used and results of these verification studies are

seldom reported in the literature. Consequently, model verification techniques need to be developed further and results of such studies need to be reported and evaluated.

In order to assess the accuracy and limitations of a sediment-contaminant transport code, each component or mechanism of the model should theoretically be tested individually with field data. The other components should be controlled to isolate the component being tested.

This study represents an initial step in the complicated process of verifying sediment-contaminant transport codes. As with most modeling efforts, more data could be collected to better represent the actual scenario. For the CMRA methodology specifically, a more complete set of field data could include: 1) suspended sediment information distributed by size fraction at various locations in the channels, 2) a more complete set of cross-sectional information for each channel, 3) surface water slopes and bed slopes for each channel, 4) the types of suspended material in each channel and their properties, 5) more intensive study of the distribution and degradation of diazinon in these channels, and 6) more hydrodynamic information describing the flow conditions. Many of these improvements are expensive and time consuming, but some need to be done only once, such as geometric descriptions of the channels--barring any significant changes in the channel slopes.

Many gaps exist in the understanding and modeling of chemical migration, fate, and effects in the environment and much room for refinement and application of present models. There is much to be gained by applying the models as a screening tool to help government and industry assess potential effects of accidental and routine chemical releases.

The facility at MERS offers an ideal location for short- and long-term study of chemicals (insecticides, pesticides, heavy metals, etc.) and their effects on the environment. Since the laboratory and field channels exist, future studies could be performed using the Chemical Migration and Risk Assessment methodology presented herein.

6.0 REFERENCES

- Allison, D. T., and R. O. Hermanutz. 1977. Toxicity of Diazinon to Brook Trout and Fathead Minnows. EPA-600/3-77-060, U.S. Environmental Protection Agency, Duluth, Minnesota.
- Allison, D. T. 1977. Use of Exposure Units for Estimating Aquatic Toxicity of Organophosphate Pesticides. EPA-600/3-77-077. U.S. Environmental Protection Agency, Duluth, Minnesota.
- Bell, H. L., unpublished data. 1971. In Water Quality Criteria 1972. EPA-R3-73-033. U.S. Environmental Protection Agency, Washington, D.C.
- Biesinger, K. E., unpublished data. 1971. In Water Quality Criteria 1972. EPA-R3-73-033. U.S. Environmental Protection Agency, Washington, D.C.
- Chow, V. T. 1959. Open-Channel Hydraulics, McGraw-Hill, New York.
- Cope, O. B. 1965. "Sport Fishery Investigations." In "The Effects of Pesticides on Fish and Wildlife." U.S. Fish and Wildlife Service, Circ. 226:51-63, U.S. Department of the Interior, Washington, D.C.
- Cowart, R. P., F. L. Bonner, and E. A. Epps. 1971. "Rate of Hydrolysis of Seven Organophosphate Pesticides." Bull. Environ. Contam. Toxicol. 6:231-234.
- Dawson, G. W., C. J. English and S. E. Petty. 1980. Physical Chemical Properties of Hazardous Waste Constituents, U.S. Environmental Protection Agency, Athens, Georgia.
- Dexter, R. N. 1979. "Distribution Coefficients of Organic Pesticides," In Methodology for Overland and Instream Migration and Risk Assessment of Pesticides. U.S. Environmental Protection Agency. p. C-22.
- Eaton, J. G. 1973. "Recent Development in the Use of Laboratory Bioassays to Determine 'Safe' Levels of Toxicants for Fish." In Bioassays Techniques in Environmental Chemistry. Ann Arbor Science Publishers, Inc., Ann Arbor, Michigan. pp. 107-115.
- Elder, J. W. 1959. "The Dispersion of Marked Fluid in Turbulent Shear Flow," J. Fluid Mech. Vol. 5, pp. 544-560.
- Fischer, H. B. 1967. "Mechanics of Dispersion in Natural Streams," J. Hydraul. Div. HY6, ASCE.
- Fischer, H. B., E. J. List, R. C. Y. Koh, J. Imberger and N. H. Brooks. 1979. Mixing in Inland and Coastal Waters. Academic Press, New York.

- Fread, D. L. 1971. "Discussion of Implicit Flood Routing in Natural Channels." M. Amein and C. S. Fang, J. Hydraul. Div. ASCE, Vol. 99, No. HY7, pp. 1156-1159.
- Fread, D. L. 1973a. "Effect of Time Step Size in Implicit Dynamic Routing," Wat. Res. Bull. AWRA, Vol. 9, No. 2, pp. 338-351.
- Fread, D. L. 1973b. "Technique for Implicit Dynamic Routing in Rivers with Major Tributaries," Water Resources Research, Vol. 9, No. 4, pp. 918-926.
- Fread, D. L. 1974. "Numerical Properties of Implicit Four-Point Finite Difference Equations of Unsteady Flow," NOAA Technical Memorandum NWS HYDRO 18, pp. 918-916.
- Fread, D. L. 1975. "Discussion of Comparison of Four Numerical Methods for Flood Routing," R. K. Price, J. Hydraul. Div. Vol. 101, No. HY3, pp. 565-567.
- Fread, D. L. 1976. "Flood Routing in Meandering Rivers with Flood Plains," Rivers '76, Vol. I, Symposium on Inland Waterways for Navigation, Flood Control and Water Diversions, Colorado State University, August 10-12, Harbors and Coastal Engineering Division of ASCE, pp. 16-35.
- Fread, D. L. 1978 (in press). "Calibration Technique for One-Dimensional Unsteady Flow Models," J. Hydraul. Div., ASCE, Vol. 104.
- Geckler, J. R., W. B. Horning, T. M. Neiheisel, Q. H. Pickering, E. L. Robinson and C. E. Stephan. 1976. Validity of Laboratory Tests for Predicting Copper Toxicity in Streams. EPA-600/3-76-116. U.S. Environmental Protection Agency, Duluth, Minnesota.
- Gomaa, H. M., I. H. Suffet and S. D. Faust. 1969. "Kinetics of Hydrolysis of Diazinon and Diazoxon. Residue Rev. 29:171-190.
- Goodman, L. R., D. J. Hansen, D. L. Coppage, J. C. Moore and E. Matthews. 1979. Diazinon(R): Chronic Toxicity to, and Brain Acetylcholinesterase Inhibition in, the Sheepshead Minnow (Cyprinodon variegatus). Trans. Am. Fish Soc. 108:479-488.
- Graf, W. H. 1971. Hydraulics of Sediment Transport. McGraw-Hill, New York.
- Gulliver, J. S. 1977. "Analysis of Surface Heat Exchange and Longitudinal Dispersion in a Narrow Open Field Channel with Application to Water Temperature Prediction," M.S. Thesis, University of Minnesota, Department of Civil and Mineral Engineering, 187 p.
- Gulliver, J. S., and H. Stefan. 1980. "Soil Thermal Conductivity and Temperature Prediction in the Bed of the Experimental Field Channels at the USEPA Ecological Research Station in Monticello, Minnesota," St. Anthony Falls Hydraulic Laboratory, University of Minnesota, External Memorandum No. 165.

- Hahn, M. G., J. S. Gulliver and H. Stefan. 1978a. "Operational Water Temperature Characteristics in Channel No. 1 of the USEPA Monticello Ecological Research Station," St. Anthony Falls Hydraulic Laboratory, University of Minnesota, External Memorandum No. 151, 46 p.
- Hahn, M. G., J. S. Gulliver and H. Stefan. 1978b. "Physical Characteristics of the Experimental Field Channels at the USEPA Ecological Research Station in Monticello, Minnesota," St. Anthony Falls Hydraulic Laboratory, University of Minnesota, External Memorandum No. 156, 36 p.
- Hahn, M. G. 1978. "Experimental Studies of Vertical Mixing in Temperature Stratified Waters," M.S. Thesis, University of Minnesota, Minneapolis, Minnesota, 179 pp.
- Henderson, F. M. 1966. Open Channel Flow, MacMillan Publishing Co. Inc., New York.
- Jarvinen, A. W., and D. K. Tanner. 1981. "Toxicity of Selected Controlled Release and Corresponding Unformulated Tehnical Grade Pesticides to the Fathead Minnow (Pimephales promelas)," Accepted for publication in the J. Environ. Pollut. Series A.
- Johnson, W. W., and M. T. Finley. 1980. Handbook of Acute Toxicology of Chemicals to Fish and Aquatic Invertebrates. U.S. Department of Interior, Fish and Wildlife Service, Resource Publication No. 137.
- Morgan, H. G. 1977. "Sublethal Effects of Diazinon in Stream Invertebrates." PhD dissertation. University of Guelph, Ontario, Canada, NIG 2W1. 188 pp.
- Olsen, A. R., and S. E. Wise. 1979. "Frequency Analysis of Pesticide Concentrations for Risk Assessment," U.S. EPA Contract 23111 03242, Battelle, Pacific Northwest Laboratories, Richland, Washington.
- Onishi, Y. 1977. Mathematical Simulation of Sediment and Radionuclide Transport in the Columbia River. BNWL-2228, Battelle, Pacific Northwest Laboratories, Richland, Washington.
- Onishi, Y., S. M. Brown, A. R. Olsen, M. A. Parkhurst, S. E. Wise and W. H. Walters. 1979. Methodology for Overland and Instream Migration and Risk Assessment of Pesticides. Battelle, Pacific Northwest Laboratories, Richland, Washington, for the U.S. Environmental Protection Agency, 6A.
- Onishi, Y., P. A. Johanson, R. G. Baca and E. L. Hilty. 1976. Studies of Columbia River Water Quality--Development of Mathematical Models for Sediment and Radionuclide Transport Analysis. BNWL-B-452, Battelle, Pacific Northwest Laboratories, Richland, Washington.
- Onishi, Y., G. Whelan and R. L. Skaggs. 1980. Development of a Multimedia Radionuclide Exposure Model for Low-Level Waste Management, PNL-3370, Pacific Northwest Laboratory, Richland, Washington.

- Onishi, Y., and S. E. Wise. 1979. "Mathematical Model, SERATRA, for Sediment-Contaminant Transport in Rivers and Its Application to Pesticide Transport in Four Mile and Wolf Creeks in Iowa." Submitted to U.S. Environmental Protection Agency, Environmental Research Laboratory at Athens, GA by Battelle, Pacific Northwest Laboratories, Richland, WA.
- Ponce, V. M. 1980. "Stability, Consistency, and Convergence." Class Notes, Colorado State University, Fort Collins, Colorado.
- Sanders, H. O. 1969. Toxicity of Pesticides to the Crustacean Gammarus lacustris. Bureau of Sport Fisheries and Wildlife, Tech. Paper No. 66, U.S. Government Printing Office, Washington, D.C.
- Sanders, H. O., and O. B. Cope. 1968. "The Relative Toxicities of Several Pesticides to Naiads of Three Species of Stoneflies," Limnology and Oceanography, 13(1):112-117.
- Sethunathan, N., and M. D. Pathak. 1972. Increased Biological Hydrolysis of Diazinon After Repeated Application in Rice Paddies. J. Agr. Food Chem. 20:586-589.
- Stefan, H. G., J. Gulliver, M. G. Hahn and A. Y. Fu. 1980. "Water Temperature Dynamics in Experimental Field Channels: Analysis and Modeling," St. Anthony Falls Hydraulics Laboratory, University of Minnesota, Project Report No. 193.
- Vanoni, V. A. (ed.). 1975. Sedimentation Engineering, ASCE M and R No. 54, New York, New York.
- Zischke, J. A., J. W. Arthur, K. J. Nordlie, R. O. Hermanutz, D. A. Standen and T. P. Henry. 1981. Acidification Effects on Macroinvertebrates and Fathead Minnows (Pimephales promelas) in Outdoor Experimental Channels. Submitted to Water Research. U.S. Environmental Protection Agency. (Publication Pending).

DATE
TIME